University College of Southeast Norway
Faculty of Technology, Natural Sciences
and Maritime Sciences

Doctoral dissertation no. 33
2017

Wenjing Zhou

Modeling, Control and Optimization of a Hydropower Plant

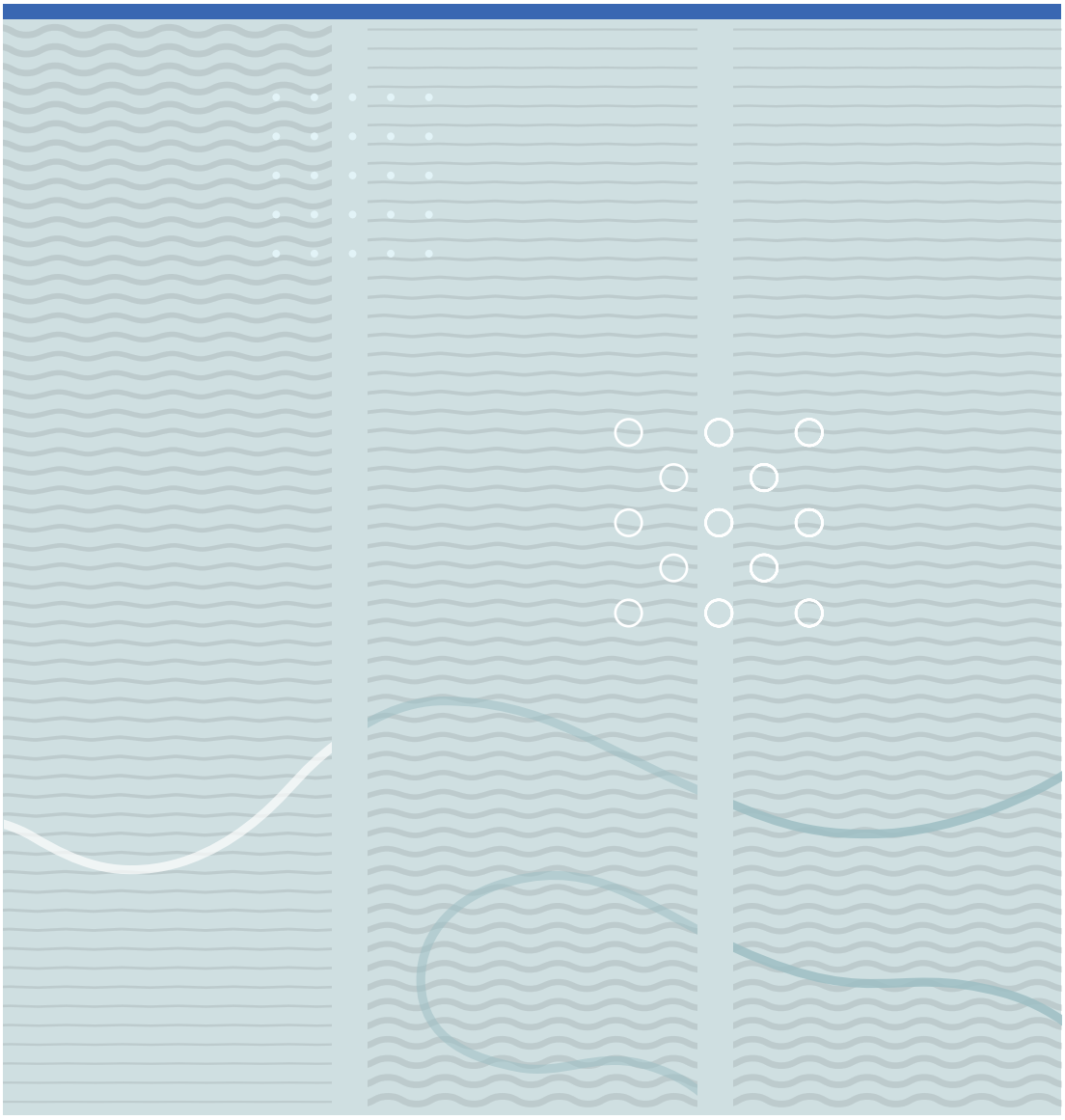

HSN

Wenjing Zhou

Modeling, Control and Optimization of a Hydropower Plant

A PhD dissertation in
Process, Energy and Automation Engineering

Faculty of Technology, Natural Sciences and Maritime Sciences
University College of Southeast Norway
Kongsberg, 2017
Doctoral dissertations at the University College of Southeast Norway no.33

ISSN: 2464-2770 (print)
ISSN: 2464-2483 (electronic)
ISBN: 978-82-7206-457-9 (print)
ISBN: 978-82-7206-458-6 (electronic)

Print: **University College of Southeast Norway**

Preface

This thesis is submitted to the University College of Southeast Norway (USN), was named Telemark University College until 31.12.2015, for partial fulfilment of the requirements for the degree of philosophise doctor.

The doctoral work has been performed at the Department of Technical Faculty, USN, Porsgrunn, with Professor Bjørn Glemmestad as main supervisor and with co-supervisor Bernt Lie.

Hydropower is renewable energy and main electricity source for Norway. My belief that it is with great interest to explore possibilities for improving this traditional industry.

Throughout these years, I have fortunately obtained different help from others, who shared their knowledge and experience with me. Even it is not possible to list all of the names, great thanks to all of you.

Abstract

Hydropower is a crucial power resource for everyday life in Norway, and a traditional industry that could be improved along with new updated technologies. The PhD work focuses on exploring new solutions, in aspect of regulation the water resource, for a hydropower plant.

Prior to develop any control strategy, a mathematical modeling for a hydropower plant is of great importance. Towards acquiring a concise and comprehensive mathematical model, various modeling approaches are introduced to represent the mechanical power input of a single-unit power plant, which contains of Simple method, Finite volume method (FVM), Method of characteristics (MOC), Electrical circuit equivalent method (EEC). From the simulation results, the Simple method demonstrated its sufficiency for representing the behaviors of the plant and its advantage with consideration of computationally complexity for subsequence controllers' developments.

For manipulation electricity production of a hydropower plant, it is the key point that controlling the input mechanical power from water, which is transferred to electrical power. According to this essential concept, nonlinear model predictive control (NMPC) is developed regarding two kinds of plants, either with only a single generation unit, or with multiple generation units. The achieved NMPC performs its function fairly better comparing with traditional PI controller under different operation situations in a single-unit plant, as well as its advantage of reducing interaction effects when manipulating multi-units simultaneously in one plant, which are presented with simulation results in this thesis.

The other concerning issue of the PhD work is to assist to security surroundings of hydropower plant from flood, and in the meanwhile, optimize the utilization of water. As a result, an optimizer is developed to achieve this purpose, which can produce a control trajectory of a Model Predictive Control (MPC) developed for floodgate with a prediction of a period ahead, and update a decision trajectory of discharging flow that

maximize electricity production under the circumstance of safety. The simulation results are presented for a water reservoir of a specific hydropower plant and made a comparison with its historical operation, which has shown that there is some room for enhancing the electricity production if it is under the operations generated from the optimizer rather than with historical operations.

Modeling, control and optimization are the main tasks of this PhD work. The thesis lays out all the details of how the NMPC and optimizer are brought out, the reasons and context for the motivations of why such a work is proposed for hydropower plant.

Contents

List of Figures

List of Tables

Nomenclature

Symbols

Symbol	Description	Unit
A	Cross sectional area	m^2
a	Water pressure wave velocity	m/s
A_G	Area of floodgate total passage	m^2
A_p	Area of penstock total passage	m^2
A_R	Area of reservoir	m^2
C	Capacitance	F
CV	Control Volume	(dimensionless)
D	Internal diameter of pipe	m
$Damp$	Damping coefficient	(dimensionless)
D_r	Droop ratio	(dimensionless)
e_{mis}	Mismatch error	Mw, or Hz
E'_d	d axis transient voltage	p.u
E_f	excitation potential	p.u
E'_q	q axis transient voltage	p.u
E_t	Tolerance error	(dimensionless)
F	Force	N
f	Frequency	Hz
f_r	Friction factor	(dimensionless)
g	Gravity acceleration	m/s^2

G	Percentage of gate opening	%
H	Water head/Water level of reservoir	m
h	Process equation	(dimensionless)
H_{loss}	Gross head loss	m
H_{net}	Net head to Turbine	m
H_{p_in} / H_{p_out}	Water head of inlet / outlet flow of penstock	m
H_r	Water head of upstream reservoir	m
H_{ref}	Reference level	m
H_T	Water head of downstream reservoir	m
H_{up}	Water head of upstream reservoir	m
I_d / I_q	d axis / q axis armature current	p.u
J	Cost function	(dimensionless)
k	Time index	(dimensionless)
K_E	Exciter gain	(dimensionless)
K_F	Stabilizer gain	(dimensionless)
k_g	Turbine gate constant	(dimensionless)
L	Length of the pipe	m
m	Mass	kg
M	Inertia constant of the machine	(dimensionless)
N_c	Control horizon	(dimensionless)
N_p	Prediction horizon	(dimensionless)
n	Index; Number of states	(dimensionless)
OP	Effective gate Opening of hydraulic turbine or floodgate	% /m

p	Pressure	bar
P	Covariance	(dimensionless)
P	Power	Mw
P_c	Total consumed power	p.u
P_d	Power demanding	p.u
P_e	Electrical power	p.u
P_m	Mechanical power	Mw
Q	Volume flow rate	m^3/s
Q_{dis}	Discharge flow to Turbine	m^3/s
Q_G	Flow rate of water pass through gate	m^3/s
Q_{in}	Inflow rate to reservoir	m^3/s
Q_{out}	Outflow rate of reservoir	m^3/s
Q_P	Production volume flow rate	m^3/s
Q_p	Volume flow rate of penstock	m^3/s
Q_S	Spill away flow	m^3/s
Q_s	Volume flow rate of surge tank	m^3/s
Q_{p_in}	Inlet flow of penstock	m^3/s
Q_{p_out}	Outlet flow of penstock	m^3/s
R	Reference vector	(dimensionless)
R_a	Armature resistance	p.u
R_e	Equivalent resistance of transmission lines	p.u
r	reference	(dimensionless)
r_c	Corrected reference	(dimensionless)

t	Time	second / hours / days
T_E	Exciter time constant	(dimensionless)
T_{FE}	Stabilizer circuit time constant	(dimensionless)
T_J	Inertia time constant	(dimensionless)
T'_{d0}	d axis open circuit time constant	second
T'_{q0}	q axis open circuit time constant	second
$u\,/\,U$	Control variable / Control variable vector	(dimensionless)
U_r	Reference voltage	p.u
U_s	Stabilizer voltage	p.u
U_t	Generator terminal voltage	p.u
U_t	Effective opening of turbine	%
$U_{td}\,/\,U_{tq}$	d axis / q axis component of terminal voltage	p.u
v	velocity	m/s
V_0	Infinitive bus voltage	p.u
V_t	Terminal voltage, ref. Figure9	p.u
x	State	(dimensionless)
X_e	Equivalent reactance of transient line	p.u
X_d	Synchronous reactance	p.u
X'_d	d axis transient reactance	p.u
X_q	q axis synchronous reactance	p.u
X'_q	q axis transient reactance	p.u
y	Process output	(dimensionless)
z	Measurements	(dimensionless)

Z_U / Z_D	Upstream / Downstream reservoir level	m

* p.u: per unit

Superscripts

Superscript	Description
atm	atmosphere

Subscripts

Subscript	Description
c / c1 / c2	conduit, conduit 1, conduit 2
c1,2	conduit 1 and 2 in multi-unit plant
loss	Head loss
neg	negative
nom	Nominal
out	Output
p / p1 / p2	Penstock, penstock 1, penstock 2
p1,2	Penstock 1 and 2 in multi-unit plant
pos	Positive
p1, p2	penstock1, 2
R / r	Water reservoir
s	Surge shaft/tank
s1 / s2	Upstream /downstream surge tank
c1 / c2	Upstream / downstream conduit
s1_in / s1_out	Inlet / outlet flow of upstream surge tank, s1

s2_in / s2_out	inlet / outlet flow of downstream surge tank, s2
p1_in / p1_out	Inlet / outlet flow of upstream conduit, p1
p2_in / p2_out	inlet / outlet flow of downstream conduit, p2
ref	Reference value
(A) / (B) / (P)	Point A, B and P on a pip, ref. Figure 6.
turbine1,2	Turbine 1 and 2 in multi-unit plant

Greek letter

Greek Letter	Description	Unit
β	Reference correction factor	Mw, or Hz
β_p	fluid compressibility at pressure P	(dimensionless)
δ	Phase angel	p.u
ε	Floodgate constant	(dimensionless)
ε_t	Turbine opening constant	(dimensionless)
η	Turbine efficiency	%
λ	Control coefficient	(dimensionless)
ρ	Water density	kg/m^3
ω	Angular velocity	p.u
ϕ	Filter parameter	(dimensionless)
χ	Sigma point	(dimensionless)

$\overline{XX}$

Abbreviation

Abbreviation	Description
HRV	Limit for highest regulated water level due to operating procedures throughout a year.
ALRV	Limit for Lowest regulated water level due to operating procedures throughout a year.
EEC	Electrical equivalent circuit
FVM	Finite volume method
FSDP	Fuzzy stochastic dynamic programming
HBV	Hydrology model
HRV	High regulated water volume limit
LMPC	Linear model predictive control
LRV	Low regulated water volume limit
MPC	Model predictive control
MIMO	Multiple inputs multiple outputs
MOC	Method of Characteristic
NMPC	Nonlinear model predictive control
NVE	Norwegian Water Resources and Energy Directorate
ODE	Ordinary differential equation
PA	Priority assignment

PDE	Partial differential equation
PI(D)	Proportional Integral (Derivative) control
SQP	Sequential Quadratic Programming
UKF	Unscented Kalman filter

1 Introduction

This opening chapter presents an overview of concerned engineering issues of hydropower plant in the PhD work. According to the topic, there are three diverse areas included for this research: modeling, control and optimization, of which control and optimization are applied to different elements of the plant respectively. As a result, the dissertation is divided into five chapters: introduction, modeling, control of hydro power plant, optimization, and conclusion.

In further, this chapter also explains the motivation for studying each aspect and corresponding research design for them. As a starting point, the principle of power generation of hydropower plant is also introduced briefly in this chapter.

1.1 Background

Hydropower is a clean, renewable energy, and the most prominent alternative to fuel thermal power or nuclear power. In Norway, hydropower supplies more than 70% (M.Aasen, 2010) of domestic electricity consumption. Prior to discussing any work developed in the thesis, an introduction of related hydropower plant in Norway is presented in this section, of which Figure 1 illustrates a prototype of a single generation unit plant.

The principle of hydro electricity generation is to transfer kinetic and potential power of falling water to electrical power. The origin of electricity generation, the water reservoir, can be a natural lake or accumulated by an artificial dam. No matter which kind of reservoir it is, as to obtain more power, more water should be gathered in the reservoir, which implies a risk of water flooding to surroundings especially in rainy season. To prevent it to happen, a floodgate is built next to reservoir to spill water to downstream reservoirs or specific waterways.

At the intake, there is a gate to control water flows from the reservoir to water conduits. This gate has been assumed normally opened with a constant value and ignored

throughout our work. The function of the surge tank is briefly to reduce water hammer pressure variations and keep the mass oscillations, caused by load changes, within acceptable limits and decreases the oscillations to stable operation as soon as possible (Kjølle, 2001). There can be two surge tanks that are separately distributed on upstream and downstream, or, alternatively only one surge tank in either water stream. Sometimes, there is no surge tank in the plant due to low-pressure waves or in a rather old plant. A water conduit after dam and a penstock after upstream surge tank guide the water flowing to the hydraulic turbine. There is another water conduit connecting downstream surge tank and downstream water reservoir or river. The hydraulic turbine is the mechanical part that transfers water kinetic power to mechanical power. There are two main types of hydraulic turbine in Norway: Francis turbine and Pelton turbine. For the Francis turbine, the water flows into the runner of the turbine through a guide vane with adjustable opening to control the rotation speed of the runner. For Pelton turbine, the water flows into runner bucket as a jet from a nozzle. Needle opening controls the rotation speed of Pelton turbine. Power generation can be manipulated by controlling the opening of turbine, because, generally speaking, almost all of the mechanical power of turbine can be converted into electrical power. However, in the control part of this work, it is not distinguished either Francis or Pelton turbine. An overall effective turbine opening stands for both of them, with a turbine opening constant ε_t that can differentiate the turbine. The elements mentioned above are classified as hydraulic system of hydropower plant. Besides, there is an electrical system that includes generator, exciter, and so on, which is not the focus in this work, but is considered in the modeling of the whole plant.

The hydropower plant can also be with several generation units. Those units share a common upstream reservoir and waterways, but a separate branch penstock before respective hydraulic turbine and then the tailor waterways.

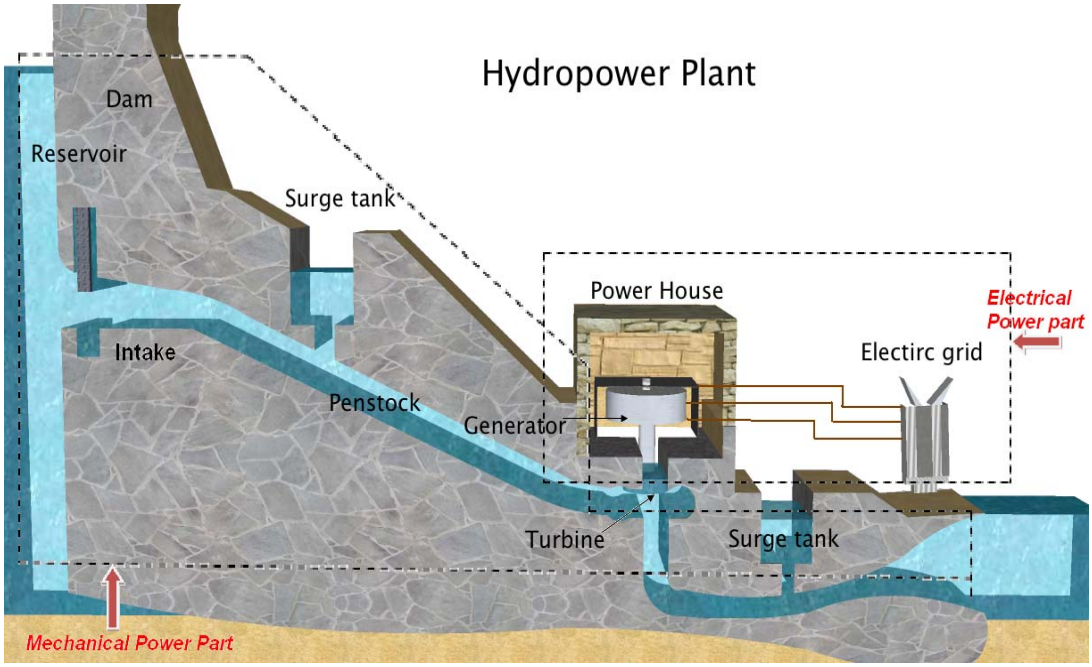

Figure 1. General drawing of a single generation unit hydropower plant

1.2 Motivation

Modern optimization and control technology becomes popular and successfully conducted for improving various processes in real industry. Even though hydropower belongs to traditional and sophisticated engineering prospect, it is still interesting to study it with relatively new solutions. Apparently, it can be seen from the research title of the PhD work that there are two main research objects involved, to control and to optimize the power generation of hydropower plant.

For control part, NMPC is introduced and simulated with a single-unit plant model and a multi-unit plant model. For optimization part, beneficial to enhance utilization of water, an optimizer is developed, which can handle floodwater efficiently, utilize available water resource of reservoir simultaneously and effectively to generate electricity for hydropower plant.

1.2.1 Motivation of NMPC

There are several motivations to implement advanced control methods to hydropower plants. One of the main intentions is to examine the feasibilities of MPC, which is a very popular and has been verified doable in other industries.

MPC technology has become a powerful control strategy for process with complex dynamics in recent decades. It uses a model to predict future process behaviour and control trajectory with an optimization process in a predefined control and prediction horizon. Furthermore, MPC is compatible to constrained control problem, since constraints can be comprised directly to the associated optimization process. Despite industry process dynamics is normally nonlinear, there are many successful linear MPC (LMPC) application examples in some industry fields (S.J Qin, 2003), especially in chemical process, petrol chemical engineering (S.J.Qin, 2000), (J. K. Gruber, 2009), (N. Daraoui, 2010), most of which are implemented with MPC based on linear models. However, the process with highly nonlinear behaviour, it is not recommended to implement conventional linear MPC, because a single LMPC cannot provide acceptance in all operating regions, the results of which a highly nonlinear system cannot be linearly modelled to be adequate in all operating regions, unless the process always works close to a nominal operating point (A. Rahideh, 2012). Solutions for this problem, like approximating nonlinear model method, are presented in (B. Aufderheide, V. Prasad, B. W. Bequette, 2001), (D. Dougherty, D. Cooper, 2003), (J. Z. Wan, 2004). Different from those works, in this work, a straightforward NMPC is implemented instead, which represents target process with a nonlinear model and succeed the principles and abilities to handle constraints of conventional MPC.

When it refers to hydropower plant, it has not only significant nonlinear behaviour, but also several different operation stages. A typical operation procedure of a hydropower plant includes: standstill, run-up, stabilization at grid frequency (speed control at no load), synchronization and connecting to operation network mode, output power

control, switch out to no load mode, and braking to shut down (A.H. Grattfelder. L. Huser). According to status of electrical network, there are three operation modes:

- operations when the plant stands alone;
- operations when plant is connected to a small grid;
- operations when connected to infinite bus;

No matter under which electrical network, with simple PI control strategy, which is widely used in power system control and other industry area, it is required tuning or choosing operation parameters depending on the interacted network. From a point of view of industrial engineering, advanced control can contribute to fulfil various operation requirements and reduce manual work.

Furthermore, speaking of hydropower, there are also some additional constraints should be considered comparing with thermal or other type of power plant. The water storage in upstream reservoir is always limited by natural conditions. Therefore, the discharging flow rate is constrained by scheduling of production. The admissible changing rate of flow is also constrained because of water hammer effect that is caused fluid inertia, which directly leads to a constraint for closing rate. These constraints are also presented and composed to the proposed NMPC. These are the reasons that NMPC is proposed for controlling a single-unit hydropower plant in this study.

Because of the water in a reservoir is limited by natural conditions, in other words, the power resource for electricity generation is limited over time, if there are several units in one plant, they are sharing this common water. Accordingly, there must be some interactions among the units. When designing an advanced controller for multi-unit hydropower plant, counting on the coupling effects, MPC would be a smarter choice due to its unique algorithm. Moreover, a two-unit hydropower plant can be treated as multiple inputs and multiple outputs (MIMO) system. The openings of hydraulic turbines are process inputs and control variables, and the power generations of the units are process outputs and control objects. Concerning to reduce the coupling effects quickly and effectively and achieve the general control goal, MPC is chosen as the control

strategy in this work, which is widely accepted in industry nowadays (Farkas, 2005), (Lu JZ, 2003), (Adetola V, 2009) and especially as a helpful tool for multivariable process control (A. Ramírez-Arias, 2012), (B. R. Maner, 1996), (D. Edouard, 2005). At each control interval, it calculates out a control trajectory with an optimization process that minimizes the cost throughout a predefined prediction horizon, and only implements the first control action to the plant process. MPC promises a great benefit to maintain the optimal and economic operation of the multivariable process and preserves the life of the equipment of the plant (Tri C.S. W, 2010). Furthermore, MPC is also characterized with its superiority of handling various constraints, for instance, the total production discharging flow rate in this case. According to the nonlinear behavior of a two-unit hydropower plant, a direct NMPC is proposed in our work, which inherits all the advantages of MPC but with a nonlinear internal model in the optimization process, even though there are some other methods to approximate nonlinear model presented in (B. Aufderheide, V. Prasad, B. W. Bequette, 2001) (B. Aufderheide, V. Prasad, B. W. Bequette, 2001), (D. Dougherty, D. Cooper, 2003), (Z. Wan, 2004).

1.2.2 Motivation of optimization

As it is known, hydroelectricity is realized by transferring mechanical power of water to electrical power. With this concept, normally, there is upstream reservoir offers water to hydropower plant, which can be a natural lake or artificially built dam to accumulate water. Then the hydropower plant uses the potential and kinetic energy of the water to rotate hydraulic turbine as well as a generator to produce electricity. However, more power implies more water should be accumulated, which usually leads to a risk that water may flood to neighbourhood. Floodgate is a facility built for avoiding it. Spilling water away by floodgate is necessary for safety reason but also a possibility of discharging unnecessary water that should be utilized for power production. Therefore, optimization of regulation of floodwater is required for increasing the efficiency of utilization of water for hydropower plant, which is another purpose of this work.

Furthermore, the optimization of floodwater certainly concerns with the scheduling of reservoir operation problem. Any result of floodgate control changes the reservoir level. Consequently, it also affects the decision on how much water should be discharged for power production. Therefore, optimal control of floodgate is a part of optimization of reservoir operation, of which the optimizing object is the electricity production under a safe circumstance of avoiding flood.

1.3 Research Design

To begin with this research, there has to be something can be manipulated with various advanced control methods and can be examined with optimization possibilities. Modeling of a hydropower plant ought to be required as a base of MPC, NMPC and optimization. Therefore, the work is divided into three parts: Modeling, Control design and Optimization. For each, there has been several works carried out and contributed.

Modeling: Finite volume method (FVM), Electrical equivalent circuit (EEC) method, Method of Characteristic (MOC) method have been proposed and established for a hydropower plant that is illustrated in Figure 1.

Controlling: NMPC of a single-unit hydropower plant, NMPC of multi-unit hydropower plant have been implemented and compared with traditional PI controller.

Optimization: Optimization of reservoir water level has been established and studied against existing operations.

NMPC and optimization are both implemented to hydropower plants that are simulated by mathematical models, in which some cases are modified by experimental data. However, since the huge surface of reservoir, the simulation time steps of these two main subjects differs greatly. The reservoir level changes with hours, whereas control response of electricity generation changes with seconds. Therefore, these two tasks can be deemed as two individual works. When regulating power generation, reservoir level is assumed constant, and when optimizing water discharging for power generation, it is

suggesting a daily average production flow. Nevertheless, some technologies are adopted for both two topics, e.g. Kalman filter. The research design then for these three topics is illustrated as shown in Figure 2.

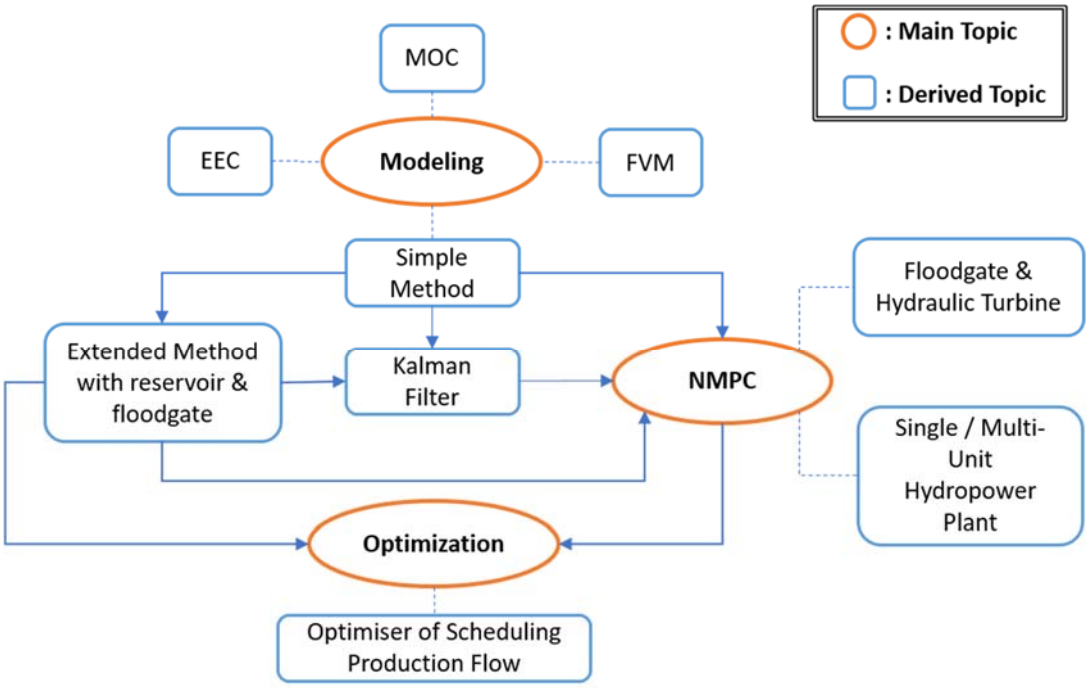

Figure 2. Research design flow chart

1.4 List of Published Papers

- "Modelling and control of a high head hydropower plant", World Congress on Engineering and Technology (WCE), IEEE, 2011.
- "The effect of compressibility of water and elasticity of penstock walls on the behaviour of a high head hydropower station", 52th Scandinavian Simulation Society conference, 2011.
- "Application of Kalman filter based Nonlinear MPC for Flood Gate control of Water Reservoir", IEEE Power & Energy Society General Meeting, 2012.
- "Implementation unscented Kalman filter for nonlinear states estimation of a hydropower plant", IEEE Power & Energy Society, Powercon, 2012.

1.5 Contributions

- A general partial differential equation (PDE) model is introduced in Modeling an overall hydropower plant, and an ordinary differential equation (ODE) mathematical model is built up and simplified from this PDE model and realized with MATLAB.
- Unscented Kalman filter is introduced for states estimation of reservoir regulation and power generation process.
- A NMPC controller is carried out for controlling single-unit hydropower plant
- A NMPC controller is developed for controlling multi-unit hydropower plant
- A NMPC controller is developed for controlling reservoir floodgate
- An optimizer is developed for enhancing water utilization for power production and, in the meanwhile, handling the flood.

2 Modeling of a hydropower plant

It is essential to have a mathematic mode to begin with for this research work, so any newly developed application for a hydropower plant can be studied and tested theoretically. The accuracy of such a plant model will affect the reliability of the applications. In this chapter, a general simple method is developed for NMPC intentionally. The simulation results of such a simple model of an overall hydropower plant have been presented in (W. Zhou, B. Lie, B. Glemmestad, 2011) with details, which is enclosed in Appendix A1. Several other commonly used modeling methods are also introduced to examine the effects of water elasticity for modeling penstock. The simulation and comparison results are illustrated and discussed for all referred models.

2.1 Simple method

The flowchart shown in Figure 3 illustrates the process how the hydropower plant with single generation unit obtains the mechanical power for electricity generation. The mathematical model of such a plant is achieved by several ODEs and two PDEs for penstock model. There are two reservoirs and two surge tanks, which are standing upstream and downstream respectively. The hydraulic turbine in the powerhouse is rotated by the water that flows in. At the same time, it drives the rotor of the generator to produce electrical power. The mechanical power, defined in this thesis, is the output from the turbine, and can be manipulated by turbine gate opening, by means of an effective opening of guide vane of Francis turbine or the effective opening of the needle of the nozzles for Pelton turbine.

Water head H is an engineering term in hydropower industry, which uses water elevation with unit of meter or feet to express pressure. The friction term of fluid, head loss H_{loss}, is customized as another form of pressure loss in this work. Darcy–Weisbach equation is introduced for head loss with considering the direction of flow:

$$H_{loss} = f_r \cdot \frac{L}{D} \cdot \frac{\bar{v} \cdot |\bar{v}|}{2g} = f_r \cdot \frac{L}{D} \cdot \frac{\bar{Q} \cdot |\bar{Q}|}{2g \cdot A^2} \quad (2.1)$$

It is a phenomenological equation that calculates the friction along a conduit from the length L, diameter D and average flow $\bar{v}$ or volume flow $\bar{Q}$ of it. The friction factor f_r is dimensionless, and can be modified to distinguish different type of pipes, such as conduits, penstocks in this work, with regards to their structures and materials. Other than head loss within a pipe, Darcy–Weisbach equation can also be used to calculate the friction loss along the hydraulic turbine, by presuming the turbine as a curly pipe with some obstructions.

2.1.1 Reservoir

The upstream reservoir is the water resource for a hydropower plant. After producing electrical power, the water is gathered in downstream reservoir or directly flows into river. It is assumed the water levels of the reservoirs, as H_r for upstream reservoir and H_T for downstream reservoir in Figure 3, are constant throughout mathematical modeling and control part, Chapter 2 and 3, of this thesis. There is another reservoir model depends on geographical measurements for a specific plant in the optimization part in Chapter 4.

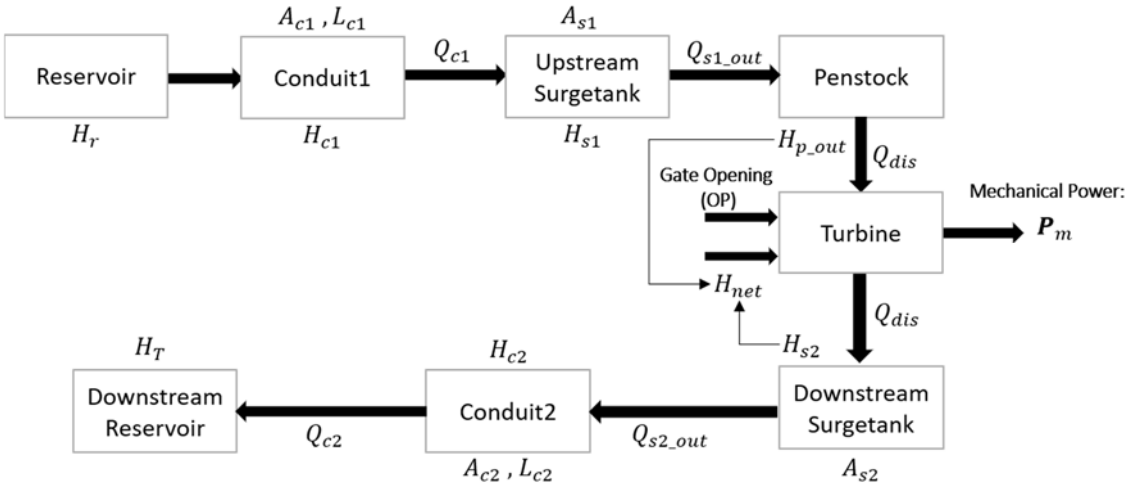

Figure 3. Flowchart for modeling mechanical power of a hydropower plant.

2.1.2 Conduits

Conduit is defined as a pipe in this study that made with concrete material and guiding water to run into the penstock. Differentiating from penstock, conduit is relatively laid in a plain area and open to the air. Therefore, for modeling a conduit, it neglects the water internal elasticity. Consequently, the mathematic model of a conduit is simply derived from Newton's second law:

$$\begin{cases} F = m \cdot a \\ a = \dfrac{dv}{dt} \\ F = \Delta p \cdot A \end{cases} \quad \Rightarrow \quad \Delta p \cdot A = m \cdot \frac{dv}{dt} \tag{2.2}$$

where the Δp is the pressure difference between inlet and outlet.

Take the conduit1 as example, its inlet pressure is equal to the bottom pressure of the upstream reservoir, and its outlet pressure is equal to the pressure of inlet of upstream surge tank. Considering the head loss along the conduits H_{c1_loss}, the (2.1) can be developed as:

$$m_{c1} \cdot \frac{dv_{c1}}{dt} = \rho \cdot g \cdot (H_r - H_{s1} - H_{c1\_loss}) \cdot A_{c1} \tag{2.3}$$

Where $m_{c1} = \rho \cdot L_{c1} \cdot A_{c1}$, $v_{c1} = \frac{Q_{c1}}{A_{c1}}$

Then the dynamic ODE for conduit1 now can be stated as:

$$\frac{dQ_{c1}}{dt} = \frac{g \cdot A_{c1}}{L_{c1}} (H_r - H_{s1} - H_{c1\_loss}) \tag{2.4}$$

Similarly, the dynamic equation for the conduit2, which connects the downstream surge tank and the tail reservoir, can be written as:

$$\frac{dQ_{c2}}{dt} = \frac{g \cdot A_{c2}}{L_{c2}} (H_{s2} - H_T - H_{c2\_loss}) \tag{2.5}$$

2.1.3 Penstock

Penstock is an enclosed pipe that guides water running from upstream to hydraulic turbine. Potential difference between inlet and outlet of a penstock is the main source for the water mechanical power. As a result, penstock is considered as a pipe that can resist internal pressure of water. Then, elasticity of water is considered only in penstock model, but not in other the models which can be an open volume. Penstock construction material can be cerement, plastic, and so on, which can be reflected with a smaller friction factor during modeling. The water heads and volume flow can be analyzed and calculated with hydraulic PDEs for pipes, which is consisted of a continuity equation (2.6) and a motion equation (2.7) (IEEE Power & Energy Society, 1992). This set of PDE is only applied and simulated for the penstock that connecting turbine and upstream surge tank.

Continuity equation:

$$\frac{a^2 \cdot \partial Q}{g \cdot A \cdot \partial x} + \frac{Q \cdot \partial H}{A \cdot \partial x} + \frac{\partial H}{\partial t} + \frac{Q}{A} sin\,\theta = 0 \qquad (2.6)$$

Momentum equation:

$$g \cdot \frac{\partial Q}{\partial x} + \frac{Q \cdot \partial H}{A^2 \cdot \partial x} + \frac{\partial Q}{A \partial t} + g \cdot \frac{dH_{loss}}{dx} = 0 \qquad (2.7)$$

2.1.4 Dealing with Penstock PDEs

In order to reduce computation complexity, especially for preparing the internal model for NMPC, the PDEs can be replaced with ODEs, which consider only one discrete space element from the set of PDEs and assume it as one-dimensional water flow through a chosen plane area (B.Strah, 2005). Then, the mathematical model of penstock is carried out as:

$$\frac{dQ_{p\_out}}{dt} = \frac{g \cdot A_p}{L_p} \cdot \left(H_{s1} - H_{p\_out} - H_{p\_loss}\right) \quad (2.8)$$

$$\frac{dH_{p\_out}}{dt} = \kappa \cdot (Q_{p\_in} - Q_{p\_out}) \quad (2.9)$$

$$\kappa = \frac{a^2}{g \cdot A_p \cdot L_p} \quad (2.10)$$

where subscripts p indicates penstock; $s1$ indicate upstream tank; $\_in$ and $\_out$ indicate inlet flow and outlet flow; t is time.

2.1.5 Surge tank

The surge tank is an open volume tank, which means there is no air compressed when water level increases inside it. The intention of such a tank is to add more open volume to reduce pressure wave in the hydraulic system while operating the hydropower plant. The surge tank equations are derived from the continuity equation of flow at the two junctions, and where the hydraulic losses at orifices of surge tank are neglected.

For upstream surge tank, $s1$:

$$A_{s1} \cdot \frac{dH_{s1}}{dt} = Q_{s1\_in} - Q_{s1\_out} \quad (2.11)$$

For downstream surge tank, $s2$:

$$A_{s2} \cdot \frac{dH_{s2}}{dt} = Q_{s2\_in} - Q_{s2\_out} \quad (2.12)$$

2.1.6 Hydraulic Turbine

The general mechanical power from water, $\boldsymbol{P}_m$, no matter which kind of the turbine it is, can be stated as:

$$\boldsymbol{P}_m = \eta \cdot \rho \cdot g \cdot H_{net} \cdot Q_{dis} \quad (2.13)$$

where η is turbine efficiency.

The net head, H_{net} , is identical to the difference of output water head of penstock, H_{p_out} , and the head of downstream surge, head loss within turbine is neglected in simple method, then:

$$H_{net} = H_{p\_out} - H_{s2} \quad (2.14)$$

Volume flow discharged into the turbine is related with the type of turbine. However, there is no detailed modeling for each type of turbine included in this work. The gate constant, k_g, is utilized for distinguishing them. The following model is generally applied to all types of turbines with an effective gate opening, OP, which is the area that water going through. Then, the discharged flow, Q_{dis} , is formulated as:

$$Q_{dis} = k_g \cdot OP \cdot \sqrt{2 \cdot g \cdot H_{net}} \quad (2.15)$$

where $OP = G \cdot A_p$

G is the percentage of gate opening. The flow before the turbine and after turbine is assumed identical. The gate opening, G , is simulated as a linear function depends on time, t , every second the gate can move 1% of full opening.

$$\Delta G = 1 \cdot \Delta t \quad (2.16)$$

2.1.7 Generator

A synchronous generator model is presented with simplification of Park transformation (Park, 1929) that illustrates the electrical transients. The fourth order model (Milano, 2010) with ODEs is as given below:

- Electrical equations:

q axis:

$$T'_{d0} \cdot \frac{dE'_q}{dt} = (X_d - X'_d) \cdot I_d - E'_q + E_f \quad (2.17)$$

d axis:

$$T'_{q0} \cdot \frac{dE'_d}{dt} = \left(X'_q - X_q\right) \cdot I_q - E'_d \quad (2.18)$$

where E' is transient voltage; E_f is excitation potential; X is synchronous reactance; X' is transient reactance; I is armature current, $\mathrm{T}'_{\mathrm{d0}}$ is *d* axis open circuit time constant, $\mathrm{T}'_{\mathrm{q0}}$ is q axis open circuit time constant. The subscripts q and d indicate q axis and d axis respectively.

- Terminal equations, *(2.19)* - *(2.22)*:

d axis component of terminal voltage:

$$U_{td} = E'_d - R_a \cdot I_d - X'_q \cdot I_q \quad (2.19)$$

q axis component of terminal voltage:

$$U_{tq} = E'_q - R_a \cdot I_q + X'_d \cdot I_d \quad (2.20)$$

Electrical power:

$$\boldsymbol{P}_e = E'_d \cdot I_d + E'_q \cdot I_q + \left(X'_d - X'_q\right) \cdot I_d \cdot I_q \quad (2.21)$$

Terminal voltage:

$$U_t = \sqrt{U_{td}^2 + U_{tq}^2} \quad (2.22)$$

where R_a is armature resistance; U_{td} and U_{tq} are terminal voltage on d and q axis respectively.

- Rotor motion equations (2.23) - (2.24):

Rotor motion phase angel, δ :

$$\frac{d\delta}{dt} = \omega_0 \cdot (\omega - 1) \quad (2.23)$$

Angular velocity, ω:

$$M \cdot \frac{d\omega}{dt} = P_{m,(p,u)} - \boldsymbol{P}_e - Damp \cdot \frac{d\delta}{dt} \quad (2.24)$$

where M is inertia constant of the machine; $Damp$ is damping coefficient.

Consider the voltage from infinite bus, v_0 , the terminal voltages on d and q axis can also be stated as (Jan Machowski, 2008):

$$U_{td} = -V_0 \cdot sin(\delta) + R_e \cdot I_d + X_e \cdot I_q \quad (2.25)$$

$$U_{tq} = V_0 \cdot cos(\delta) + R_e \cdot I_q - X_e \cdot I_d \quad (2.26)$$

where X_e is equivalent reactance of transient line.

The exciter here is simply treated as a second order (H.L.Zeynelgi, 2002) dynamic model:

$$T_E \cdot \frac{dE_f}{dt} = K_E \cdot (U_r - U_t - U_s) - E_f \quad (2.27)$$

$$T_{FE} \frac{dU_s}{dt} = K_F \cdot \frac{dE_f}{dt} - U_s \quad (2.28)$$

where T_E is exciter time constant; K_E is exciter gain; K_F is stabilized gain; U_r , U_s , U_t are the voltages at reference, stabilizer, and generation terminal respectively.

Assuming generated electrical power, $\boldsymbol{P}_e$, is equal to totally consumed, $\boldsymbol{P}_c$, and the power demanding, $\boldsymbol{P}_d$, from costumers for a steady infinite grid.

$$\boldsymbol{P}_e = \boldsymbol{P}_c = \boldsymbol{P}_d \quad (2.29)$$

On account of that the work is made out as simulation based, the equations, from (2.4) to (2.16) constitute the hydraulic elements of a simple model for both modeling and internal model of NMPC for a hydropower. However, the electrical parts, (2.17) - (2.29) are only described in this chapter, since they are not the focal points. The overall modeling results of a hydropower plant with electrical parts are presented in Appendix A1.

2.2 Finite volume method

The simple method converts the penstock modeling problem of solving a set of PDE into solving two ODEs. The intention is to make a model not complicated to be implemented into model based prediction control. However, it may bring some deficiency of precision. Conducive to verify it is good enough to represent the flow transients of penstock, other existing but more detailed modeling methods are also introduced for penstock. Comparisons are presented along with simulation results.

The PDEs of penstock model are derived from the momentum and mass balance of a one-dimensional infinitely volume. FVM is developed and presented in (B. R. Sharefi, 2010), which is a method for representing physical behaviors inside the penstock as an alternate for solving the set of PDE. It divides the penstock into finite segments. For each segment, there is an ODE represents the conservation of mass and another ODE represents the conservation of momentum (H. K. Versteeg, 1995), instead of the PDE for the whole penstock. The purpose of introducing FVM is the discretized governing equations can retain their physical interpretation, rather than possibly distorting the physics (Chung, 2002), and somewhat reducing computation complexity. For applying this method, the penstock is ideally divided into $2N$ segments with identical length in the work. The first segment is from $i = 0$ to $i = 1$, where the last one is from $i = 2N - 1$ to $i = 2N + 1$. However, the discretized momentum equations have unrealistic behavior for behavior for spatially oscillating pressures (H. K. Versteeg, 1995). The solution to this possible problem, which is suggested in (H. K. Versteeg, 1995), is to use a so-called "staggered grid". Staggered grid is applied to define the volume determined by each couple of pipe segments located between $\mathrm{X_{2i+1}}$ and $\mathrm{X_{2i+3}}$ (for $i = 0, 1, 2, \dots, N - 2$) as a control volume for application of the momentum conservation and define the volume determined by each couple of pipe segments located between $\mathrm{X_{2i}}$ and $\mathrm{X_{2i+2}}$ as a control volume for application of the mass conservation.

2.2.1 Discretized continuity equation

Continuity equations are derived from the mass balance law to the control volumes enclosed between penstock segment $\mathrm{X_{2i}}$ and $\mathrm{X_{2i+2}}$ (for $i = 1, 2, \dots, N - 1$), (H. K. Versteeg, 1995). Mass balance here states that the rate of change of the fluid mass inside the control volume is equal to the difference between the mass flow, $\dot{m}$, into and out of the same control volume, which is presented with equation as:

$$\Delta x \frac{d}{dt}(\rho_{2i+1} A_{2i+1}) = \dot{m}_{2i} - \dot{m}_{2i+2} \qquad (2.30)$$

where the mass of fluid in any segment of penstock can be stated:

$$m_{2i+1} = \int_{X=X_{2i}}^{X_{2i+2}} \rho_{2i+1} A_{2i+1} dx = \rho_{2i+1} A_{2i+1} \Delta x \qquad (2.31)$$

For discrete system, the integral term is replaced by summation. The density and cross section of each segment are assumed constant. However, at the boundaries, for the continuity equation, the density is assumed as the average value of two adjacent volumes:

$$\rho_{2i+1} \cdot A_{2i+2} = \frac{(\rho_{2i+1} \cdot A_{2i+1} + \rho_{2i+3} \cdot A_{2i+3})}{2} \qquad (2.32)$$

Considering water elasticity, the pressure inside the penstock, p, can affect the water density, ρ. The relationship between them is presented with a fluid compressibility factor β:

$$\beta = \frac{1}{\rho} \cdot \frac{\partial \rho}{\partial p} \qquad (2.33)$$

Consequently, the water density at location i can be described as a term based on the atmosphere pressure:

$$\rho_{2i+1,2i+2} = \rho^{atm} \cdot e^{\beta(p_{2i+1,2i+2} - p^{atm})} \qquad (2.34)$$

Then, the left side of mass balance in (2.30) can be developed as in (2.35) at location $(2i+1)$:

$$\begin{aligned} \frac{d}{dt}(A_{p,2i+1} \cdot \rho_{2i+1}) &= \frac{d}{dp_{2i+1}}(A_{p,2i+1} \cdot \rho_{2i+1}) \cdot \frac{dp_{2i+1}}{dt} \\ &= \beta_p^{total} \cdot A_p^{atm} \cdot \rho^{atm} \cdot \frac{dp_{2i+1}}{dt} \end{aligned} \qquad (2.35)$$

Then, the mass balance in (2.30) turns into:

$$\Delta x \beta_p^{total} A_p^{atm} \rho^{atm} \frac{dp_{2i+1}}{dt} = \dot{m}_{2i} - \dot{m}_{2i+2} = \Delta x \cdot A_{p,2i} \cdot \rho_{2i} \cdot v_{p,2i} - \Delta x \cdot A_{p,2i+2} \cdot \rho_{2i+2} \cdot v_{p,2i+2} \quad (2.36)$$

where $i = 1, \dots, N-1$

2.2.2 Discretized momentum equation

The momentum conservation law is applied to the segment from point x_{2i+1} and x_{2i+3} (for $i = 0, 1, \dots, N-2$) for control volume CV_{2i+2}, which is stated as:

$$\int_{CV_{2i+2}} dm \cdot v = \int_{CV_{2i+2}} \ddot{m}\, dx = \ddot{m}_{2i+2} \cdot \Delta x \quad (2.37)$$

In this work, the velocity throughout segment $2i+1$ and $2i+3$, are assumed constant. According to the momentum balance, the rate of momentum in segment $2i+2$ is equal to the difference of the momentum flow in and flows out it, plus the force (F_p for pressure, F_G for gravity, F_F for friction) applied to the segment:

$$\Delta x \cdot \frac{d\dot{m}_{2i+2}}{dt} = \dot{m}_{2i+1} v_{2i+1} - \dot{m}_{2i+3} v_{2i+3} + F_{p,2i+2} + F_{G,2i+2} + F_{F,2i+2} \quad (2.38)$$

where

$$F_{p,2i+2} = A_{2i+2} \cdot (p_{2i+1} - p_{2i+3}) \quad (2.39)$$

$$F_{G,2i+2} \cong \Delta x \cdot A_{(2i+2)} \cdot \rho_{2i+2} \cdot g \cdot \sin\theta \quad (2.40)$$

$$H_{loss} = f_r \cdot \frac{L}{D} \cdot \frac{\bar{v} \cdot |\bar{v}|}{2g} = f_r \cdot \frac{L}{D} \cdot \frac{\bar{Q} \cdot |\bar{Q}|}{2g \cdot A^2} \quad (2.41)$$

$$\begin{aligned} F_{F,2i+2} &= -\rho_{2i+2} \cdot g \cdot H_{loss} \cdot A \\ &= -f_r \cdot \frac{\Delta x}{D} \cdot \frac{Q|Q|}{A} \cdot \frac{1}{2} \cdot \rho_{2i+2} \\ &= -\frac{1}{2} f_r \cdot \frac{\Delta x}{D} \cdot \rho_{2i+2} |Q_{2i+2}| \cdot v_{2i+2} \\ &= \varepsilon_{fr} \cdot v_{2i+2} \end{aligned} \quad (2.42)$$

where $$\varepsilon_{fr} = -\frac{1}{2} \cdot f_r \cdot \frac{\Delta x}{D} \cdot \rho_{2i+2} |Q_{2i+2}| \quad (2.43)$$

The momentum balance can be written as:

$$\begin{aligned} \Delta x \cdot \frac{d\dot{m}_{2i+2}}{dt} = {} & \dot{m}_{p,2i+1} \cdot v_{2i+1} - \dot{m}_{p,2i+3} \cdot v_{p,2i+2} + F_{G,2i+2} + F_{p,2i+2} \\ & + \varepsilon_{fr} \cdot v_{2i+2} \end{aligned} \quad (2.44)$$

If the velocities are positive at the boundaries of the control volume, using the upwind difference scheme

$$\dot{m}_{p,2i+1} = \frac{\dot{m}_{p,2i} + \dot{m}_{p,2i+2}}{2} \quad (2.45)$$

$$\dot{m}_{p,2i+3} = \frac{\dot{m}_{p,2i+2} + \dot{m}_{p,2i+4}}{2} \quad (2.46)$$

And according the upwind scheme, the $v_{p,2i+1}$ and $v_{p,2i+3}$ in (2.44) be replaced with $v_{p,2i}$, and $v_{p,2i+2}$ respectively. Then:

$$\Delta x \cdot A_{p,2i+2} \cdot \rho_{2i+2} \cdot \frac{dv_{p,2i+2}}{dt} + \left(\frac{\dot{m}_{p,2i} + \dot{m}_{p,2i+2}}{2} - \varepsilon_{fr,2i+2}\right) \cdot v_{p,2i+2} = \frac{\dot{m}_{P,2i} + \dot{m}_{P,2i+2}}{2} \cdot v_{p,2i+1} + F_{G,2i+2} + F_{p,2i+2} \quad (2.47)$$

which satisfies Scarborough's condition for stability (H. K. Versteeg, 1995) [p. 112].

If the velocities are negative at the boundaries of the control volume, according the upwind scheme, the $v_{p,2i+1}$ and $v_{p,2i+3}$ in (2.44) be replaced with $v_{p,2i+2}$and $v_{p,2i+4}$. Then:

$$\Delta x \cdot A_{p,2i+2} \cdot \rho_{2i+2} \cdot \frac{dv_{p,2i+2}}{dt} + \left(-\frac{\dot{m}_{p,2i+2} + \dot{m}_{p,2i+4}}{2} - \varepsilon_{fr,2i+2}\right) \cdot v_{p,2i+2} = \left(-\frac{\dot{m}_{p,2i+2} + \dot{m}_{p,2i+4}}{2}\right) \cdot v_{p,2i+1} + F_{G,2i+2} + F_{p,2i+2} \quad (2.48)$$

In another situation, if one velocity is positive and the other is negative, the term of transported momentum can be ignored. Then:

$$\Delta x \cdot A_{p,2i+2} \cdot \rho_{2i+2} \cdot \frac{dv_{p,2i+2}}{dt} - \varepsilon_{fr,2i+2} \cdot v_{p,2i+2} = F_{G,2i+2} + F_{p,2i+2} \quad (2.49)$$

2.3 Electrical equivalent circuit of method

If neglecting the advective terms, the PDE set of penstocks can be reorganized as:

$$\frac{\partial H}{\partial x} + \frac{1}{g \cdot A} \cdot \frac{\partial Q}{\partial t} + \frac{f_r \cdot |Q|}{2g \cdot D \cdot A^2} \cdot Q = 0 \quad (momentum) \quad (2.50)$$

$$\frac{\partial H}{\partial t} + \frac{a^2}{g \cdot A} \cdot \frac{\partial Q}{\partial x} = 0 \quad (continuity) \tag{2.51}$$

It is very similar to the mathematical model of a RLC circuit with the basic idea of treating the hydraulic components equivalent to electrical elements. The equations of the traveling wave in a transmission line are presented in (J. Robert Eaton, 1983) as below, which neglects the shunt conductance of the transmission line. Dividing the penstock into several segments. For each segment, the following RLC equations, (2.52) and (2.53) can represent the momentum and continuity equations in (2.50) and (2.51).

$$L \cdot \frac{\partial i}{\partial t} + \frac{\partial u}{\partial x} + R \cdot i = 0 \tag{2.52}$$

$$C \cdot \frac{\partial u}{\partial t} + \frac{\partial i}{\partial x} = 0 \tag{2.53}$$

In this work, the penstock is assumed uniform. There is no consideration for varying of volume flow, pressure or friction loss due to cross section change.

Defining:

$$L_0 = \frac{1}{g \cdot A} \tag{2.54}$$

$$R_0 = \frac{f_r \cdot |Q|}{2g \cdot D \cdot A^2} \tag{2.55}$$

$$C_0 = \frac{g \cdot A}{a^2} \tag{2.56}$$

With regard to reduce complexity during the calculations, the volume flow in R_0 is considered as the average flow throughout the segment at last time interval. For each segment, the PDE set of penstocks can be written as:

$$L_0 \cdot \frac{\partial Q}{\partial t} + \frac{\partial H}{\partial x} + R_0 \cdot Q = 0 \quad (2.57)$$

$$C_0 \cdot \frac{\partial H}{\partial t} + \frac{\partial Q}{\partial x} = 0 \quad (2.58)$$

Approximating:

$$\left.\frac{\partial H}{\partial x}\right|_{i+\frac{1}{2}} = \frac{H_{i+1} - H_i}{\Delta x} \quad (2.59)$$

$$\left.\frac{\partial Q}{\partial x}\right|_{i+\frac{1}{2}} = \frac{Q_{i+1} - Q_i}{\Delta x} \quad (2.60)$$

where $i = 1, \dots, N+1$; N is the total amount of divided pipe segments.

Then, altering equation (2.57) and (2.58) to ODE:

$$L_0 \cdot \frac{dQ_{i+\frac{1}{2}}}{dt} + R_0 \cdot Q_{i+\frac{1}{2}} + \frac{H_{i+1} - H_i}{\Delta x} = 0 \quad (2.61)$$

$$C_0 \cdot \frac{dH_{i+\frac{1}{2}}}{dt} + \frac{(Q_{i+1} - Q_i)}{\Delta x} = 0 \quad (2.62)$$

Assume:

$$Q_{i+\frac{1}{2}} = \frac{Q_{i+1} + Q_i}{2} \quad (2.63)$$

Equation (2.61) and (2.62) become:

$$C_0 \cdot \Delta x \cdot \frac{dH_{i+\frac{1}{2}}}{dt} = -(Q_{i+1} - Q_i) \quad (2.64)$$

$$H_{i+1} + \frac{L_0}{2} \cdot \Delta x \cdot \frac{dQ_{i+1}}{dt} + \frac{R_0}{2} \cdot \Delta x \cdot Q_{i+1} = H_i - \frac{L_0}{2} \cdot \Delta x \cdot \frac{dQ_i}{dt} - \frac{R_0}{2} \cdot \Delta x \cdot Q_i \quad (2.65)$$

Correspondingly, equivalent circuit can be described as either in Figure 4 or in Figure 5:

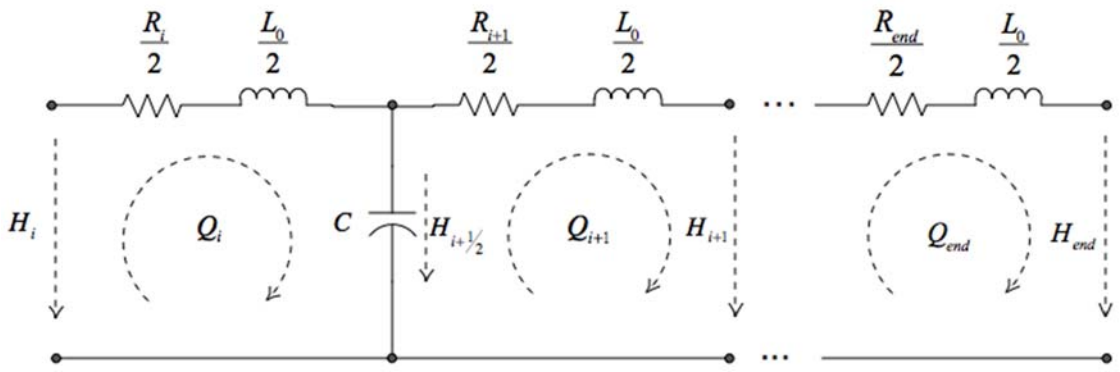

Figure 4. Equivalent circuit diagram for PDEs for a penstock

Or:

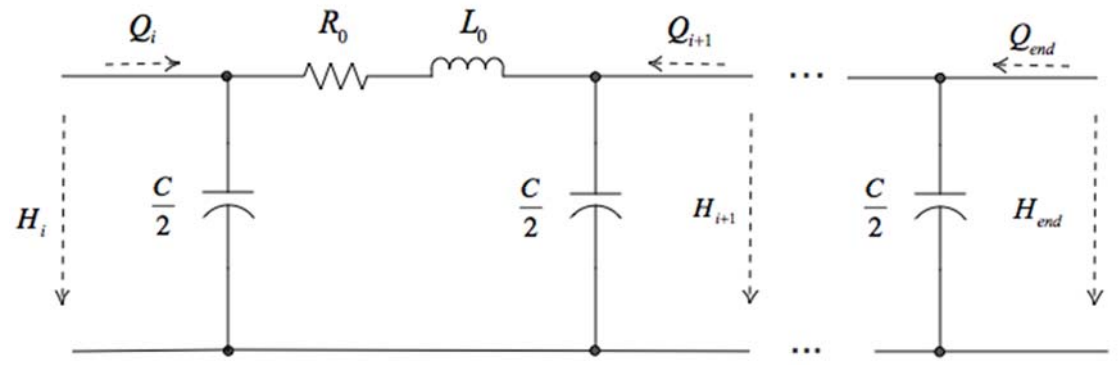

Figure 5. Alternative equivalent circuit diagram for PDEs for a penstock

According to the equivalent circuits shown two above figures, the penstock model can be represented with several ODEs:

$$\frac{L_0}{2}\cdot\Delta x\cdot\frac{dQ_i}{dt}+\frac{R_0}{2}\cdot\Delta x\cdot Q_i+H_{i+\frac{1}{2}}-H_i=0 \qquad (2.66)$$

$$\frac{L_0}{2}\cdot\Delta x\cdot\frac{dQ_{i+1}}{dt}+\frac{R_0}{2}\cdot\Delta x\cdot Q_{i+1}-H_{i+\frac{1}{2}}+H_{i+1}=0 \qquad (2.67)$$

$$C_0\cdot\Delta x\cdot\frac{dH_{i+\frac{1}{2}}}{dt}=-(Q_{i+1}-Q_i) \qquad (2.68)$$

The volume flow and water head at the outlet of penstock are equal to those values at the inlet of hydraulic turbine. By neglecting pressure loss within turbine, it can be stated:

$$Q_{end} = Q_{p\_out} = k_g \cdot G \cdot A_p \cdot \sqrt{2 \cdot g \cdot H_{net}} \quad (2.69)$$

$$H_{end} = H_{p\_out} = H_{net} + H_{S2} \quad (2.70)$$

2.4 Method of characteristic

Method of characteristic (MOC) is a popular method for calculation of the hydraulic transients in pipeline due to its simplicity and superior performance in comparison with other methods (M.H. Afshar, 2009). The basic idea of this method is to use a characteristic line, which is upon to time and extension direction of the pipe, to describe the dynamic equations with ordinary differential equations of the pipe that is parted to several segments. For each internal point of the pipe, the pressure and volume flow can be represented with the values at up and down neighbour points.

One premises for developing ODEs for modeling hydraulic transient of pipeline is, which is different than any method else, the length of every segment should be eligible to the following condition in (2.71):

$$\frac{\Delta x}{\Delta t} = a \quad (2.71)$$

2.4.1 Formulation

The characteristic lines are shown in Figure 6:

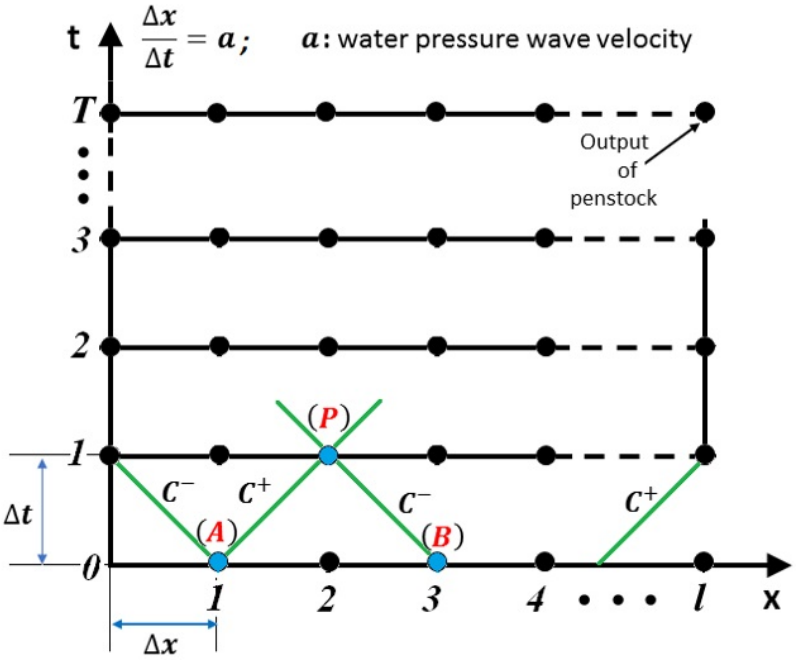

Figure 6 Illustration MOC method principle

When it is on positive characteristic line C^+:

$$\frac{dx}{dt} = a \tag{2.72}$$

When it is on negative characteristic line C^-:

$$\frac{dx}{dt} = -a \tag{2.73}$$

The total derivatives of H and Q are:

$$\frac{dH}{dt} = \frac{\partial H}{\partial x} \cdot \frac{dx}{dt} + \frac{\partial H}{\partial t} \tag{2.74}$$

$$\frac{dQ}{dt} = \frac{\partial Q}{\partial x} \cdot \frac{dx}{dt} + \frac{\partial Q}{\partial t} \tag{2.75}$$

If it is along the positive characteristic line, the momentum equation (2.50) multiply a and plus continuity equation (2.51), we can get:

$$\left(\frac{\partial H}{\partial t}+a\cdot\frac{\partial H}{\partial x}\right)+\frac{a}{g\cdot A}\cdot\left(\frac{\partial Q}{\partial t}+a\cdot\frac{\partial Q}{\partial x}\right)+a\cdot\frac{f_r\cdot|Q|}{2g\cdot D\cdot A^2}\cdot Q=0 \qquad (2.76)$$

It can be rewritten as:

$$\left(\frac{\partial H}{\partial t}+\frac{dx}{dt}\cdot\frac{\partial H}{\partial x}\right)+\frac{a}{g\cdot A}\cdot\left(\frac{\partial Q}{\partial t}+\frac{\partial x}{\partial t}\cdot\frac{\partial Q}{\partial x}\right)+a\cdot\frac{f_r\cdot|Q|}{2g\cdot D\cdot A^2}\cdot Q=0 \qquad (2.77)$$

If it is along the negative characteristic line, momentum equation (2.50) multiply a and minus continuity equation (2.51) we can have:

$$-\left(\frac{\partial H}{\partial t}-a\cdot\frac{\partial H}{\partial x}\right)+\frac{a}{g\cdot A}\cdot\left(\frac{\partial Q}{\partial t}-a\cdot\frac{\partial Q}{\partial x}\right)+a\cdot\frac{f_r\cdot|Q|}{2g\cdot D\cdot A^2}\cdot Q=0 \qquad (2.78)$$

It can be rewritten as:

$$\left(\frac{\partial H}{\partial t}+\frac{dx}{dt}\cdot\frac{\partial H}{\partial x}\right)-\frac{a}{g\cdot A}\cdot\left(\frac{\partial Q}{\partial t}+\frac{dx}{dt}\cdot\frac{\partial Q}{\partial x}\right)-a\cdot\frac{f_r\cdot|Q|}{2g\cdot D\cdot A^2}\cdot Q=0 \qquad (2.79)$$

Using the total derivatives to replace the partial derivative terms, then the characteristic equation becomes:

$$C^+:\ \frac{dH}{dt}+\frac{a}{g\cdot A}\cdot\frac{dQ}{dt}+\frac{dx}{dt}\cdot\frac{f_r\cdot|Q|}{2g\cdot D\cdot A^2}\cdot Q=0 \qquad (2.80)$$

$$C^-:\ \frac{dH}{dt}-\frac{a}{g\cdot A}\cdot\frac{dQ}{dt}+\frac{dx}{dt}\cdot\frac{f_r\cdot|Q|}{2g\cdot D\cdot A^2}\cdot Q=0 \qquad (2.81)$$

According to characteristic grids, simply assuming the volume flow along the C^+ and C^- are constant, discretize the equations above taking the point (P), referring to Figure 6, as an example, it arrives:

$$C^+:\ H_{(P)}-H_{(A)}+C_M\cdot\left(Q_{(P)}-Q_{(A)}\right)+R_M\cdot Q_{(A)}\cdot\left|Q_{(A)}\right|\cdot\Delta x=0 \qquad (2.82)$$

$$C^-:\ H_{(B)}-H_{(P)}-C_M\cdot\left(Q_{(B)}-Q_{(P)}\right)+R_M\cdot Q_{(B)}\cdot\left|Q_{(B)}\right|\cdot\Delta x=0 \qquad (2.83)$$

where:

$$R_M = \frac{f_r}{2 \cdot g \cdot D \cdot A^2} = \frac{8 f_r}{g \cdot \pi^2 \cdot D^5} \quad (2.84)$$

$$C_M = \frac{a}{g \cdot A} \quad (2.85)$$

Because all the values, at last time interval, are known, defining the following constants:

$$C_{pos} = H_{(A)} + C_M \cdot Q_{(A)} - R_M \cdot Q_{(A)} \cdot \left|Q_{(A)}\right| \cdot \Delta x \quad (2.86)$$

$$C_{neg} = H_{(B)} - C_M \cdot Q_{(B)} + R_M \cdot Q_{(B)} \cdot \left|Q_{(B)}\right| \cdot \Delta x \quad (2.87)$$

The characteristic equations become:

$$C^+: \; H_{(P)} - C_{pos} + C_M \cdot Q_{(P)} = 0 \quad (2.88)$$

$$C^-: \; H_{(P)} - C_{neg} - C_M \cdot Q_{(P)} = 0 \quad (2.89)$$

Then, the water head and volume flow at point (P) can be solved as:

$$H_{(P)} = \frac{C_{pos} + C_{neg}}{2} \quad (2.90)$$

$$Q_{(P)} = \frac{C_{pos} - C_{neg}}{2 C_M} \quad (2.91)$$

In the same way, all the knot points, except the boundary points, shown in Figure 6 can be calculated.

2.4.2 Boundary conditions

The first point of the characteristic grid is located at the inlet of the penstock. The pressure of it, H_1 , is equal to the outlet pressure of the upstream hydraulic element, H_{s1} , which can be surge tank or reservoir. In this work:

$$H_1 = H_{s1} \quad (2.92)$$

Applying it to the C^- equation (2.89), since it hits the first point:

$$Q_1 = \frac{H_1 - C_{neg}}{C_M} \quad (2.93)$$

Similarly, the volume flow at the outlet of the penstock, Q_{end} , is equal to the inlet flow of turbine, Q_{dis}:

$$Q_{end} = Q_{dis} = k_g \cdot G \cdot A_p \cdot \sqrt{2 \cdot g \cdot H_{net}} \quad (2.94)$$

Applying it to the C^+ equation (2.88), since it hits the ending point. Neglecting head loss within turbine, the water head at the ending point, H_{end} , is:

$$H_{end} = C_{pos} - C_M \cdot Q_{end} = H_{net} + H_{S2} \quad (2.95)$$

2.5 Results

In this work, no matter which modeling method is applied for the penstock, the mathematical models of the other parts are all the same. This is due to the necessity of including water elasticity. If the hydraulic element of such a plant is an open volume, under a macroscopic scale of developing controller for mechanical power, it is not demanded deeply to see the transients because of water internal elasticity. However, if it is a closed volume, such as a penstock, the effect of transient pressure will be more significant. In this section, the simulations are carried out without considering the generator side. It is focusing the modeling of mechanical power and presuming all the mechanical power is transferred to electrical power.

The initial conditions and parameter settings are identical for all the models in order to compare their outputs. The applied modeling simulation conditions and parameter settings are given in Table 1 and

Table 2 . To generate some dynamics, the hydraulic turbine gate was closed from 50% to 35% at 200th second.

Table 1: Modeling simulation initial conditions

Variable:	***Value:***	***Unit:***
G	50	%
P_m	85	Mw
Q_{C1}	30	m^3/s
Q_{C2}	30	m^3/s
Q_{s1_out}	30	m^3/s
Q_{s2_out}	30	m^3/s
H_{s1}	344	m
H_{s2}	11	m
H_r	350	m
H_T	10	m

Table 2: Modeling simulation parameter settings

Data:	***Value:***	***Unit:***
Simulation Period	500	s
Simulation step	0.1	s
L_{c1}	4000	m
D_{c1}	7	m
D_{s1}	15	m
L_{c2}	1000	m
D_{c2}	7	m
D_{s2}	10	m
L_p	1100	m
D_p	2.5	m
a	1100	m/s
f_r	0.05	dimensionless
η	0.9	dimensionless

Data:	***Value:***	***Unit:***
k_g	0.0016	dimensionless
ρ	1000	kg/m^3

As it is shown in Figure 7 and Figure 8, the simulations results of different modeling methods illustrate very similar characteristic responses on 'water head before turbine' and 'mechanical power' when implementing equivalent turbine operations for the same hydropower plant, but they end with different steady state values. This is mainly due to the differences of their modeling algorithms. The simple method gave the highest power production while the least water head loss, which lead to a more reactive inverse pressure response than the other methods when closing the turbine gate. The pressure rise increased to around 355m water head, which is approximate 15m higher than FVM and EEC, and about 20m higher than MOC. It is caused probably by simplification of the penstock PDE model with one dimensional ODE for a pseudo plane area. Apparently, this method introduced less complexity, but more imprecision with regards to energy loss due to friction is considered as for a one-segment penstock. The other three methods, MOC, EEC and FVM gained comparable results. All of them divided the penstock into several segments, and deployed the finite ordinary differential equations to represent partial differential equations. Comparing results of EEC and MOC, which are broadly alike with each other's, if using $\frac{dx}{dt} = a$ to replace dx or dt in (2.66) to (2.68) of EEC, it will be very close to (2.80) or (2.81) of MOC. However, EEC and FVM used ODE solver in Appendix C, instead of approaching $\frac{dH}{dt}$ by $\frac{H_{(A)}-H_{(P)}}{\Delta t}$ as MOC, they derived results with higher power generation and higher water head. Aside of MOC or EEC, FVM considered the density variation depending on pressure along the penstock as described in (2.34), so FVM got the lowest water head in the steady state before turbine closing. However, its water head is the second lowest but higher than MOC in post steady state. This would be an effect of linear approaching derivatives in MOC method. It is hard to say which method is better without examining against with real measurements.

However, any of them can be adapted to simulate the real plant. The model fitting can be carried out by, e.g. modifying the friction factor, which is not completely certain since the internal material and condition of penstock varies. From the perspective of developing NMPC, as long as it reflects homogeneous behaviour of a hydropower plant with other relatively sophisticated methods, the simple method appears to have a slight advantage in aspect of saving computational cost when it comes to compounded algorithm of NMPC.

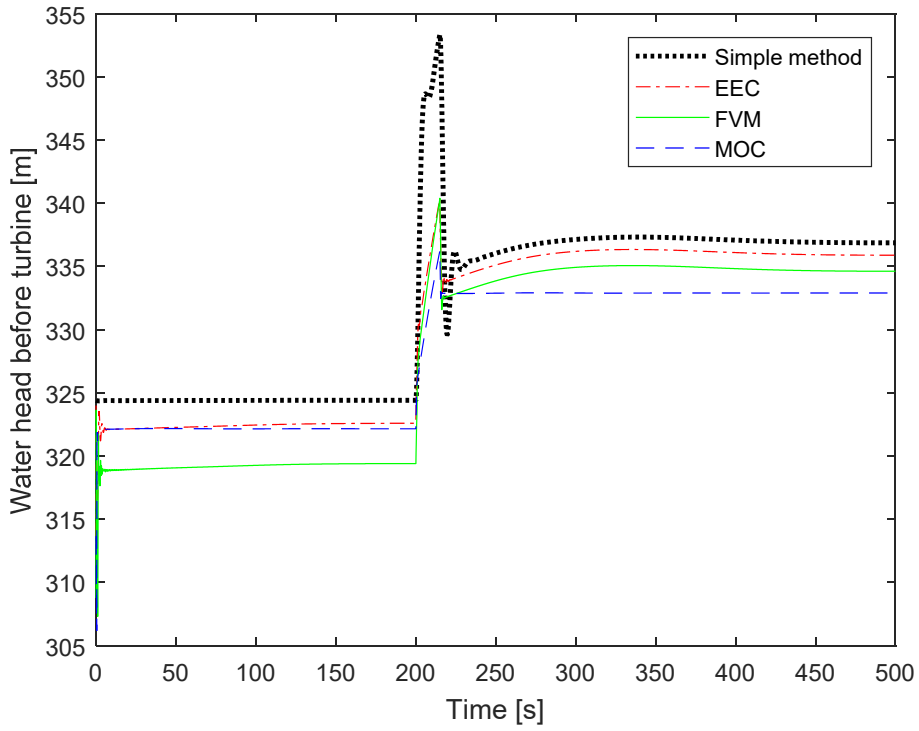

Figure 7. Simulation results of water head before turbine using different modeling methods

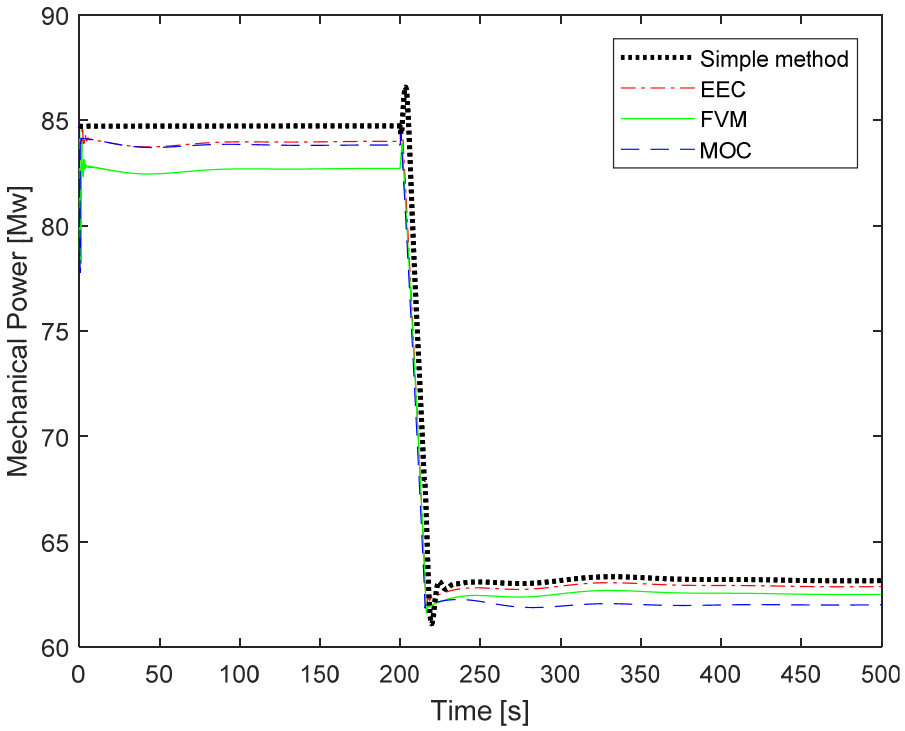

Figure 8. Simulation results of mechanical power using different modeling methods

3 Control of hydropower plant

To control the production of a hydropower plant, two aspects needs to be taken into account. One is controlling the water inputs to the plant, which is in terms of mechanical power regulation. The other is controlling the electrical outputs, which is in terms of regulation of frequency and terminal voltage. This work is primarily focusing on the regulation of mechanical power. Nevertheless, the traditional controller is simulated and presented for both turbine and generator control as for the basis of further comparison. The nonlinear controller is developed afterwards for turbine input water regulation. Different scenarios of using NMPC are performed for single-unit plant and multi-unit plant. Its advantage for handling various situations has been demonstrated and discussed in this chapter.

3.1 Traditional controller

This section describes the traditional control of hydropower plants. The modeling from the previous chapter results in a MIMO system, the mechanical power from water and excitation voltage of synchronous machine are the inputs, while the frequency and voltage are the outputs in this system. A traditional PI controller combining Droop control method is implemented with this model for frequency and another controller for voltage. The working process of this interacting and controlled MIMO system working process is shown in Figure 9.

3.1.1 Frequency control

The frequency control is also called speed/torque control or the active power control. The controller is meant to keep the rotational speed of turbine-generator unit stable and constant at any grid load to maintain the frequency. Besides, it should also respond to any change of electrical power.

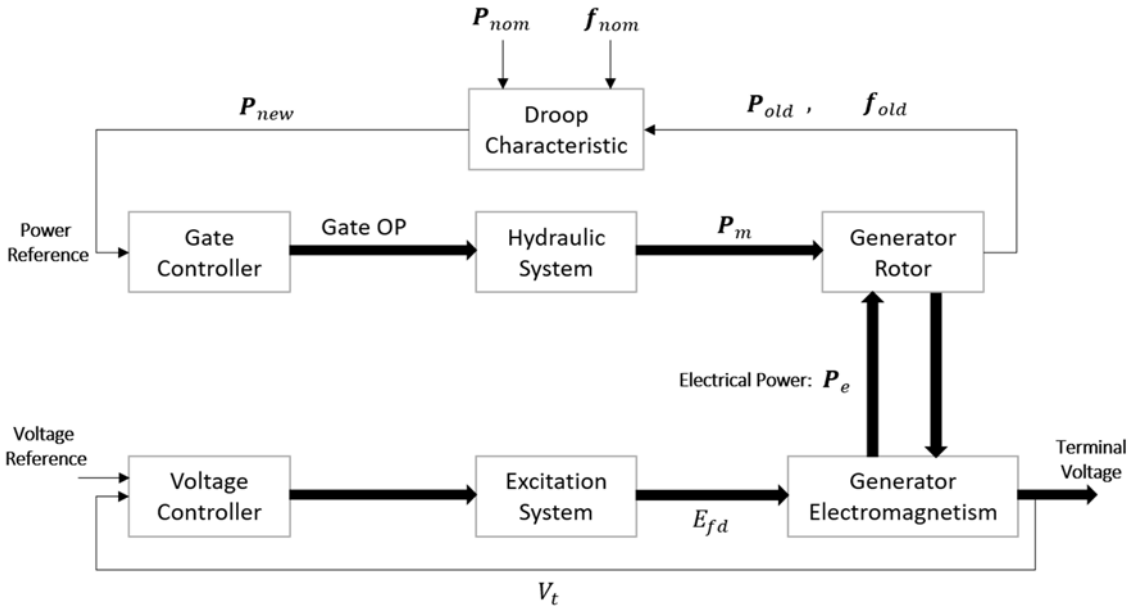

Figure 9. Flow chart of a controlled MIMO hydropower plant

When a real hydropower plant is connected to an isolated load, in case of a load decrease, the excess power will accelerate the rotation of the turbine. Then the controller should reduce turbine speed by closing the turbine gate. In the meanwhile, considering avoiding too much pressure rise caused by closing as observed in the simulation results that shown in Figure 7, the closing rate, G , should be limited. To fulfil these two demands, a PI controller with step change limit is a traditional solution in hydropower industry. Assuming the generator is a single machine connected to infinite bus, the PI controller is usually implemented with a Droop characteristic, D_r , which is a commonly used method to decide how much a single machine should contribute to the network at present, for active power, $\boldsymbol{P}$, and frequency, f. The Droop relationship (Sluis, 2008) for them is described as:

$$\frac{\Delta f}{f_{nom}} = -Dr \cdot \frac{\Delta \boldsymbol{P}}{\boldsymbol{P}_{nom}} \qquad (3.1)$$

At every simulation control interval, the function of Droop control will calculate the frequency variation, $f_{new} - f_{old}$, and obtain a reference power, $\boldsymbol{P}_{ref}$, for PI controller:

$$\begin{cases} \boldsymbol{P}_{new} = -\frac{1}{Dr} \cdot \frac{f_{new} - f_{old}}{f_{nom}} \cdot \boldsymbol{P}_{nom} + \boldsymbol{P}_{old} \\ \boldsymbol{P}_{ref} = \boldsymbol{P}_{new} \end{cases} \quad (3.2)$$

3.1.2 Voltage Control

The voltage control was carried out with the generator excitation system using a controller with a stabilizer. The controller was embedded in the second order model of exciter, which is shown in (2.27). The purpose of the controller is to hold the terminal voltage magnitude of a synchronous generator at a specific value. An increase in reactive power load of the generator should be accompanied by a drop in the terminal voltage magnitude. This voltage is rectified and compared to a setpoint signal. The difference between them is the input into the controller which controls the exciter field and increases the exciter voltage. Thus, when the generator field current is increased it will result in an increase of the generated voltage (H.L.Zeynelgi, 2002).

3.2 State estimation

State estimation is introduced in the control part of this work, since a traditional hydropower plant may lack physical sensors for monitoring and feedback to the control loops. A Kalman filter has been developed per this purpose, details refer to Appendix A3.

According to the working condition at a hydropower plant, the pressure in the penstock is most critical state to be estimated and be predicted. The reason is that if the hydraulic turbine is shut down abruptly, the pressure will rise to a very high value that may damage the hydraulic turbine or penstock. This inverse pressure response is described as water hammer in hydropower industry (Wahba, 2009) and presented in Figure 7, which can occur too quickly to respond, thus monitoring and prediction of it are required to secure the plant. As reported by research practice of Fjone power plant, there is only one single pressure meter functioning with this purpose, and there is no back-up

monitoring physically placed. In case of this single meter fails, the state estimation is suggested as in Appendix A3.

3.3 NMPC for a single-unit hydropower plant

3.3.1 Algorithm

MPC is a popular advanced control technique for industry during recent decades. In principle, MPC is an optimization process to minimize an object function that synthesizes cost of control actions and predicted process output deviations from the reference values. There is a prediction horizon N_p and a control horizon N_c in a typical MPC algorithm. The model predictions are carried out using internal model based, thoroughly along the prediction horizon, under the responses of a trajectory of control actions that are calculated by the optimization process just mentioned. The control horizon is for defining how many control actions ought to be worked out, so that process outputs are closest to or equal to references. Generally, control horizon is shorter than the prediction horizon, since it makes no sense to predict a process is still under controlling. At every control interval, only the first control action, which is calculated out by the optimization process, is applied to the plant. As well as the optimization process is repeated at every control interval. The scheme of NMPC is the same as MPC but with a nonlinear internal mode. Some constraints are considered as industry practical and consisted in optimization procedure that minimizes an object function that returns the difference between predicted process trajectory and the reference value. At next control step, it repeats the procedure and computes a new control trajectory.

Then, a basic NMPC working procedure at each control step n would be (L. Grüne, 2011):

- Measure the state $x(n)$ that is the control target. In this case, the corresponding system output is $y(n)$.

- Set the system initial output $y_0 = y(n)$, solve an optimal control problem, which is the object function in next section 3.3.2, and denote, U, as the obtained optimal control trajectory.
- Define the NMPC output value, $u = U(1)$, and use this control value in the next sampling period.

3.3.2 Cost function

The nonlinear process can be formulated with state space form as discrete form:

$$x(k+1) = f\big(x(k), u(k), d(k)\big), \quad x(0) = x_0 \tag{3.3}$$

$$y(k+1) = h(x(k+1), v(k)) \tag{3.4}$$

In the equations above, x is process variable, y is the plant output, u is manipulated variable, d is measured disturbance, v is unmeasured disturbance. d and v are neglected in the simple model derived in Chapter 2. The basic NMPC algorithm, which is expressed in equation (3.5), states clearly the general control purpose, to track the reference value. Furthermore, normally, with optimization process, NMPC works out a series control actions that fulfil the purpose of tracking reference and reducing the cost with least system consumptions at the same time. The cost function, $\boldsymbol{J}$, can be seen from the discrete mathematical expression below:

$$Minimize: \boldsymbol{J} = \sum_{i=0}^{N_p} [y(k+i) - r(k+i)^2] + \lambda \cdot \sum_{j=i}^{N_c} [\Delta u(k+j-1)]^2 \tag{3.5}$$

Where N_c is the control horizon and N_p is the prediction horizon; λ is the weighting parameter. With (3.4), the prediction of future outputs can be obtained. There are usually some offsets in plant measurements comparing with the mathematical model. To implement a mismatch plant model, a steady state error, e_{mis}, is added to process outputs, y, in mathematical model for plant, which distinguish the plant model from

internal model of NMPC. In this way, if only depending on internal model predictions, the calculated control action cannot make the process output tracking the reference. To cope with the mismatch, a corrector is accomplished to modify the reference. At every control interval, the plant process output vector y is measured and sent to the corrector. The internal model provides an output vector $\hat{y}$ under the same operation circumstance with the knowledge of all the process states, which can be measured or estimated. A mismatch error vector can be detected as:

$$e_{mis} = \hat{y} - y \tag{3.6}$$

To compensate this mismatch error, e_{mis}, a corrector is made. A filtered discrepancy (3.7) is implemented for correction (P. Potocnik, 2002):

$$\beta(k) = \phi \cdot e_{mis} + (1 - \phi) \cdot \beta(k-1) \tag{3.7}$$

where $\phi \in [0, 1]$ determines the filter setting. β is added to correct the reference, r, as:

$$r_c(k+i) = r(k+i) + \beta(k) \tag{3.8}$$

where r_c is corrected reference.

This correction is modified and replaces the reference, r, in cost function (3.5) during horizon $[0, N_p]$. Then the cost function can be rewritten as:

$$Minimize: \boldsymbol{J} = \sum_{i=0}^{N_p} [y(k+i) - r_c(k+i)]^2 + \lambda \cdot \sum_{j=1}^{N_c} [\Delta u(k+j-1)]^2 \tag{3.9}$$

3.3.3 Constraints

There are always practical constraints for a real process, like the range of the control variable, u, and the gradient of it, Δu, because of the mechanical structure of the actuator. The constrains for u and Δu are given in (3.10) and (3.11) respectively. Except for these normal constraints, there are also special constraints for hydropower plant. As

mentioned above, the production flow rate,Q, cannot be over the scheduled admission flow that is discharged from the reservoir. The constrains for the Q is given in (3.12).

$$u_{min} \leq u(k) \leq u_{max} \quad (3.10)$$

$$-\Delta u_{max} \leq \Delta u(k) \leq \Delta u_{max} \quad (3.11)$$

$$Q_{min} \leq Q \leq Q_{max} \quad (3.12)$$

Another inequality constraint is the pressure, p, or the water head, H, in the penstock, as given in (3.13):

$$p_{min} \leq p \leq p_{max} \quad or \quad H_{min} \leq H \leq H_{max} \quad (3.13)$$

A reverse pressure response happens when the hydraulic turbine is in motion, which is also entitled as water hammer (Wahba, 2009), in some circumstances. This characteristic response of hydropower is proved possible to be estimated in (W. Zhou B. G., 2012). Concerning safety, this pressure should not be too high that it may damage the turbine or penstock. With the purpose of coping with this problem, the closing movement of the hydraulic turbine is constrained with a maximum rate in the hydropower industry. But even in the same plant, when the pressures across the turbine are different, for example when the upstream and downstream reservoir level is varying, with a constrained closing rate, the highest pressure happens before the turbine would be different. This is demonstrated in Figure 10. The hydraulic turbine is closed from 80% to 65% at 100th second with the closing rate 1% per second for both two cases. With the identical initial conditions and 10m downstream level, when the upstream reservoir level is 357m, the highest pressure in penstock is around 34.36bar, while it is around 32.97bar when the upstream level is 347m. The reservoir level can change because of the seasons and rainfall. The pressure across the turbine also can vary when

encountering different operations. This proves the traditional PI controller with a constrained closing rate cannot adaptive to for all these situations.

Furthermore, constraining the closing rate also constraints the speed of generation to track the reference value. It somehow reduces the production efficiency. One remarkable advantage of NMPC is its ability to handle various constraints. For the sake of maintaining production and avoiding high pressure at the same time, a straightforward pressure constraint is added to the optimization process. The control signal of the NMPC is automatically divided with small steps when it is risk to approach the pressure limit. Those steps are not assigned with fix highest values, but a shifty and tolerated value that can abide to pressure constraint, which is illustrated and compared with the traditional way in Figure 11, Figure 12, Figure 13. The closing rate of hydraulic turbine is also limited by its mechanical structure. The corresponding highest speed is set as 5% per second in this work. This speed limit is assigned to both NMPC and PI. An extreme situation is simulated to test the function of the two controllers for handling pressure constraint. The pressure that the turbine or penstock can endure is set to 300m water head, or 29.41bar, which is a very small value and not realistic. The permitted max speed of PI controller is 3% per second for reverse pressure consideration. In this simulation, the power generation setpoint is changed from 60Mw to 55Mw at 20^{th} second. The PI parameters here are only valid for this simulation, and certainly differs from values used in real hydropower plants.

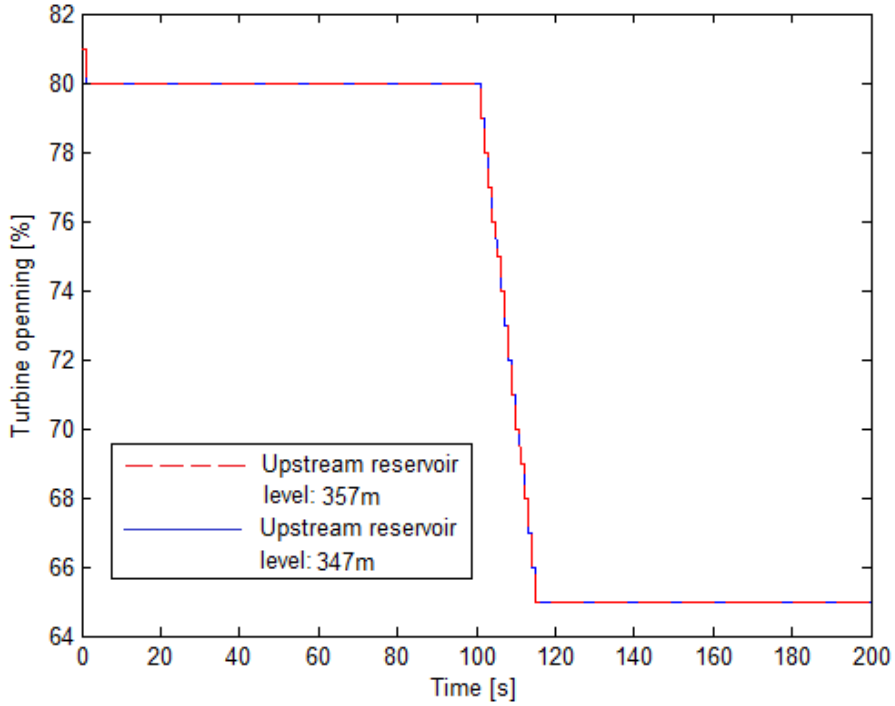

(a)

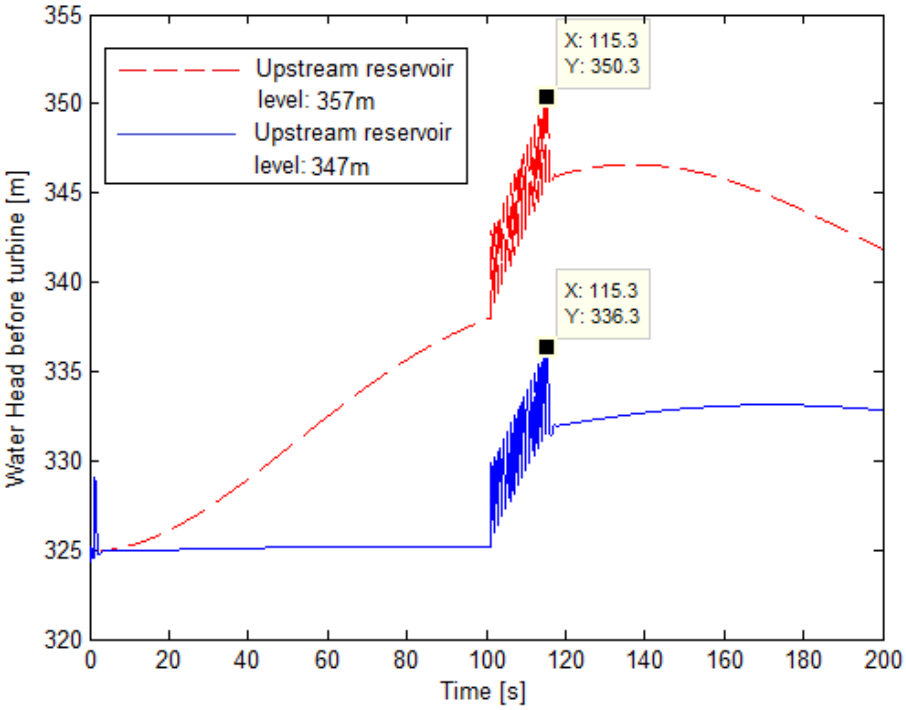

4

(b)

Figure 10. Turbine opening (a) and pressure response (b) according to different upstream reservoir level

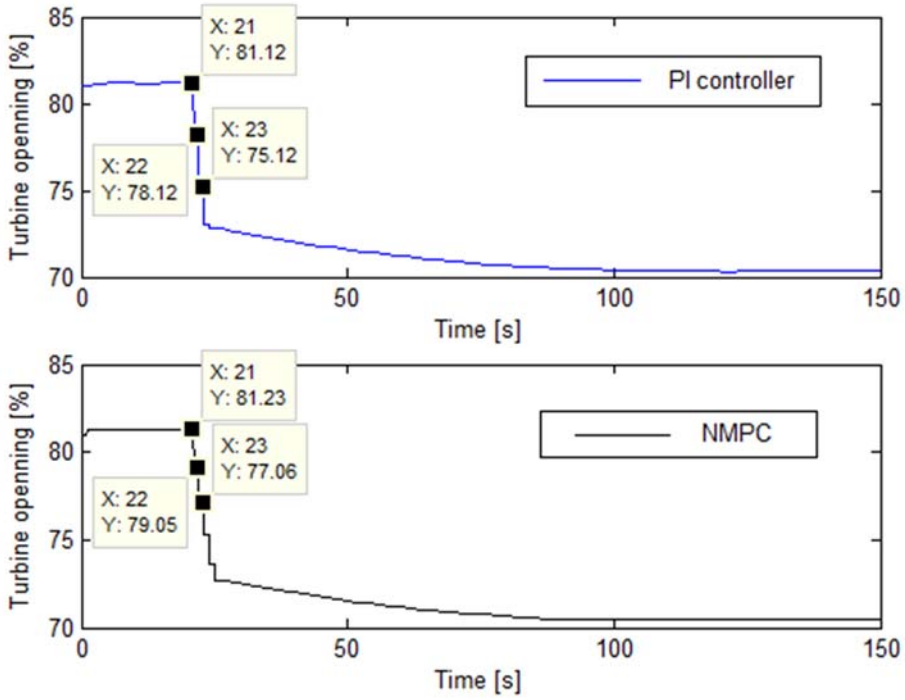

Figure 11. Turbine movements comparison when pressure constraint is 29.14 bar or 300m

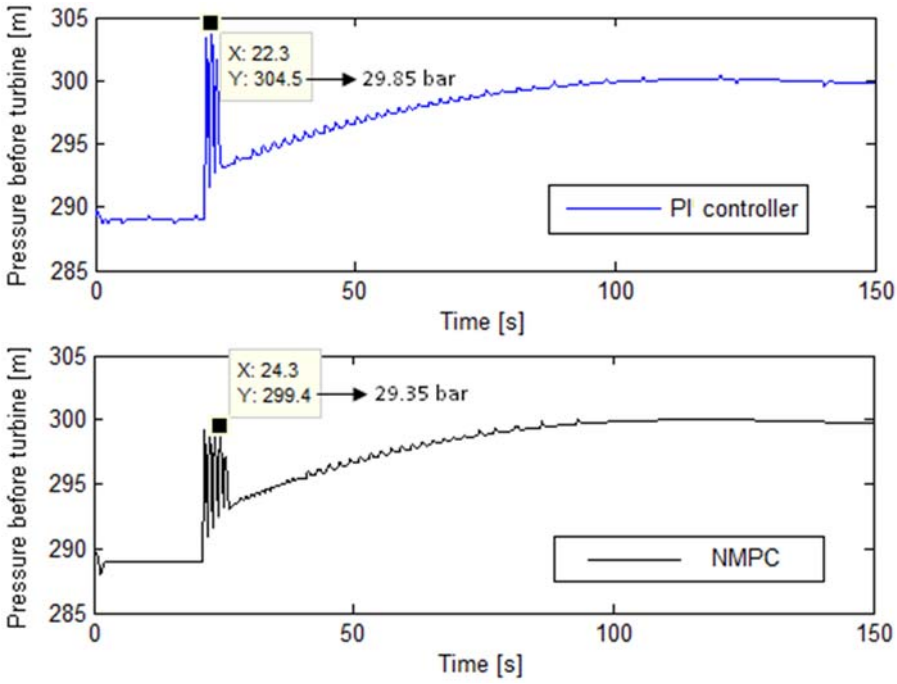

Figure 12. Pressure comparison when pressure constraint is 29.14 bar or 300m water head

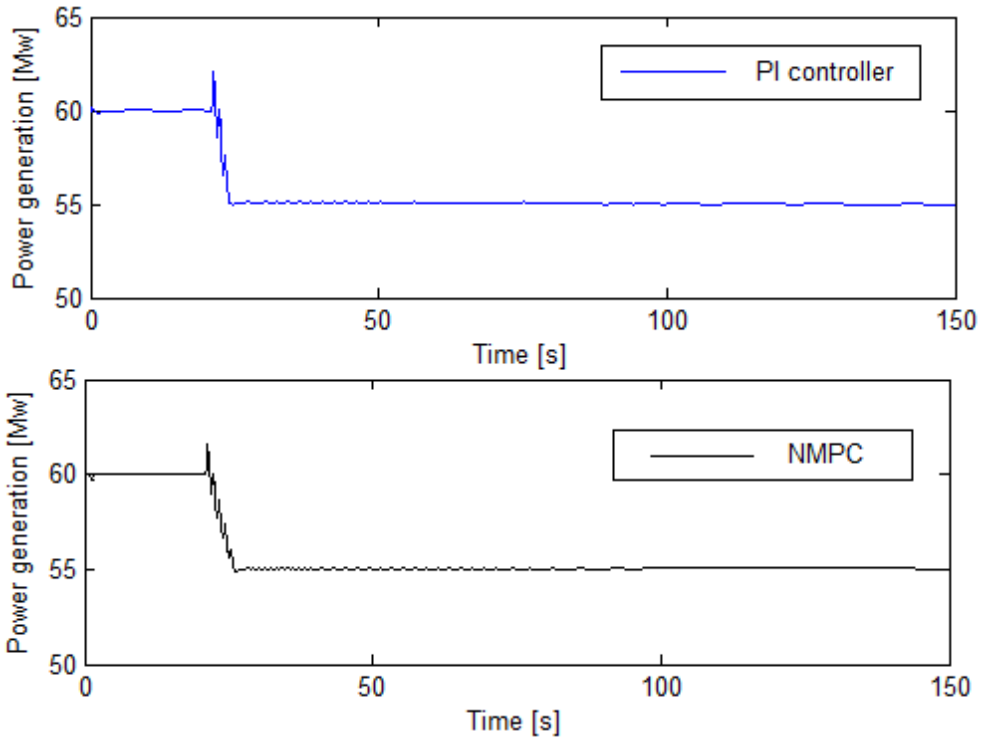

Figure 13. Power generation comparison when pressure constraint is 29.14bar or 300m water head

It is shown in Figure 11, the general trend of NMPC and PI controller is similar. As to comply with the pressure constraint, NMPC gave out a series hydraulic turbine opening, which is 81.23%, 79.05%, and 77.06% at first 3 seconds with shifty step length, whereas PI controller output openings with fixed maximum value 3%, in order to track the power reference. In both two cases, the highest pressure emerges at 22.3 second, but the resulted pressure of PI controller is higher than 300m pressure limit, even following the allowed step change. These two simulations, shown from Figure 11 to Figure 13, have demonstrated that either PI controller or NMPC can achieve the general goal of controlling, but the NMPC is more reliable and strict to pressure safety constraint.

3.3.4 Optimization process

The developing process of a NMPC is generally to solve a constrained nonlinear problem for optimization. Solving the most economic control trajectory of NMPC is an optimization problem that searching a solution for minimizing the cost functions $\boldsymbol{J}$ above.

During this process, there are a lot of gradient calculations involved. According to the affordable computation complexity, sequential quadratic programming (SQP) method is utilized in this work, which converts the optimization calculation into a set of quadratic sub problems to search the directions that decreases the value of the cost function (Y. Xiang, 2006) by assuming the quadratic turns out to be positive definite. The details about this algorithm can be checked in (C. Buskens, 2000). Considering the practical constraints that should not be exceeded from the engineering prospect, the optimization process is realized by *fmincon* function with active-set algorithm of MATLAB optimization toolbox, which is based on SQP method.

3.3.5 Implementation

The differential equations of the internal model of NMPC are approximated by finite differences method to decrease computation complexity. And then, the model is discretized with Euler's method, shown in equation (3.14):

$$\begin{cases} x_{k+1} = x_k + \Delta t \cdot f_c(x_k, u_k) = f(x_k, u_k) \\ y_k = h(x_k, u_k) \end{cases} \quad (3.14)$$

where f_c presents the control function; h presents the process function.

The time step of internal model is set to 0.1 second. With too large time step, it may lose some dynamics when doing the prediction. For instance, the highest pressure before the turbine may only last for a very short while. Compromising computation speed and precision of process dynamics, the Δt is set as 0.1 second, the same as for the plant model. Obviously, it is no need for internal model to catch more information of process than the real plant. On the other hand, An ODE solver with a fix simulation step works out the plant model as mentioned. The implementation structure for this work is presented in Figure 14. The control step is set as 1s, which means controller sends out a signal at every second. This is on the basis of the movement speed of hydraulic turbine. The hydraulic turbine is bearing tons of water, so it cost time for the turbine to start up and not possible for the turbine to move too quickly.

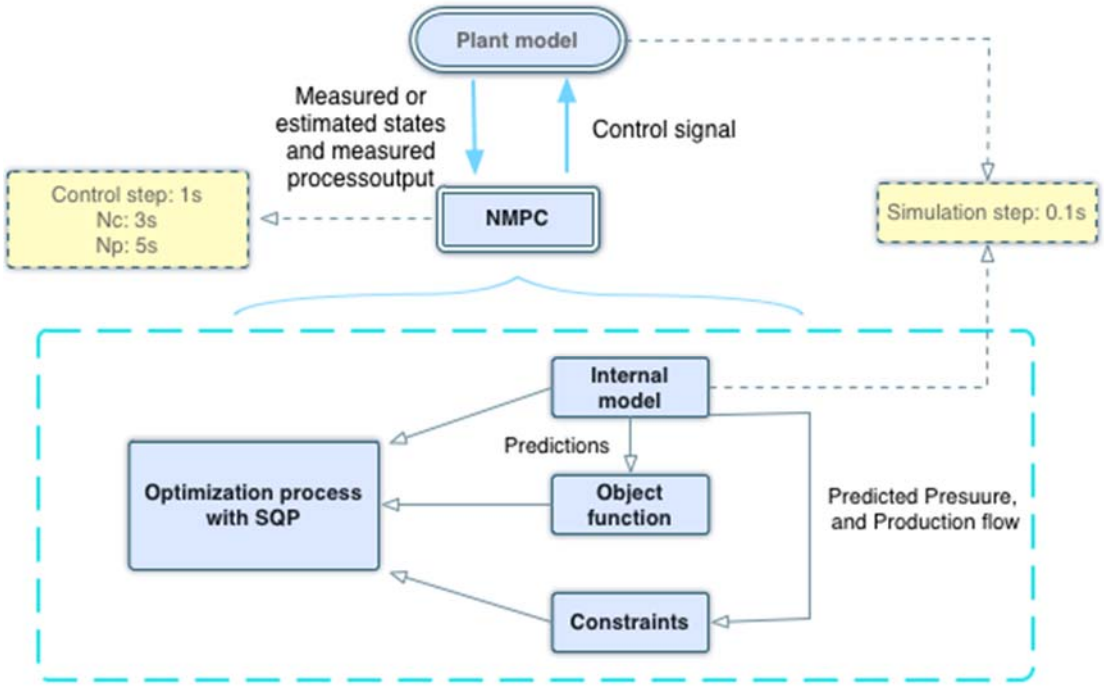

Figure 14. Implementation structure of NMPC

The control horizon of NMPC is 3 seconds forward, which means three control actions, and the prediction horizon is 5 seconds forward. The process resulted from every control action should comply with the constraints. However, the extreme value can happen between two control actions, hence it is important to predict the dynamics with a smaller interval than control step for the internal model. According to the simulation step and control step, one control action output from NMPC can engender 10 further values for each state, all of which should abide to the constraints, especially the production flow and penstock pressure. For each optimization process, there are 50 predicted discrete values for each state.

3.3.6 Results

The NPMC of this work is made for controlling the active power or frequency of hydropower plan and being adapted to different operation modes by using parameters setting given in Table 3 and initial conditions given in Table 4. The performance of this NMPC is tested in a closed loop of a mismatch plant model and under three situations:

- connecting to infinite bus
- connecting to small grid
- standing alone plant

When a hydropower plant is going to be coupled to any network, there are some common preparations. After the plant starting up, before activating excitation system, it should accelerate the hydraulic turbine until it arrives at 80% of the speed setpoint. And then starting excitation system, the rotation speed may decrease little due to the coupling effect of the two systems. When the differences of frequency, terminal voltage, phase angle between generator and grid reaches a specified range, it is ready to be connected into the electrical network.

Table 3: Simulation parameters of NMPC of single-unit hydropower plant

Data:	***Value:***	***Unit:***
$Simulation\ period$	150	s
$Simulation\ step$	0.1	s
$Control\ step$	1	s
a	1100	m/s
N_c	3	s
N_p	5	s
D_r	0.01	dimensionless
F_{nom}	50	Hz
$\boldsymbol{P}_{nom}$	60	Mw
Q_{max}	35	m^3/s
Q_{min}	4	m^3/s
H_{max}	550	m, water head
H_{min}	0	m, water head
u_{max}	100	%
u_{min}	0	%
Δu_{max}	5	% per second

λ	0.1	dimensionless
ϕ	0.5	dimensionless
L_{c1}	15000	m
D_{c1}	10	m
D_{s1}	10	m
L_{c2}	1000	m
D_{c2}	3.5	m
D_{s2}	5	m
L_p	300	m
D_p	2	m

Table 4: Initial conditions of NMPC of single-unit hydropower plant

Variable:	***Value:***	***Unit:***
G	81	%
$\boldsymbol{P}_m$	60	Mw
$\boldsymbol{P}_e$	1	p.u
Q_{c1}	23	m^3/s
Q_{c2}	23	m^3/s
Q_{p_in}	23	m^3/s
H_{s1}	345	m
H_{s2}	35	m
H_{p_out}	324	m

3.3.6.1 Connecting to infinite bus

There may be thousands of generators contributing in the infinite bus. When the hydropower plant is connected to the infinite bus, it is cooperating with the other units. Furthermore, every unit is normally scheduled with a power flow setpoint that is decided by control center of grid with a dispatching calculation system. The frequency

is relatively stable with this scheduling. Therefore, the simulation of this situation with NMPC is carried out with different setpoints for generated power. The generated power here is simply treated as a proportional to the mechanical power, under the assumption of almost all the mechanical power is transferred to electrical power. The generator side mathematical model is not included for simulation. The result is shown in Figure 15 and Figure 16. The power generation setpoint is changed from 60 Mw to 50Mw at 20th second. The simulation results from NMPC can achieve the control goal and track the reference quickly in the simulation.

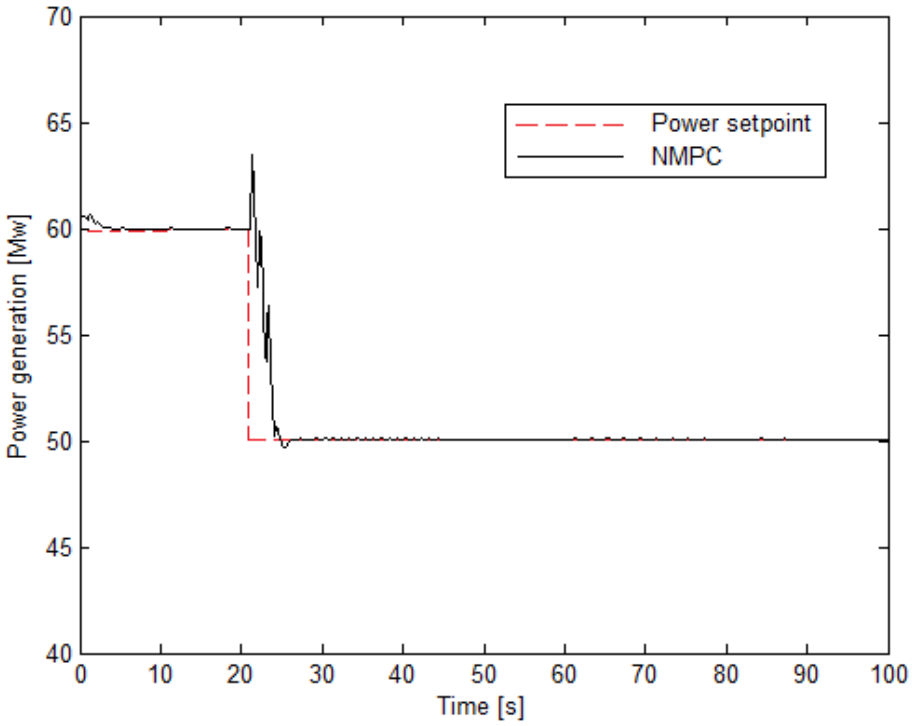

Figure 15. Simulation result, power generation, when connecting to infinite bus

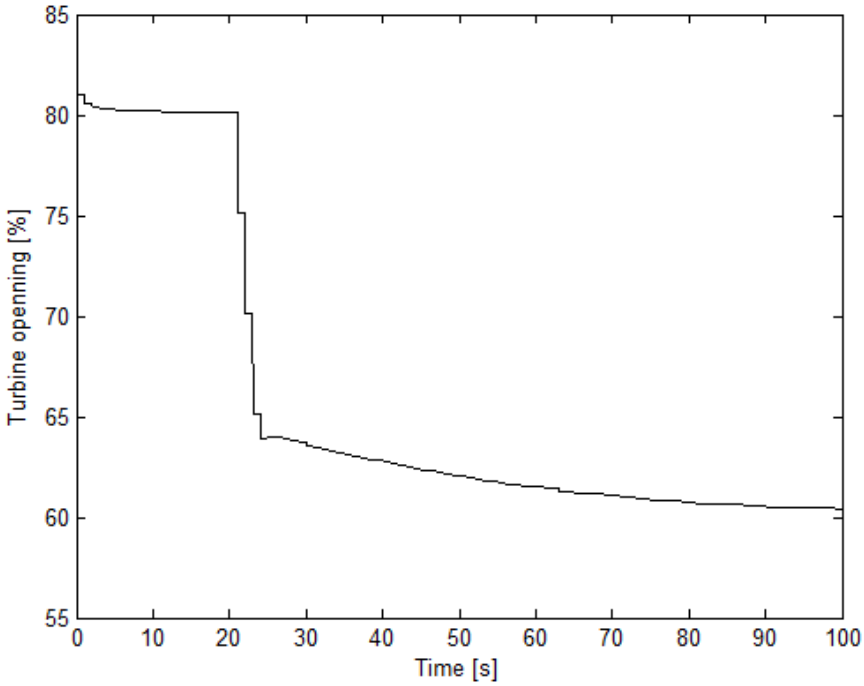

Figure 16. Simulation result, turbine opening, when connecting to infinite bus

3.3.6.2 Connecting to small grid

A hydropower plant also can be connected to a small grid that is built by less than 10 units. This can happen when the unit is in a regional grid that is caused by tie line failing. In this situation, every unit has a significant influence on the grid. The load frequency control effect becomes more significant. Consequently, the frequency is controlled by manipulating power from each unit. After the same starting procedure as connecting to infinite bus, a droop control combined NMPC is applied. Droop control is the first loop control that decides how much power should each unit contributes to the grid. A droop ratio is assigned to each unit, so the deviation of frequency can be transferred to difference of the generated power from previous, which is presented in (3.1) and (3.2). Then a new power reference is given to the NMPC. A frequency deviation is simulated by reducing power demanding in the network. Consequently, to maintain the frequency, the power generation of this unit is also reduced. The simulation result is presented in Figure 17.

The power demand is reduced from 1p.u to 0.9p.u at 50th second. As a result, disturbances happen to the frequency. According to the droop control, new setpoints are created for power generation as shown in the 3rd plot in Figure 17. After about 5 seconds, disturbances are eliminated by NMPC, and the whole system is back to balance.

3.3.6.3 Standing alone

When a hydropower plant is standing alone and with a single unit, the power that should be generated is depending on the electricity consuming. This situation could happen when the tie line is failed, and the plant is offering emergency power for a local use. The frequency is related with power generation and consumption and it is a result of balancing of them. The power consuming is hard to be forecasted and measured. Therefore, the setpoint is shifted directly to frequency in this simulation. Controlling is still completed by NMPC, but with different reference and process output. The corrector to the reference is also applied, since the power offset still have effects to the frequency output, and it is with the same value for the filter factor, ϕ.

This function of NMPC is simulated with manipulating the consumed electrical power in equation (2.29). And the corresponding results are presented in Figure 18. The power consumption is increased from 1p.u to 1.1p.u at 50th second and decreased to 0.9p.u at 100th second. Because the consumption cannot be predicted and varied a lot, there are some deviations in frequency. However, they only last less than 10 seconds under controlling of NMPC.

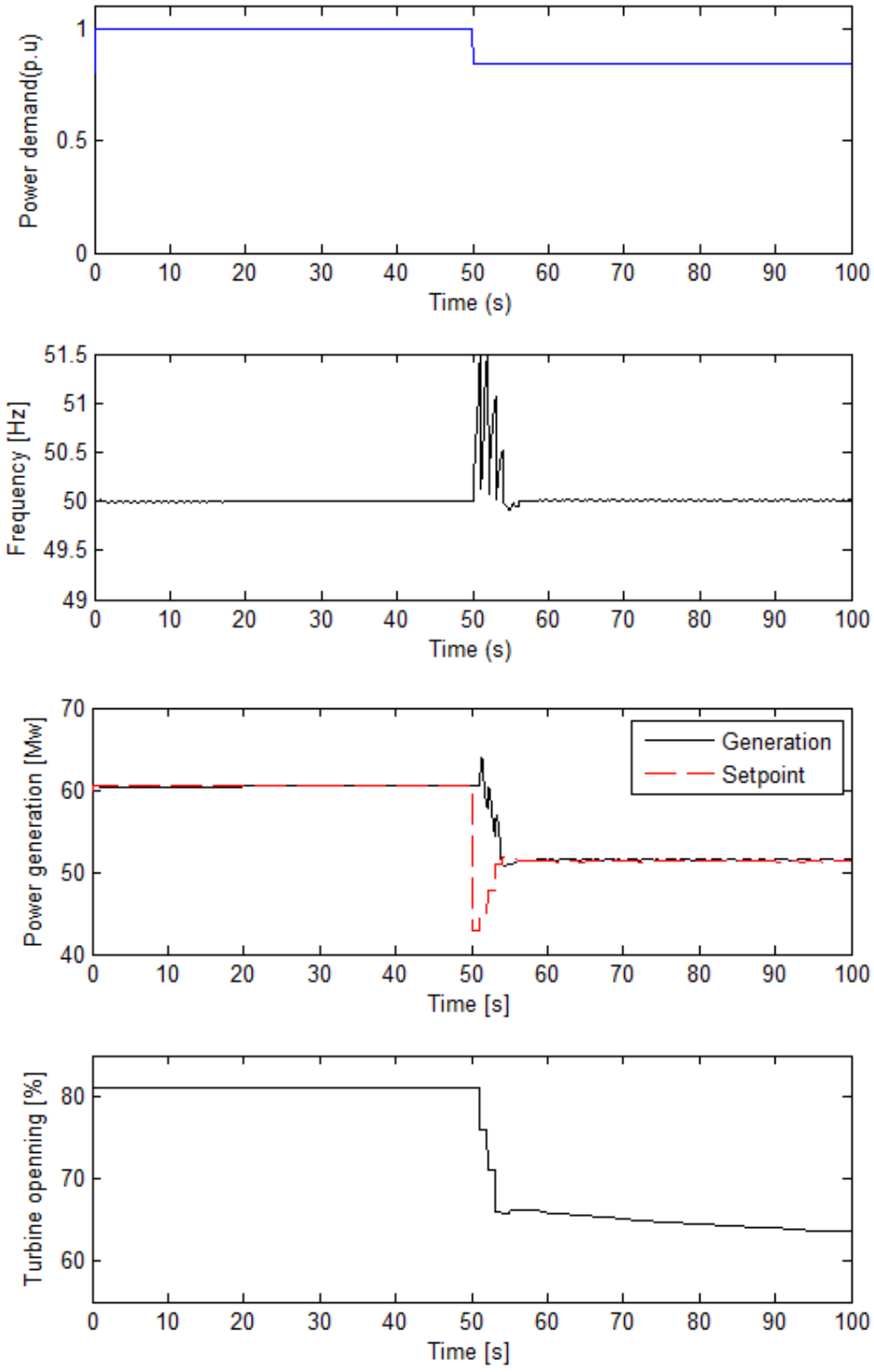

Figure 17. Simulation results when under connecting to small grid condition.

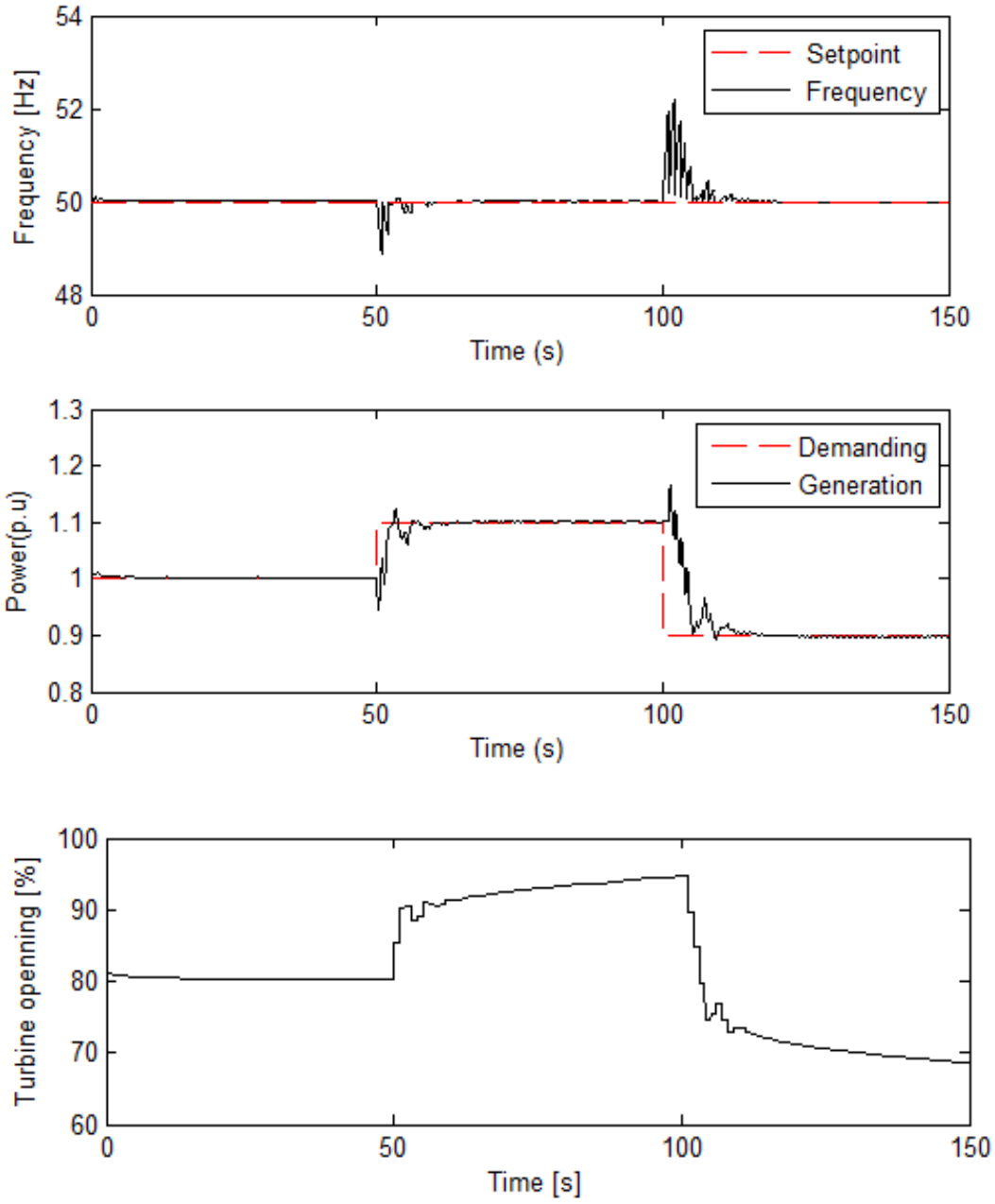

Figure 18. Simulation results of frequency (top), power generated (middle) and turbine opening (bottom), when under standing alone condition.

3.3.7 Overall NMPC strategy

Because of load conditions according to the different operation mode, traditional PI controller would need to adapt with tuning PI parameters. In the contrary, the proposed NMPC does not need to do any adjustments, except changing reference variable for

situation of standing alone. The general control strategy of this NMPC controller is presented in Figure 19. It has shown that the only imperative action of this NMPC strategy is to select the operation mode. Any deviation of frequency or power can be corrected by manipulate hydraulic turbine opening, which has been tested in Section 3.3.6.1, 3.3.6.2 and 3.3.6.3. In the sense of industry engineering, comparing with PI controller, NMPC can help to improve the reliability of control actions and working efficiency.

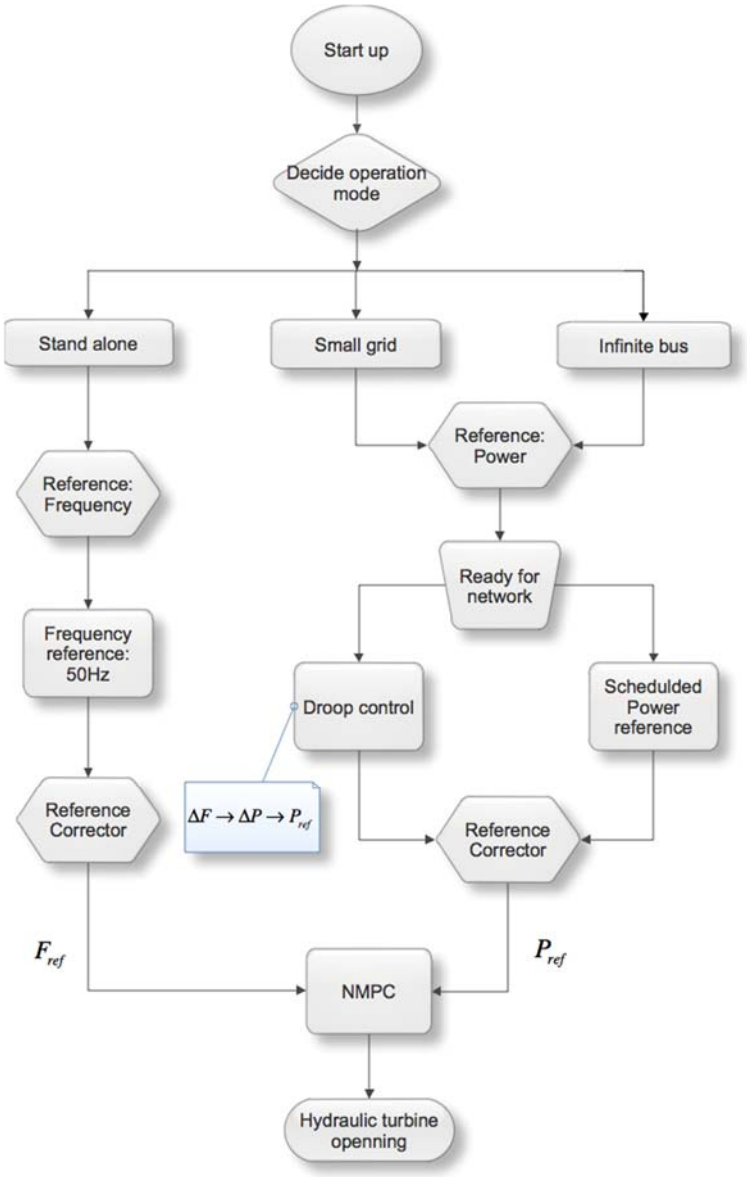

Figure 19. Overall working procedure of NMPC

3.3.8 Conclusion

A NMPC strategy is presented in this work for controlling a single unit hydropower plant. The scheme of NMPC with a reference corrector is carried out. Working procedure of overall NMPC strategy is put forward. Various simulations are applied for testing the functions of NMPC. It has proved that NMPC has predominance on handling pressure and flow constraints than PI controller with fixed maximum closing rate. In other word, NMPC is more reliable for production scheduling issue and pressure safety concerning of hydropower plant. Furthermore, no matter under which operation mode, it has shown that the NMPC can achieve the control purpose steadily and smoothly. All in all, the proposed NMPC can contribute to satisfy a variety of requirements for controlling a single unit hydropower plant and reduce manual work.

3.4 NMPC for a multi-unit hydropower plant

3.4.1 Problem description

Take a plant with two units as an example. When one unit reduces production, it closes hydraulic turbine opening to a smaller value. Then, the water flowing into this turbine is decreased. As a result of that, a total smaller passage for water comes about to this plant. If there is no manipulation for the other turbine in the plant, because the same water level in reservoir for a short while, which implies same energy is offered for the plant, it precipitates more water running into the other turbine. Consequently, the production flow, net head, even the power production for the other unit are different from the way that they were, without changing turbine's opening. This situation is demonstrated in Figure 21 and Figure 22, which utilized the mathematical model of a multi-unit hydropower plant below, and described in (Vournas & Zaharakis, 1993), (Hannett, Feltes, Fardanesh, & Crean, 1999).

A flow chart of multi-unit hydropower plant is illustrated in Figure 20. Other than characteristics that are presented for a single-unit hydropower plant model in section 2.1, water is split into branch penstocks before it flows to hydraulic turbine.

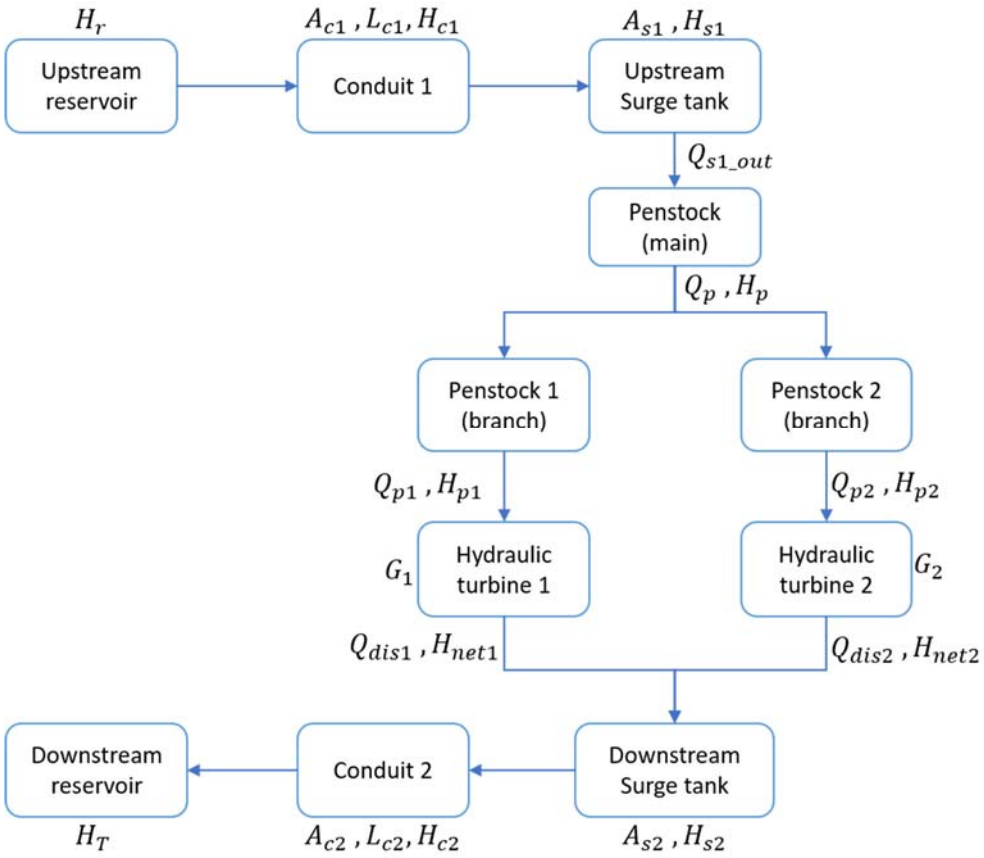

Figure 20. Flowchart of a two-unit hydropower plant

Furthermore, it is supposed that there should be two different turbines. Therefore, it is expressed by two different gate constants k_1 , k_2 and different turbine efficiency η_1, η_2. To sum up above, and reorganize the simple model in Chapter 1, the mathematical model of a multi-unit hydropower plant can be stated as:

Upstream conduit:

$$\frac{dQ_{c1}}{dt} = \frac{g \cdot A_{c1}}{L_{c1}}(H_r - H_{s1} - H_{loss\_c1}) \qquad (3.15)$$

Surge shaft:

$$A_{s1} \cdot \frac{dH_{s1}}{dt} = Q_{s1\_in} - Q_{s1\_out} \qquad (3.16)$$

Main penstock:

$$\frac{dQ_{p\_in}}{dt} = \frac{gA_p}{L_p}(H_{s1} - H_{p_{out}} - H_{loss\_p}) \quad (3.17)$$

$$\frac{dH_{p\_out}}{dt} = \kappa \cdot (Q_{p\_in} - Q_{p\_out}) \quad (3.18)$$

Branch penstocks:

$$\begin{cases} \frac{dQ_{p1,2\_in}}{dt} = \frac{g \cdot A_{p1,2}}{L_{p1,2}}(H_{p\_out} - H_{p1,2\_out} - H_{loss\_p1,2}) \\ \frac{dH_{p1,2\_out}}{dt} = \kappa_{1,2} \cdot (Q_{p1,2\_in} - Q_{p1,2\_out}) \end{cases} \quad (3.19)$$

where: $\kappa = \frac{a^2}{g \cdot A_p \cdot L_p}$, $\kappa_{1,2} = \frac{a^2}{g \cdot A_{p1,2} \cdot L_{p1,2}}$

While the total amount of water is not changed and only divided into two branches.

So,

$$Q_{p\_out} = Q_{p1\_in} + Q_{p2\_in} \quad (3.20)$$

Downstream conduit:

$$\frac{dQ_{c2}}{dt} = \frac{gA_{c2}}{L_{c2}}(H_{s2} - H_T - H_{loss\_c2}) \quad (3.21)$$

Downstream surge shaft:

$$A_{s2} \cdot \frac{dH_{S2}}{dt} = Q_{s2\_in} - Q_{s2\_out} \quad (3.22)$$

The head loss along the conduits and penstock are calculated by Darcy-werch's equation:

Head loss:

$$H_{loss} = f_r \cdot \frac{L}{D} \cdot \frac{\bar{Q}}{2g} \cdot \frac{|\bar{Q}|}{A^2} \quad (3.23)$$

Hydraulic turbine:

$$Q_{p1,2\_out} = Q_{dis1,2} = k_{1,2} \cdot A_{p1,2} \cdot G_{1,2} \cdot \sqrt{H_{net1,2}} \quad (3.24)$$

$$H_{net1,2} = H_{p1,2\_out} - H_{s2} - H_{loss\_turbine1,2} \quad (3.25)$$

At connections:

$$\begin{cases} Q_{c1} = Q_{s1\_in} \\ Q_{s1\_out} = Q_{p\_in} \\ Q_{s2\_in} = Q_{p1\_out} + Q_{p2\_out} \\ Q_{s2\_out} = Q_{c2\_in} \end{cases} \quad (3.26)$$

The mechanical power:

$$\boldsymbol{P}_{m1,2} = \eta_{1,2} \cdot \rho \cdot g \cdot H_{net1,2} \cdot Q_{dis1,2} \quad (3.27)$$

The process outputs are generated active powers from the two units, whereas model can only calculate the mechanical power, $\boldsymbol{P}_m$. It is assumed that all the mechanical power is transferred to electrical power for both units. Moreover, the electrical power, $\boldsymbol{P}_e$, is totally consumed, $\boldsymbol{P}_c$, and fulfils the electricity market demands. In other words, there is no inverse power to the units. This assumption can be defined as:

$$\boldsymbol{P}_e = \boldsymbol{P}_c = \boldsymbol{P}_m \quad (3.28)$$

The simulation results that shown in Figure 21 and Figure 22 is so-called coupling effects when there are several units in the same plant. When unit2 production is decreased from 40Mw to 20Mw, its turbine opening is closed from around 65% to 30% with a speed 5% per second. Meanwhile, the turbine of unit1 does not move, but unit1 arrives at a higher power generation, higher net head and higher production flow, because of the identical water level in reservoir during a short period but a smaller passage to turbine of unit2.

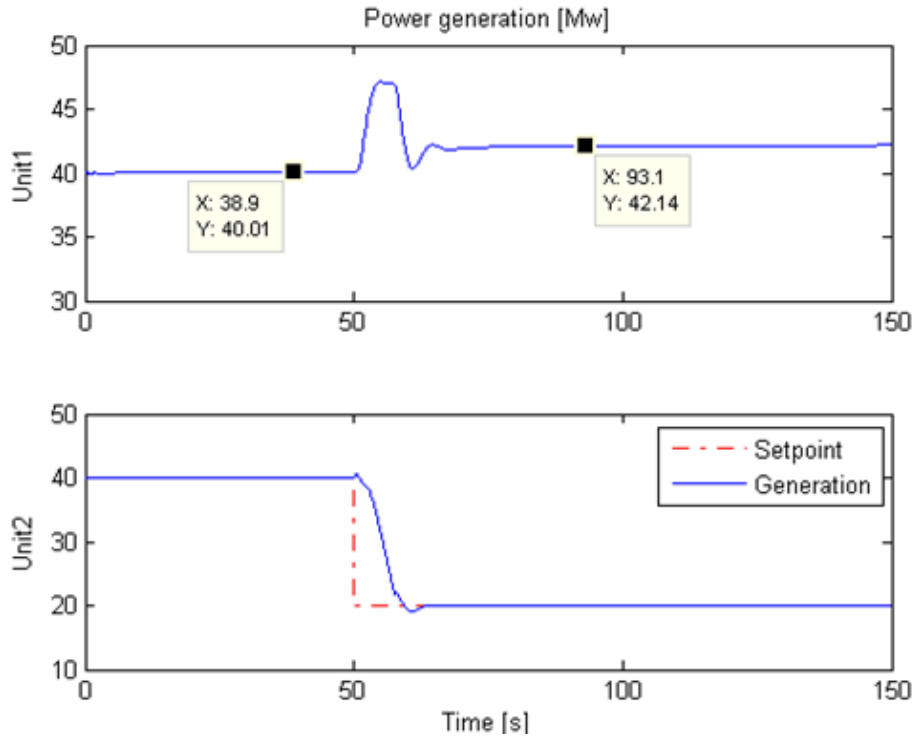

(a)

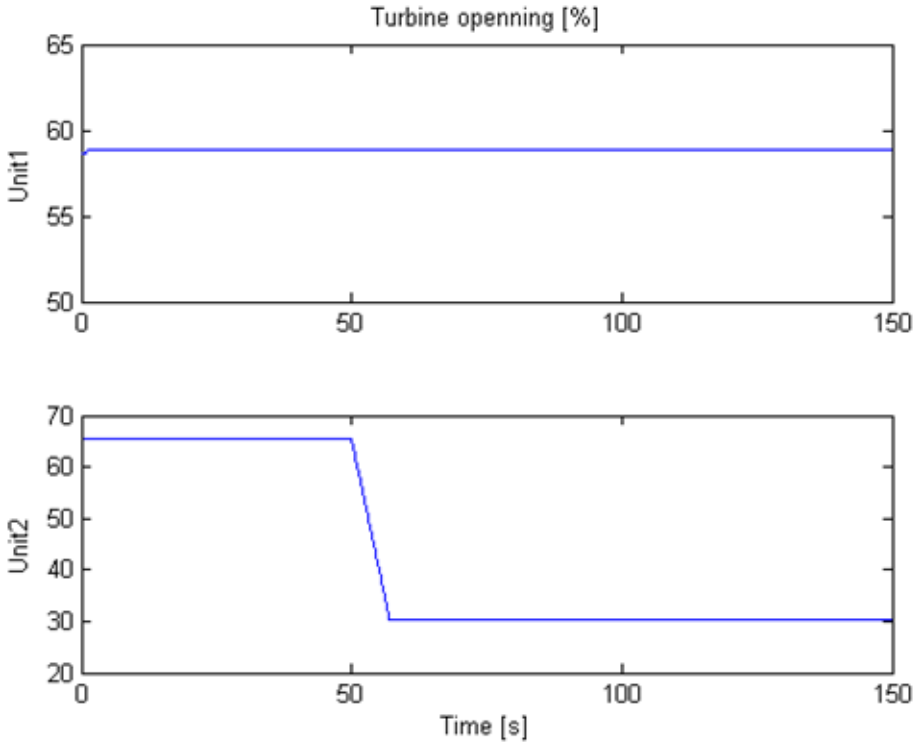

(b)

Figure 21. Demonstration of coupling effects of power generation (a) among units with their corresponding turbine opening percentage (b).

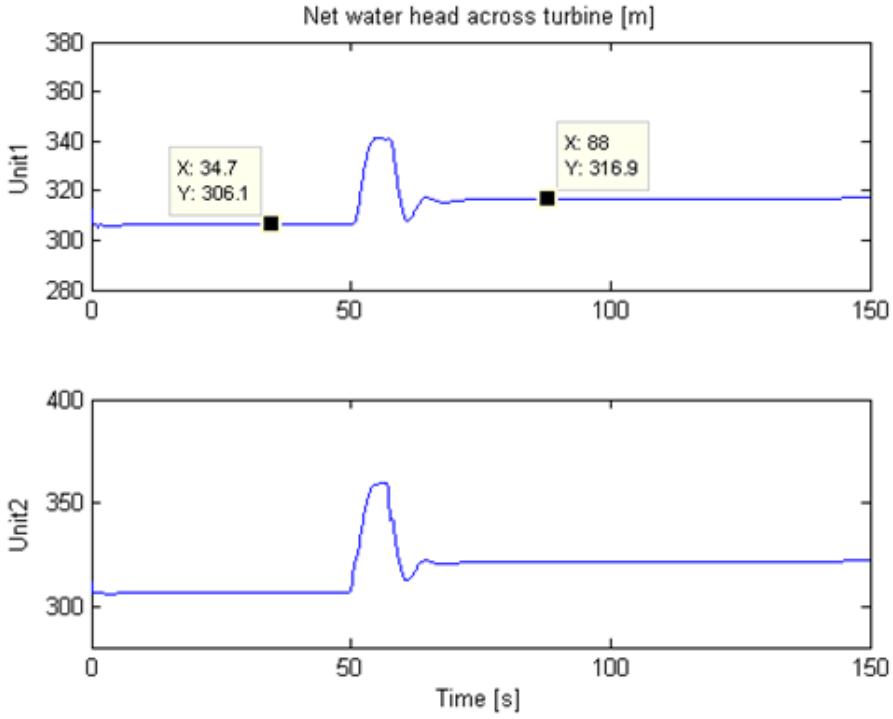

(a)

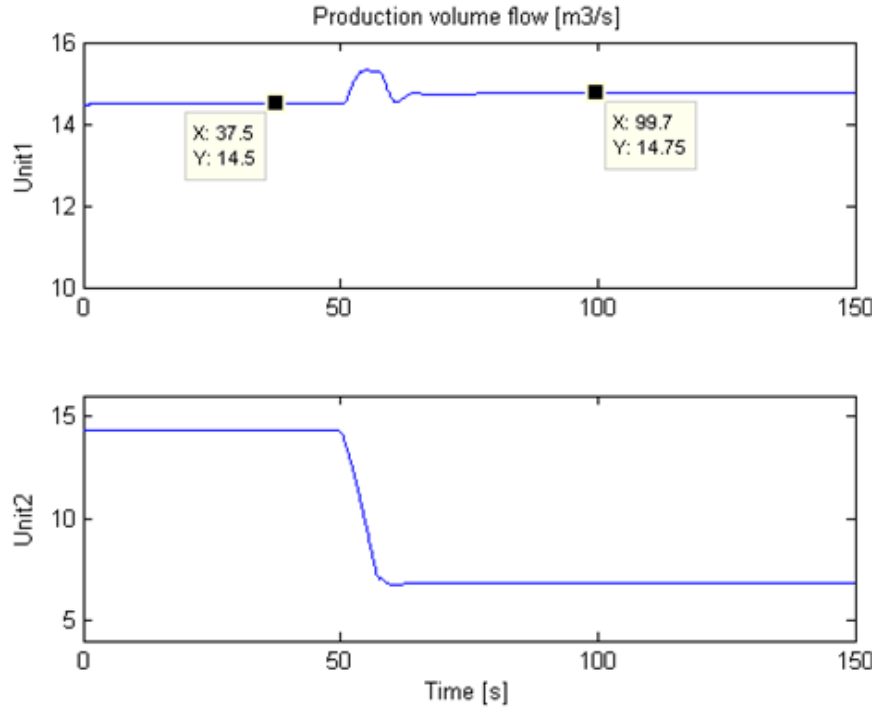

(b)

Figure 22. Demonstration of coupling effects of net head(a) and production volume flow rate (b) among units.

3.4.2 Cost function

There is no difference in the cost function, either when the NMPC is applied to a single generator unit hydropower plant or a multi-unit hydropower plant. The overall cost function is the same as a target that can minimize the deviation between process output and the reference that is preferred for the process with appropriate cost, which is described in section 3.3.2. However, due to multi-unit hydropower plant is generally a MIMO control problem, vectorizing the variables are required. So, the process model can be rewritten as:

$$\begin{cases} X(k+1) = f\big(X(k), U(k), D(k)\big) \\ Y(k+1) = h(X(k+1), V(k)) \end{cases} \quad (3.29)$$

Where

$$U = [G_1\,, G_2]^T \quad (3.30)$$

$$X = \left[Q_{c1}\,, Q_{c2}, H_{s1}, H_{s2}, Q_{p_{in}}, Q_{p1_{in}}, Q_{p2_{in}}, H_{p\_out}, H_{p1\_out}, H_{p2\_out}\right]^T$$

$$Y = [P_{e1}\,, P_{e2}]^T \quad (3.31)$$

Due to SQP method is selected for optimization in this work, a vectorized cost function is rearranged from (3.5) and presented as:

$$\begin{aligned} \boldsymbol{J}(k) = &\sum_{i=0}^{N_p} [\hat{Y}(k+i) - R(k+i)] \cdot Q_y' \cdot \left[\hat{Y}(k+i) - R(k+i)\right] \\ &+ \sum_{j=1}^{N_c} \Delta U(k+j-1) \cdot Q_u' \cdot \Delta U(k+j-1) \end{aligned} \quad (3.32)$$

Where, $Q_y' \in R^{2\times 2}$, $Q_u' \in R^{2\times 2}$

$Q'_y$and Q'_u should be symmetric and positive semi-definite weighting matrices. In this work, they are simply defined as $Q'_y = I_{2\times2}$, $Q'_u = \lambda \times I_{2\times2}$

3.4.3 Constraints

One of dominant advantage of NMPC is to handle various constraints comparing with traditional controllers. As a MIMO system, the constraints of hydropower plant are presented with vectors. To be realistic, not only because of the production requirements in the industry, but also concerning the actuators' movements constrained by their mechanical structures, several constraints are embedded into NMPC. The range of the control variable is from 0% to 100%, which is opening of the turbine. The gradient of the hydraulic turbine is constrained to maximum 5% per second since they are bearing tons of water, not easy to move too fast. These two constraints for each element in U vector can be described as:

$$u_{min} \leq u(k) \leq u_{max} \quad (3.33)$$

$$-\Delta u_{max} \leq \Delta u(k) \leq \Delta u_{max} \quad (3.34)$$

Because of the water resource in reservoir is limited, as spoken previously, utilization of the water is scheduled in an optimal way that is responding to the electricity market. As a result of this, the admission flow, or gross flow should be discharged from reservoir, is constrained by the scheduling value, which can be stated as:

$$Q_{min} \leq (Q_{dis1} + Q_{dis2}) \leq Q_{max} \quad (3.35)$$

The pressure in the penstock is another state that should be constrained. When the hydraulic turbine is closed, the water flow is reduced, but because of smaller passage, the pressure is increased in a short duration and reduced afterwards. The increased pressure should be limited to avoid damaging the equipment. Therefore, constraints are added to the highest pressure, which is allowed to happen throughout plant manipulation. This constraint vector can be described with the inequality below:

$$p_{min} \leq p \leq p_{max} \quad or, \quad H_{min} \leq H \leq H_{max} \tag{3.36}$$

3.4.4 Optimization process

With regard to reduce the computation complexity of the optimization process, the internal differential mathematic model of NMPC is simplified with discretized form that is achieved by Euler's method, whereas, the plant model is still carried out with (3.29).

ODEs that are solved by ODE solvers in MATLAB. A simulation time step of 0.1 second is used for both models. An illustration of the optimization process is presented in Figure 23. The control step is 1 second every actuation. The control horizon of NMPC is 2 seconds forward with 20 samples, and the prediction horizon is 5 seconds forward with 50 samples.

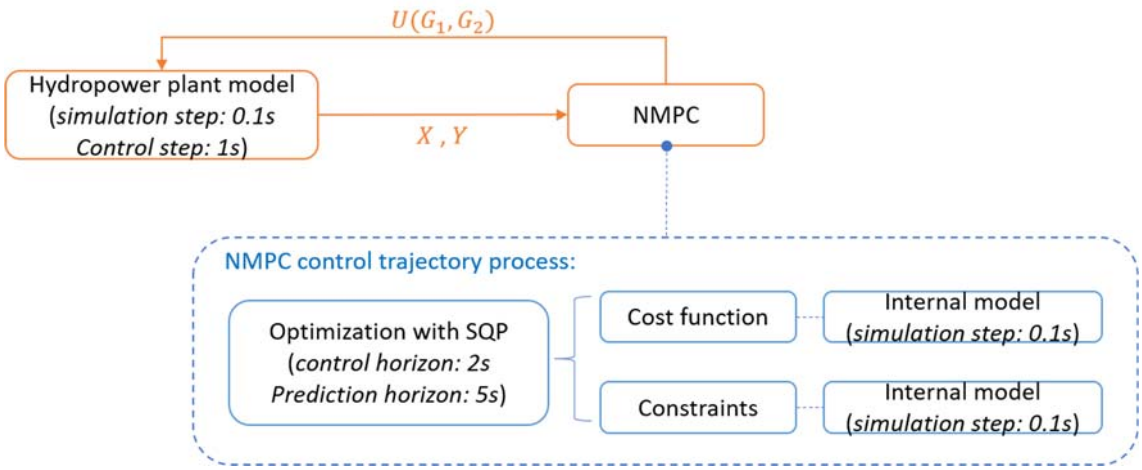

Figure 23. Optimization process of NMPC controller for multi-unit plant

3.4.5 Results

The two-unit hydropower plant is considered as a MIMO system. The control variable vector, U , in equation (3.29) includes two turbines' openings, and the output vector, Y , includes two units' power generations. Each unit is assigned a set point for power generation, which lies in reference vector, R. A simulation result of controlling a 2-unit

plant using NMPC and traditional PI controller are presented in Figure 24, which is done by manipulating power generation setpoint of unit2 from 40Mw to 20Mw at 50th second. The parameters and initial conditions are set as Table 5 and Table 6.

Table 5: Simulation parameters of NMPC of single-unit hydropower plant

Data:	***Value:***	***Unit:***
$Simulation\ period$	150	s
$Simulation\ step$	0.1	s
$Control\ step$	1	s
a	1100	m/s
N_c	2	s
N_p	5	s
G_{nom}	50	%
$\boldsymbol{P}_{nom}$	30	Mw
Q_{max}	35	m^3/s
Q_{min}	0	m^3/s
H_{max}	350	m, water head
H_{min}	0	m, water head
u_{max}	100	%
u_{min}	0	%
Δu_{max}	5	% per second
λ	0.1	dimensionless
ϕ	0.5	dimensionless
L_{c1}	4000	m
D_{c1}	7	m
D_{s1}	15	m
L_{c2}	1000	m
D_{c2}	7	m
D_{s2}	10	m

L_p	1200	m
D_p	2.5	m
L_{p1}	200	m
D_{p1}	1.5	m
L_{p2}	200	m
D_{p2}	1.5	m

Table 6: Initial conditions of NMPC of single-unit hydropower plant

Variable:	***Value:***	***Unit:***
G_1	58	%
G_2	65	%
$\boldsymbol{P}_{m1}$	40	Mw
$\boldsymbol{P}_{m2}$	40	Mw
Q_{s1_in}	30	m^3/s
Q_{s2_out}	30	m^3/s
Q_{p_in}	30	m^3/s
Q_{p1_in}	15	m^3/s
Q_{p2_in}	15	m^3/s
H_{s1}	342	m
H_{s2}	11	m
H_{p1_out}	317	m
H_{p2_out}	317	m
H_{p_out}	323	m

The PI parameters are only for the simulations, and certainly different with those that are using in industry. The coupling effects are counted in predictions when NMPC is working, which is achieved by the developed model, whereas PI controllers, shown in Figure 24 and Figure 25, only attempt to eliminate error between reference and output

respectively for each unit. Because the pressure inverse response, when the turbine is closed any opening, the generated power is increased on the contrary for a short period, and it will be reduced later, vice versa. The PI controller handles it in a straightforward way. When the power generation is higher, it reduces the turbine opening. When the power generation is lower, it increases the turbine opening. In this way, the PI controller consumed more time to track the reference comparing with NMPC in this case. The reason is, not that the PI parameters are tuned not good enough, but when the reverse response happens, PI controller may lead the control variable make excessive force and need to compensate it subsequently. Tuning PI parameters cannot assist to improve controller's performance any further for covering the inverse response elimination quickly and effectively.

Nevertheless, the NMPC can predict 5 seconds forward, which integrates 50 samples with time interval 0.1 second for each. In this plant, the highest pressure-deviation of inverse response happens at 0.3 second after every movement of turbine. Then the prediction horizon with 5 seconds, 50 samples, is certainly sufficient for capturing the inverse response. Therefore, the NMPC can foresee it and produce the most economic control trajectory.

The results of two controllers for unit2 are presented in Figure 24, Figure 25 and reveal this advantage of NMPC, which is reflected directly by the time consumption for achieving next steady state after changing the setpoint of power generation of unit2. Reaching the new setpoints takes about 25 seconds using PI-controllers and only about 10 seconds using NMPC

The other advantage of NMPC for controlling a multi-unit hydropower plant would be the prediction function of the coupling effects among the units that has been demonstrated in Figure 22. It can be seen that, when decreasing power generation one unit, it causes some fluctuations for the other unit and a relatively higher generation under a same turbine opening eventually. If increasing power generation of one unit, it will result in a relatively lower generation from the other unit with no manipulation.

The PI controller, as spoken above, pays no more attention to these effects except do its own job. However, NMPC can produce envisioning control trajectories for the coupling effects among the units. In this simulation, it is more apparently displayed from the controlling results of unit1 presented in Figure 24, even though the effects are mutual. When unit2 is reducing its production, it causes a rise of power generation to unit1. PI controller makes the turbine close to attempt to reach the reference value again, while NMPC can predict it only a temporary rise and output different control actions. On the contrary with PI controller, after the first control step, the NMPC open the turbine for one control step and later, it closes the hydraulic turbine. As a result, the NMPC lower the deviation and smaller the total duration of eliminating the deviation for unit1. Under NMPC controlling, the deviation is from 0 to 9.37Mw, and under controlling with PI controller, it is -6.11 to 4.01 Mw. Duration with NMPC is 12 seconds, with PI controller is 37.3 seconds.

3.4.6 Conclusion

This paper has presented a simulation-based NMPC application for a multi-unit hydropower plant. A nonlinear mathematical model is developed for the internal model and plant model. A mismatch error is added to the power output of each unit. The algorithm of NMPC is presented and applied to the mismatch plant model. Simulations with manipulation power generation setpoint of unit2 are carried out and compared with traditional PI controller. Under the influences of inverse response and coupling effect, NMPC has shown its advantage. With NMPC, when manipulating generation of one unit, the range of deviation from reference value and duration of eliminating deviation for both two units are effectively diminished, according to the control results of traditional PI controller.

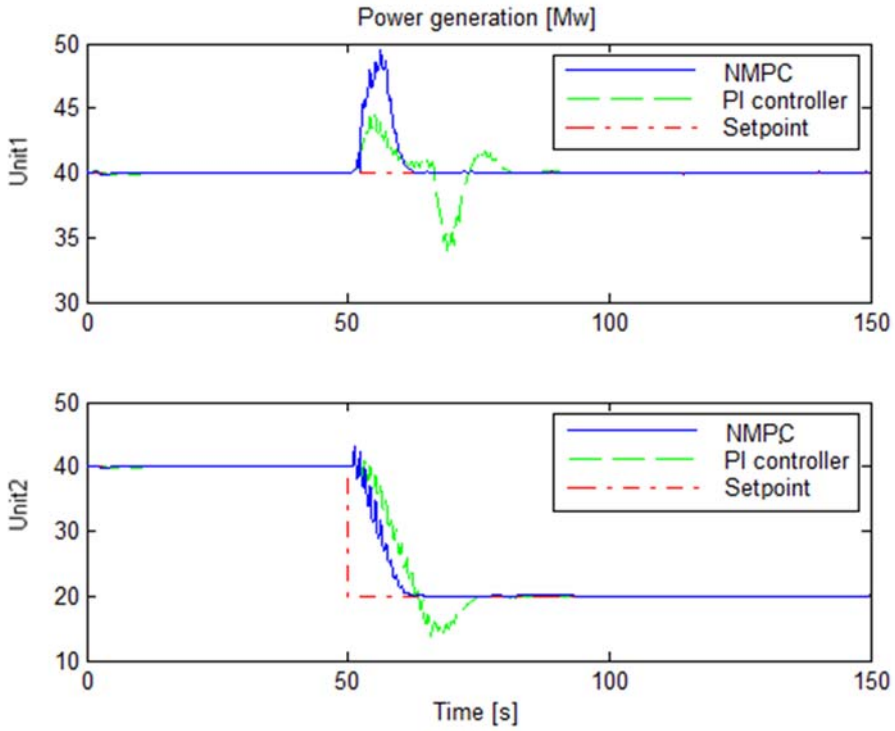

(a)

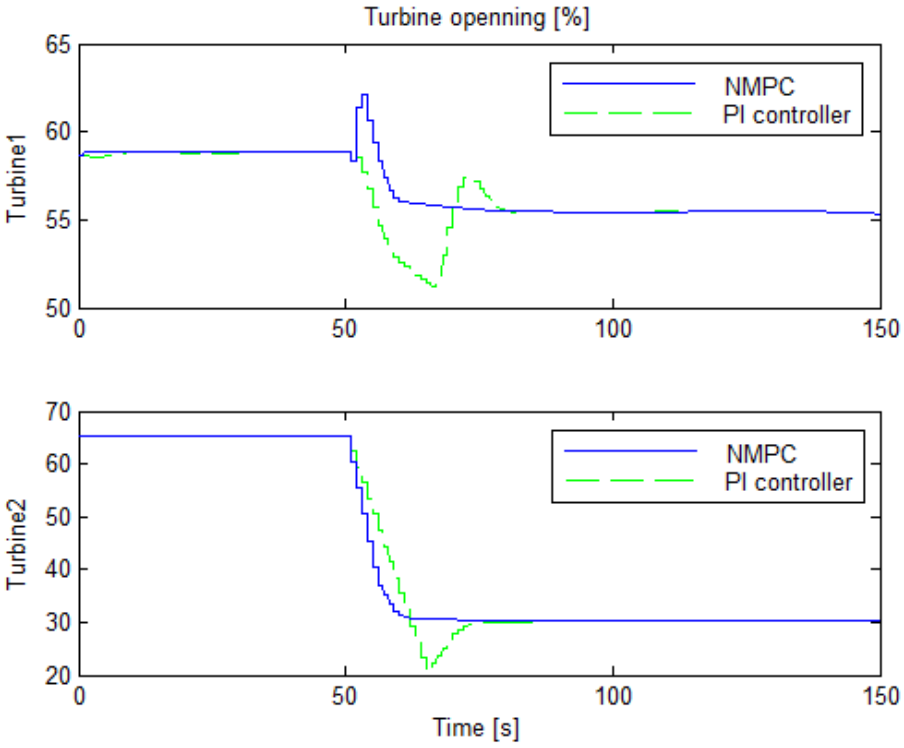

(b)

Figure 24. Simulation results of power generation (a) and turbine opening (b) of controlling two-unit hydropower plant with NMPC and PI controller

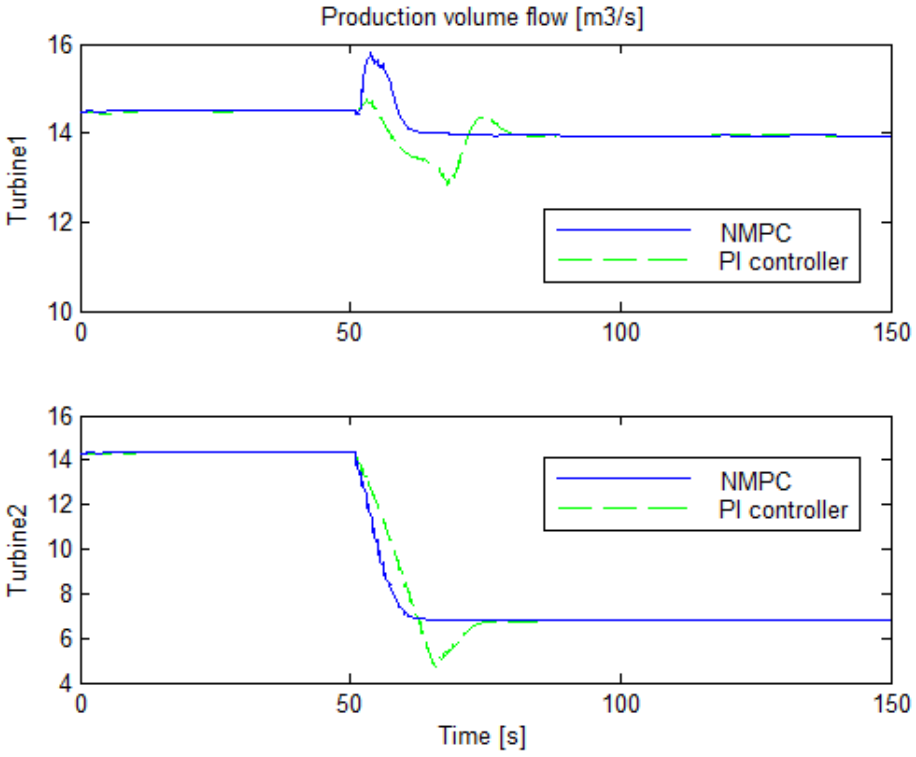

(a)

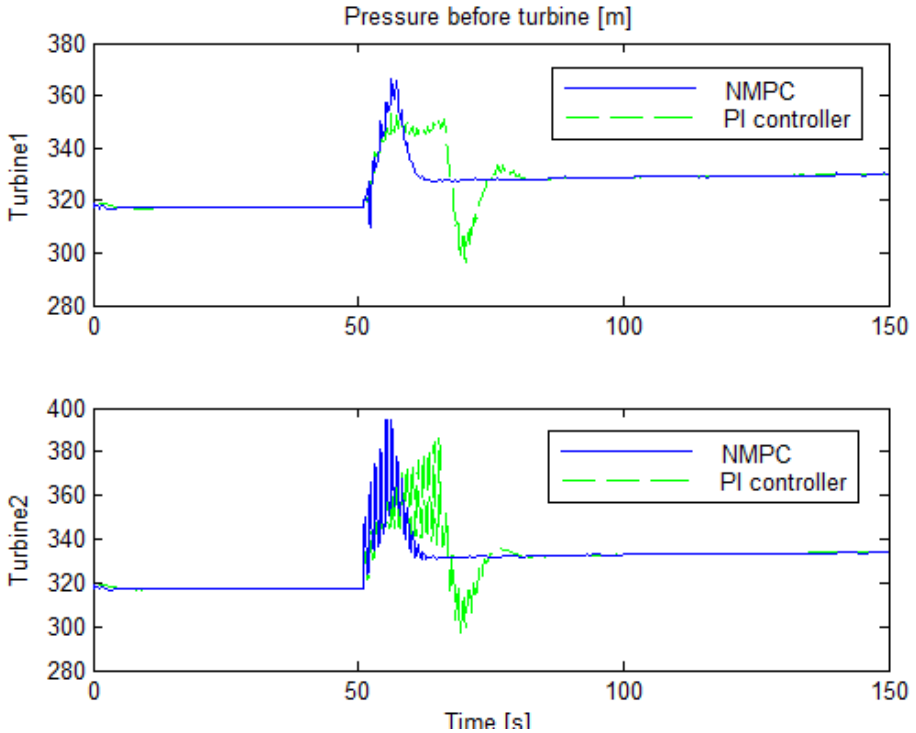

(b)

Figure 25. Simulation results of production volume flow rate (a) and pressure before turbine (b) of controlling two-unit hydropower plant with NMPC and PI controller

4 Optimization

The other concern of this work is to optimize the accumulation of water in reservoir for electricity production with the premises of avoiding flood to surroundings. The optimization is accomplished with a floodgate regulation to offer more water for electricity production and systematizing spillage of water when there is a potential flood situation. Optimized results are compared with historical operations, from which, it can be seen there are some possibilities to produce more electricity with the same amount of water but no flood.

The optimization of floodwater certainly concerns with the scheduling of reservoir operation problem. Any result of floodgate control changes the reservoir level. Consequently, it also affects the decision making on how much water should be discharged for power production. Therefore, optimal control of floodgate is a part of optimization of reservoir operation, of which the optimizing object is the electricity production under a safety premises of avoiding flood. Diverse works have been carried out for scheduling or optimizing operation for water reservoir of hydropower plant. Short term reservoir operation scheduling was formulated as a large-scale linear programming algorithm and solved by a commercial package in (M.R. Piekutowski, 1994). Needham etc. presented reservoir optimization study for Iowa/Des Moines in (J.T. Needham, 2000) with also a linear programming model. In (Yoo, 2009), linear programming model was also used for maximizing power generation with different decision weights on variables. Fuzzy stochastic dynamic programming (FSDP) approach was presented in (A. Tilmant, 2002) for deriving steady state multipurpose reservoir operation policies and implemented to Mansour Eddahi reservoir (Morocco) with inflow as the hydraulic state variable. Another two-stochastic programming (K. Reznicek, 1991) (D.W. Watkins Jr., 2000) were also applied to Modeling reservoir operations. Different optimization methods have also been carried out for reservoir operation. Hybrid particle swarm optimization has been implemented for short term scheduling for cascade hydropower plants in (W. Jiekang, 2008). The scheduling problem is considered as

mixed-integer nonlinear optimization problem in (M. Kadowaki, 2009) and with decision outputs as generated power and unit committed

Other than those studies, in the interest to see the effects of optimization, this work is made simulation based. Different dynamic nonlinear models are introduced, which are called system simulation models. Responses of variables can be observed according to optimal control actions with those models. Furthermore, this work uses Sequential Quadratic Programming (SQP) method to do constrained nonlinear optimization that comprises of optimizing production flow discharged by reservoir, handling of flood situation with floodgate control, higher accuracy of prediction of inflow to reservoir, as well as subject to various constraints. However, the electricity price market is not considered in the optimization. The main purpose of this work is to provide a possible capability of how much electrical power can be supplied for the market. The final power output should combine with consideration of the market requirement and the best profit it can make, which are not included in the work. At last, with this simulation based optimization work, optimized results for a specific hydropower plant are compared with its historical operation data and discussed.

4.1 System simulation models

Several simulation models are accomplished with optimization work. Reservoir model and floodgate model are calibrated and validated with real measurements. Forecasting and estimation inflow is briefly achieved with an unscented Kalman filter (UKF). Power generation model is included for calculation how much electricity can be produced.

4.1.1 Reservoir model

In this work, the optimizing object is the operation to a reservoir called Tokevatn, which is the main upstream reservoir for five cascaded hydropower plants. The tailor water reservoir is not considered, since lacking historical data, and assumed with a constant water level. A simple dynamic reservoir model of Tokevatn is:

$$\frac{dH_{up}}{dt} = \frac{1}{A_{R[H_{up}(t)]}} \cdot (Q_{in} - Q_{out}) \quad (4.1)$$

$$Q_{out} = Q_p + Q_s \quad (4.2)$$

This model is validated with reservoir storage measurements carried out by the hydropower supply company Skagerak, Norway. Area of Tokevatn is calculated as a function of reservoir elevation on the basis of water storage measurements. Unmeasured points are evaluated by interpolation method. The geometry of the reservoir is complex and lead the reservoir model to a nonlinear model.

4.1.2 Forecast inflow

Forecasting of inflow to the reservoir is not included in this work, but a forecast result of a so-called HBV model can be introduced to associate with the optimization process. Forecasting inflow is a common challenge for optimization of reservoir operation and brings many uncertainties to predict reservoir level. Different modern technologies are implemented to acquire an accurate forecasting in research works. There is a hydrology model, HBV model (Otnes.J, 1978), which is utilized by Skagerak to predict total inflow to Tokevatn with the information of rainfall, snow melting and runoff of branches. According to the rainfall information is updated by weather report every two hours, with HBV model, it is supposed to predict inflow at least two-hour ahead. Consequently, the simulation step of all the models is also made to every two hours. In favor of obtaining a more accurate forecasting, in this work, a UKF is implemented to modify the result of the HBV model. The inflow is treated as an unknown parameter to be estimated by this UKF where the state is the reservoir level.

4.1.3 Flood gate model

The floodgate is equipment that controlled to spill away water to specific water ways so that the reservoir level can maintain in a feasible operation zone. A simple sketch and

model is presented in (W. Zhou H. B., 2012 IEEE Power and Energy Society General Meeting) and as:

$$Q_s = \varepsilon \cdot OP \cdot A_G \cdot \sqrt{2 \cdot g \cdot \Delta H} \quad (4.3)$$

$$\Delta H = Z_U - Z_D, \quad Z_U = H_{up} \quad (4.4)$$

where Z_U and Z_D are the upstream and downstream reservoir level respectively.

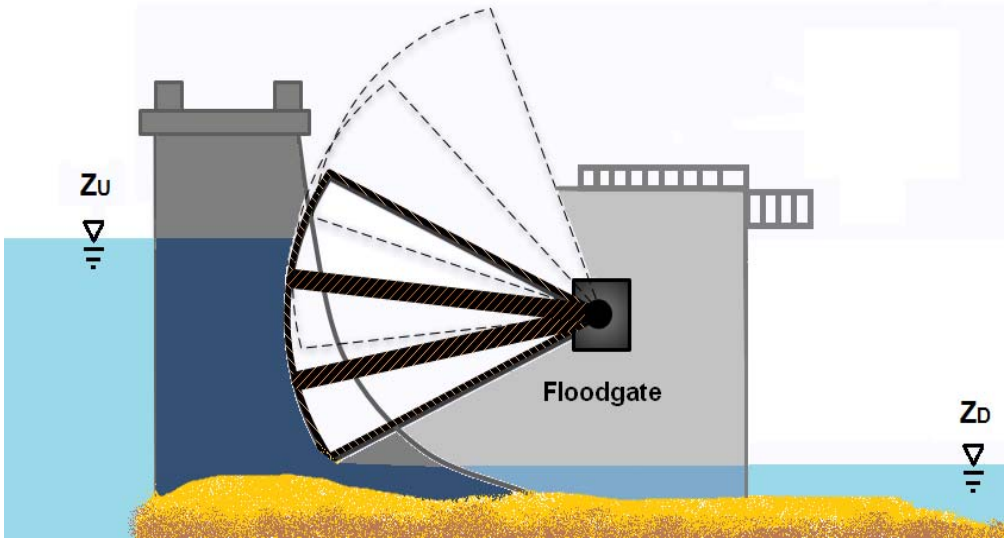

Figure 26. Illustration of a flood gate

This model is also validated with flow rate measurement depending on gate opening measurements carried out by Skagerak. Coefficient ε is determined to adapt the model to fit the real measurements. For submerged gate it will be in the range 0.3 -0.6 and for free discharge it is in the range 0.5 –0.7 (Lewin, 2001). Maximum capacity of flood gate is 1000 m^3/s.

$$\varepsilon \in \left[\frac{1000}{A_G \times \sqrt{2g \times 6.3}}, \frac{1000}{A_G \times \sqrt{2g \times 7.5}}\right]$$

This model also follows an assumption that there is no consideration of inverse flow from the discharging water ways back to the reservoir.

4.1.4 Power production model

A general mathematic model of power generation is presented in equation (2.13) and (2.14) . The net head in (2.14) is decided by upstream, downstream reservoir levels and the head loss throughout the whole process. Similar with upstream reservoir, there are also many uncertainties involved for determination of downstream elevation, like imponderable natural inflows, rainfall and snow melting. Besides, Tokevatn is also a common shared upstream reservoir by several hydropower plants. The potential flood of it can be spilled via guided paths to downstream reservoir or to natural rivers which can run into sea. As well as because lacking information or measurements of downstream reservoir, its elevation is assumed constant for modeling. So, the HBV is only implemented for the main upstream reservoir Tokevatn.

4.1.5 Production flow model

The mathematic model for discharged production flow by hydraulic turbine is in equation (2.15). There are normally several hydraulic turbines in one hydropower plant. The production flow and power generation model are included for calculation of a total power that one plant can generate. The production flow is treated as an output from the optimizer and a targeted total volume flow that can be manipulated and achieved by all together the hydraulic turbines. A detailed effective opening of each hydraulic turbine is not considered in this work.

4.2 Optimization process

This work aims at developing an optimizer for floodgate control to avoid flood and utilize floodwater efficiently for power production. On the other hand, this optimizer should also achieve the purpose of better operation of the reservoir to associate with the regulation of floodgate, so that a higher efficiency of water utilization can improve

electricity generation efficiency. However, with this optimizer, the reservoir operation is carried out without consideration of the electricity market and only brings out maximum electricity that can be generated under the conditions of handling flood optimally and abiding by specified operation zone. The function of the optimizer is illustrated in Figure 27. The work here only suggests a production flow that makes best use of water under the requirement of avoiding any water flooding to the surroundings of reservoir. The ultimate operation should be concerned with the market demanding and the best interest that it can make.

4.2.1 Challenges for optimization

There are some common challenges when optimization the operation of the reservoir. First, from the power generation model (2.13), with assuming downstream reservoir also equipped with a floodgate which can maintain its water level as a constant, it can be obviously found that power production is maximized when both upstream reservoir level and discharged production flow reach their maximum in meanwhile. However, that is not applicable when look at reservoir level dynamic model (4.1), (4.2). They are two conflicting objectives. When it refers to operation of reservoir, increasing production flow must lead to a lower water level. On the other hand, as for handling of flood, the higher reservoir level results in a higher risk to confront flood. However, more water spilled away also implies that less water is utilized for production. An effective way is to store flood water as much as possible to production of hydropower plant, simultaneously ensure the security for the neighbourhood. Thirdly, the optimizing object is power production in (2.13), where the manipulate variables are upstream reservoir level and production flow. However, referring to reservoir level, discharged flow and opening of floodgate are the manipulate variables, which can be seen from (4.1), (4.2), (4.3). Thus, optimization work can be treated as multiple inputs and single output problem shown in (2.15). Eventually, the power is the output, but the floodgate opening, and production flow are manipulated variables. How to make these two manipulate variables cooperate with each other is another problem in optimization.

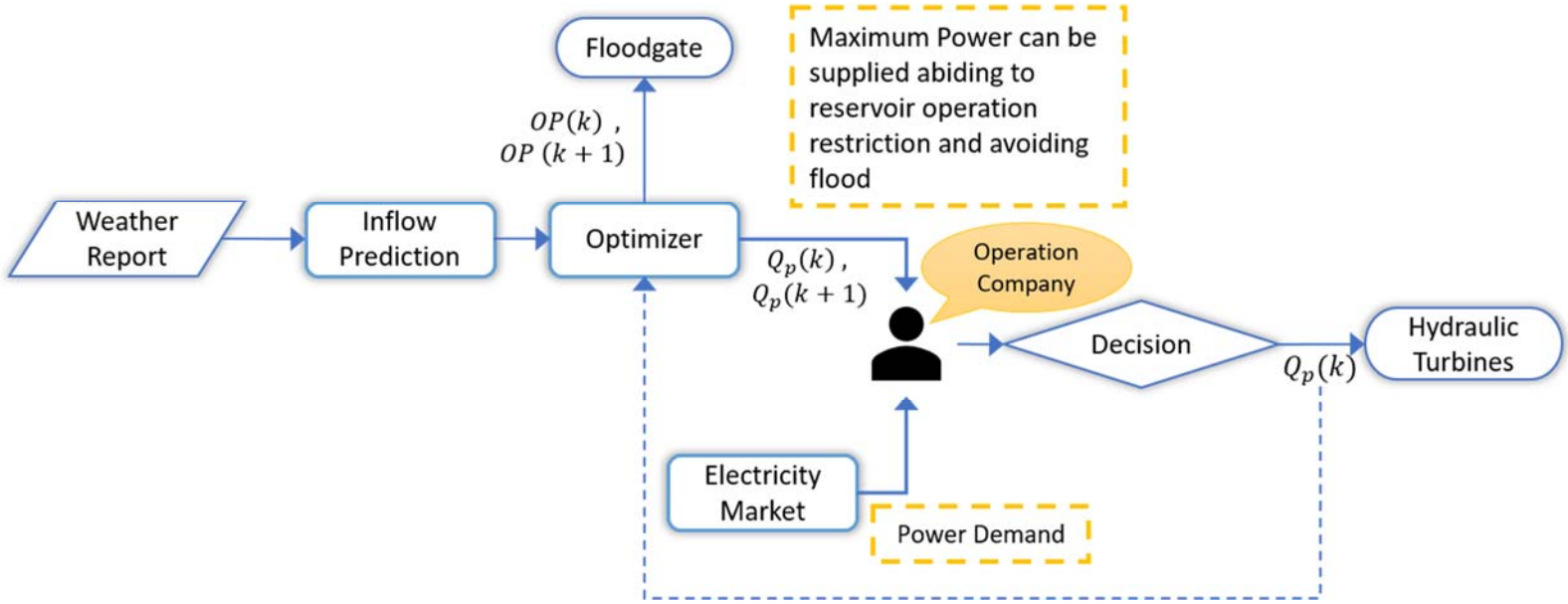

Figure 27 Illustration of optimizer function

4.2.2 Limitations

During the optimization process, different limitations are added for realistic consideration, e.g. reservoir level operation bounds, hydraulic turbine production flow bounds, bounds of spill away flow. Example: are explained in the following subsections.

4.2.2.1 Reservoir level bounds

Norwegian Water Resources and Energy Directorate (NVE) formulate a feasible operation zone for reservoir Tokevatn, which varies with season and rainfall of Norway throughout a year. As it is illustrated in Figure 28, from spring to autumn, the operation zone is stricter according to target of avoiding flood and storing water for dry seasons, whereas the allowed variation range is broad when it is autumn and winter, since it may be frozen and less inflow. These reservoir level bounds are set as level constraints for the optimal controller.

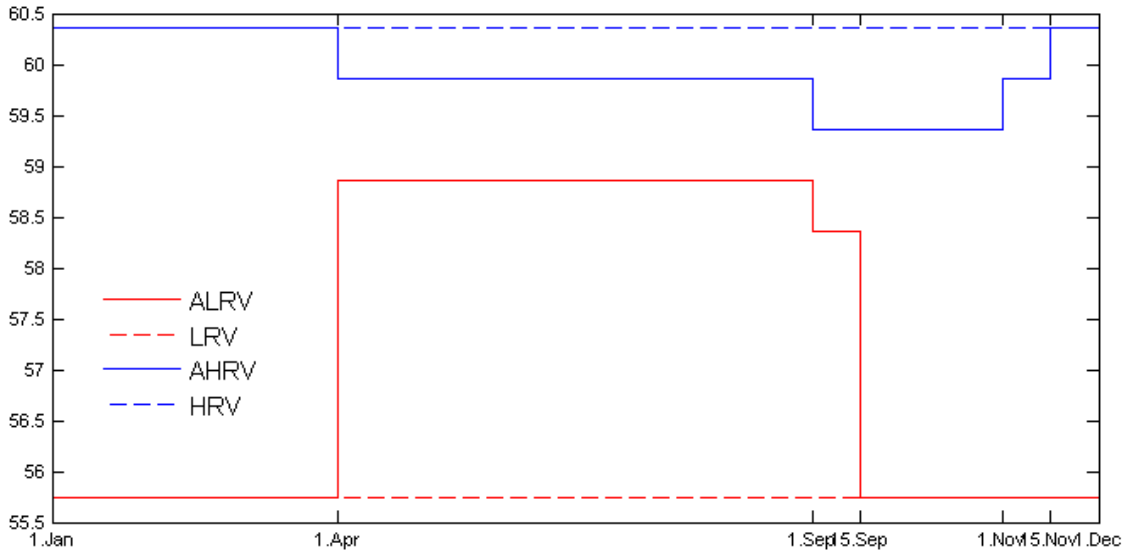

Figure 28. An example of Tokevatn reservoir operation constraints throughout a year

4.2.2.2 Production flow bounds

Discharged production flow should not exceed the capacity of hydropower plant by all means. Moreover, as to reservoir operation, any previous decision would cause

sequence results, which is the reason that reservoir operation needs a logical scheduling. In accordance with the habitual behaviour of electricity consumption, during night time, it uses up less power than during day time. Therefore, it is not necessary to keep the production as day time, which means less water is required to be discharged from reservoir. In this way, it also can maintain reservoir level higher and save rather more water for next day production.

4.2.2.3 Handling of flood and spill flow limitations

At Tokevatn, it experiences floods almost one third of a whole year. Water must be spilled away to a preplanned path when there is a big flood, to secure neighbourhood people and environment. Spill water ways and floodgates are built with this purpose. Two exactly same floodgates with total capacity 1000 m^3/s are implemented to reservoir Tokevatn. The discharge of those floodgates should be subject to this capacity. According to HBV model and weather forecast, it can predict natural inflow at least six hours forward. Therefore, floodgate control is established as a NMPC that release some water to prepare for flood and break off working to store more water when there is less inflow that not threaten overwhelming of reservoir. But this floodgate model based predict control is carried out without a fixed set point for reservoir elevation whereas only comply with the level bounds mentioned.

4.2.3 Priority assignment

To overcome those challenges for optimization of reservoir operation, an optimizer with priority assignment (PA) is proposed. Considering the uncertainties of downstream reservoir mentioned previously, the reservoir level control is not appropriate to be put in the first place. To give the production flow the highest control priority is more practical and straightforward. Then, to optimize is to maximize production flow with the purpose of increasing power generation as well as not exceeding any constraints. Under ensuring production flow, keep the elevation would be secondly important, not only because it affects power generation but also because it concerns how and when to prepare for flood. Two manipulate variables contributes to level control of the reservoir:

one is the production flow, the other is floodgate opening. As far as production flow is already decided by the highest priority, the opening of floodgate is assigned with a lower priority in the optimizer. By this priority assignment, floodgate predict-control is executed when and only when level tends to exceed the upper reservoir level limit. No matter production flow manipulation either floodgate manipulation, resulted reservoir level should always be restricted within operation zone made by NVE. In this way, upstream water level control and production flow control can be associated with each other, maximizing power generation and handling of flood can be realized at the same time, two manipulate variables can work simultaneously with proper steps.

4.2.4 Nonlinear optimization

Since the models are nonlinear, SQP method is applied for the optimization. Because of the conflict operation variables mentioned, in this work, *fminimax* function of MATLAB optimization toolbox is implemented, which is appointed to be companied with 'active-set' algorithm using Karush-Kuhn-Tucker conditions as necessary optimality conditions. To select 'active-set' algorithm is because it is effective on problems with non-smooth constraints and can take large steps. As it is discussed previously, the reservoir level constraints are with step changes during a year and the control step is 6 hours, therefore it is more appropriate to use 'active-set' algorithm than using 'sqp' algorithm directly. Those two algorithms in MATLAB are almost the same and both developed from sequential quadratic programming method. Furthermore, it can be deemed as a multi-objective optimization problem. If all the objectives are minimized or maximized simultaneously, there is normally no unique optimum. In general, solution of multi-objective optimization is a set of trade off points that satisfy the optimization model. Despite of it, with priority assignment, different objective functions are optimized sequentially, so it is not required for selection of those trade-off points. In a summary, the Optimization work comprises of reservoir level control with optimal controller, optimization of production flow discharged to hydraulic turbine, handling of flood situation with floodgate control.

4.2.4.1 Cost model

For consideration of increasing power production and preparing for flood, the first object function with the highest priority is:

$$\min_{-Q_p(k)} max\,(\boldsymbol{P}_m(k) = \eta \cdot \rho \cdot g \cdot H_{net}(k) \cdot Q_p(k)) \quad (4.5)$$

For consideration of safety issue to avoid flood, utilization of floodwater and power production, the second cost functions with lower priority is:

$$\min_{OP(k)} \max\left(H_{up} = \frac{1}{A[H_{up}(k)]} \cdot \left(Q_{in}(k) - Q_p(k) - \varepsilon \cdot OP(k) \cdot A_G \cdot \sqrt{2 \cdot g \cdot \left(H_{up}(k) - Z_D\right)} \cdot \Delta t\right) + H_{up}(k-1)\right) \quad (4.6)$$

Subjects to:

- Reservoir level operation bounds, $\mathrm{H_{up}}$:

$$H_{LRV} \leq H_{up}(k) \leq H_{HRV} \quad (4.7)$$

- Hydraulic turbine production flow bounds, $\mathrm{Q_p}$:

$$Q_{p\_min} \leq Q_p(k) \leq Q_{p\_max} \quad (4.8)$$

- Spill away flow limitations, $\mathrm{Q_S}$:

$$Q_{S\_min} \leq Q_S(k) \leq Q_{S\_max} \quad (4.9)$$

- Flood gate opening bounds, OP:

$$OP_{min} \leq OP(k) \leq OP_{max} \quad (4.10)$$

4.2.4.2 Optimization process

The whole working procedure is shown in Figure 29. The red blocks are the main process elements. The blue ones are sub-functions that included in main process. Yellow blocks are constraints added to optimization. Estimated inflow is acquired from UKF for HBV model. It can estimate inflow at least one-time step forward and the reservoir level as well, thus it assists in floodgate predictive control. The cost model is implemented with PA. It decides the value of the manipulate variables, and then output them to simulation model. With knowledge of them and the value of current estimated inflow, simulation model can resolve reservoir level. Eventually, power production model can simulate how much mechanical power can be supplied to electric power generation.

4.3 Results and discussion

- Study case: Dalsfoss hydropower plant which is the first plant with other four cascaded hydropower plants sharing the reservoir Tokevatn. Dalsfoss has three Francis turbine units with a capacity of 6.2Mw. The average generation of it is 32Gwh during a year. There are two floodgates located beside Tokevatn with a total spilling capacity of 1000 m^3/s
- Simulation time step: 2 hours. Because the surface of reservoir is huge, it takes time to make any measurable small change to the reservoir level.
- Control time step: 6 hours.
- Duration: 3 days
- Production flow limits: $5m^3/s$ to $40m^3/s$
- Reservoir level limits: 58.85m to 59.85m

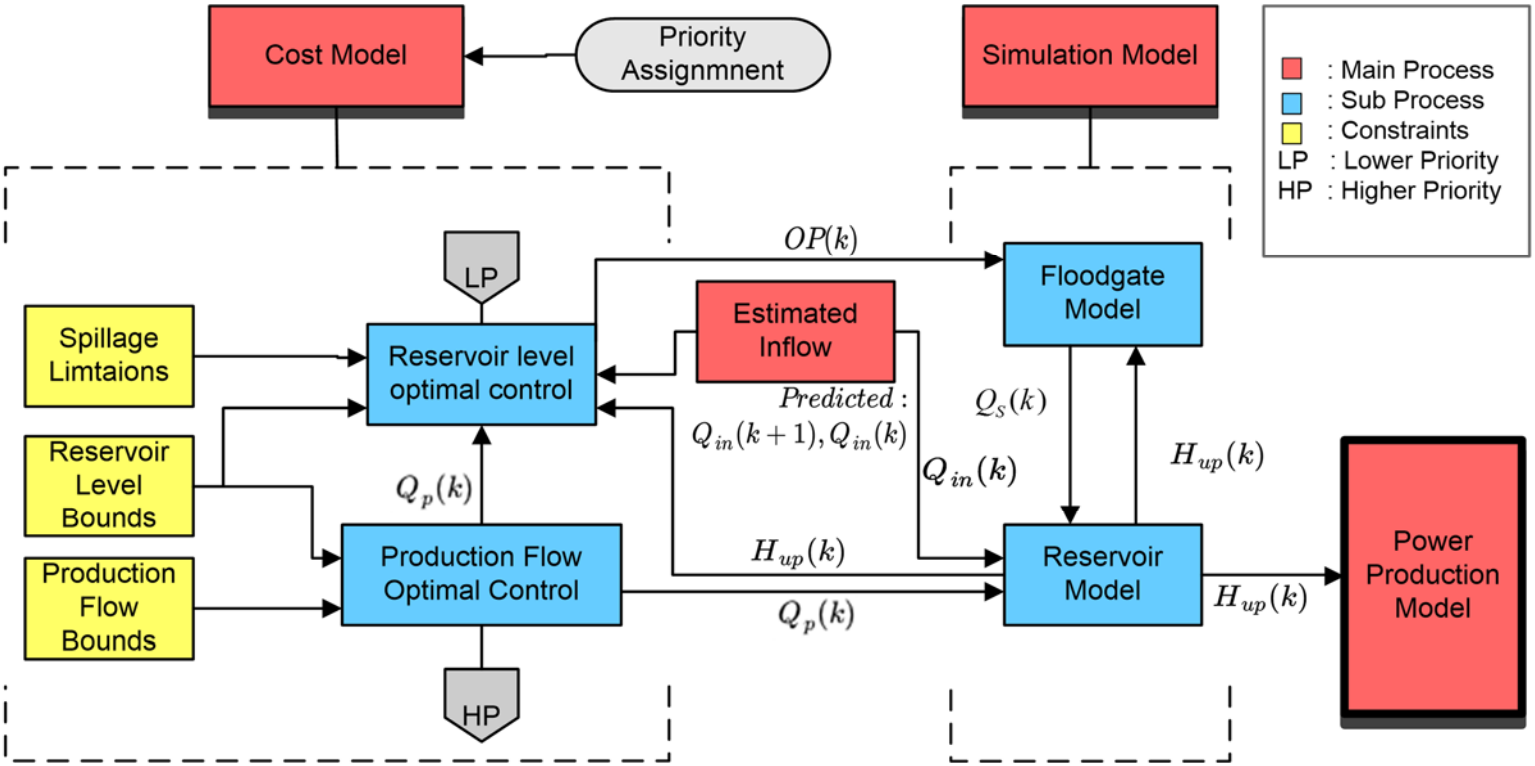

Figure 29 Optimization process

4.3.1 Scenario one: flood situation

A simple simulation for three days ahead experiencing extreme flood is made to demonstrate how the optimizer working and to present the results it can achieve. The inflow is simulated by step changes with white noise and estimated by UKF, which is shown in Figure 30. Resulted reservoir level and production flow are presented in Figure 31, and floodgate control result is in Figure 32. The best variation zone of reservoir level is from 58.85 to 59.85 in this scenario as in summer time. On the first day, it is initialized with production flow 15 m^3/s and reservoir level 59.5m as can be seen in Figure 31. After the initialization, because reservoir level is far from LRV, as well as the production flow is assigned with higher priority, optimizer decides to discharge more water to hydraulic turbine, which can reach the maximum production capacity 40m^3/s which is shown in Figure 31.

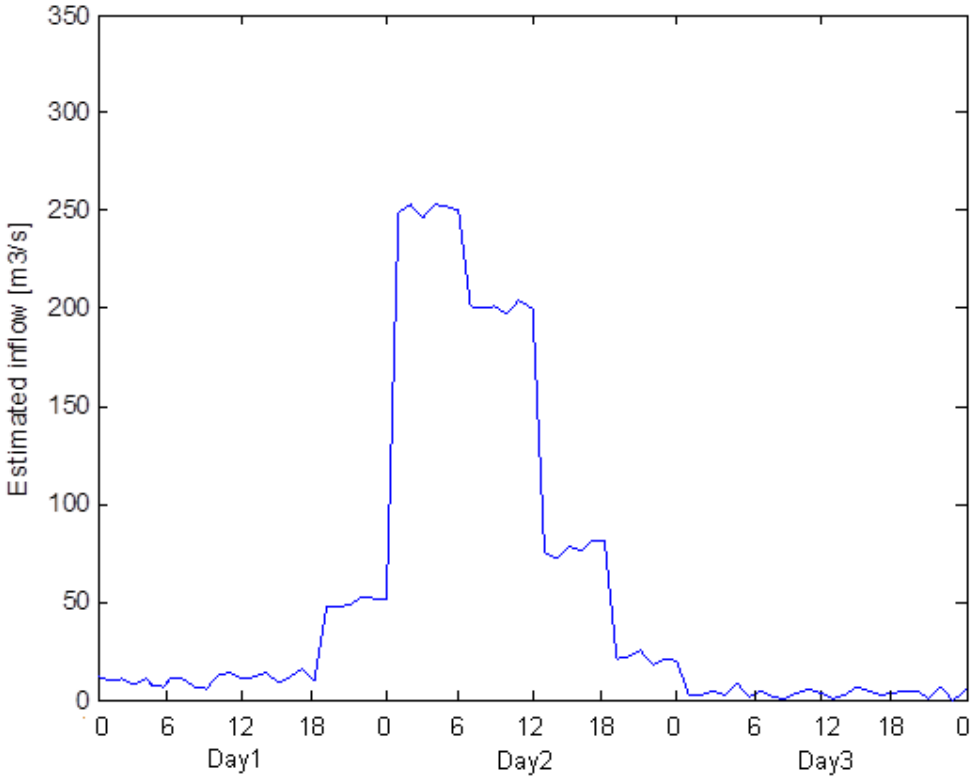

Figure 30. Estimated inflow of reservoir for scenario one: flood situation

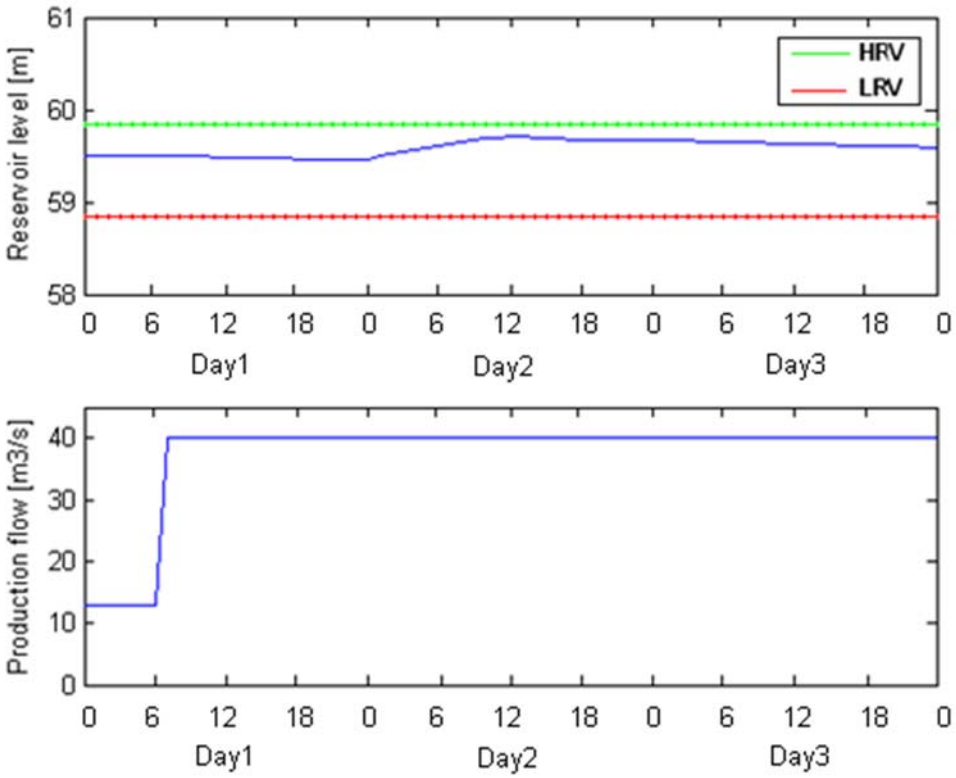

Figure 31. Optimized reservoir level and production flow of scenario one: flood situation

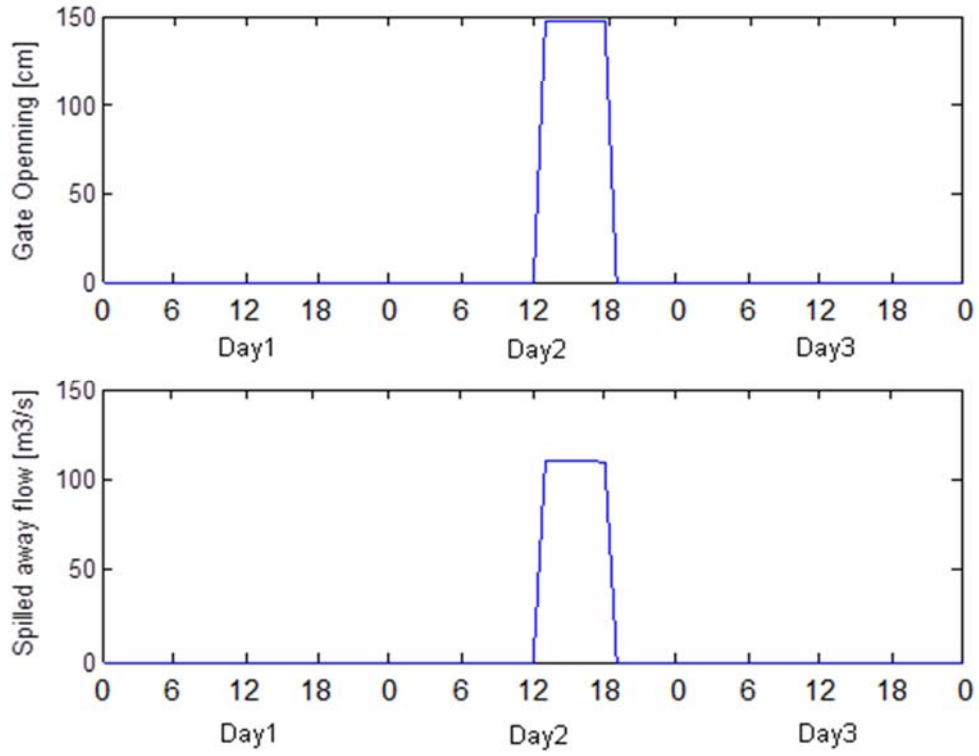

Figure 32. Floodgate opening and spilled away flow of scenario one: flood situation

On second day, there is an extreme flood up to 250m^3/s, as shown in Figure 30,that lasts from 06:00 to 18:00. The production flow is certainly at its maxima since massive water can be utilized, while the floodgate can be found only be activated when reservoir level approaching to the risk level. The flood happens from midnight. But during the period clock 0:00 to 12:00, the floodgate is closed, so it can store water for power generation. At clock 12:00, the predictive controller of floodgate senses that if it does not begin to open, the water would overflow and hazard neighbour. Therefore, it makes the floodgate opened to 149cm, seen in Figure 32, synthesizing the intention of maintaining a rather high reservoir level. However, there is still a persistently big inflow and level is still approaching to HRV, so the predictive controller keeps opening to floodgate to avoid overflowing. From clock 18:00, the floodgate breaks off working to keep zero opening because of less inflow and reservoir level in safe range. On day three, after the flood, even with less water flow into reservoir, it is enough to keep the maximum production flow discharged to hydraulic turbine. The floodgate is assuredly not opened since without any risk of overflow.

This simulation has shown that with PA, production flow control is considered on the first place and reservoir level manipulation is considered afterwards. When there is any inflow, it always increases the production flow firstly like the simulation of day one. The optimizer can manage to discharge production flow to hydraulic turbine as much as possible if reservoir level does not approach to LRV. What is more distinctly advanced with the optimization in this scenario and also has been demonstrated, in a flood situation, the floodgate predictive controller only output an opening when it happens to be dangerous to overflow. The rest time, floodgate suspends working so as to accumulate more water for power production.

In this simulation, totally around 15Mm^3 volume water flew into reservoir. Approximately 4.58Mm^3 volume water was utilized for power production and 2.76 Mm^3 water was spilled away. The rest water was stored in reservoir. As a result, this optimization with PA can use the flood water as much as possible. In other words, it can

realize a higher utilization efficiency of water and then increase the efficiency of hydropower plant.

With the same inflow series, another simulation is made to compare the reservoir operation with optimizer and a NMPC control with a fix setpoint for reservoir level to handle flood, which is shown in Figure 32 and Figure 33. The setpoint is decided as the central line of the level constraints to have some space preparing for flood or avoid running down out of the lower limit if it is a dry situation in future. Then, it consequently spilled away more water to track the setpoint. There is around 13Mm^3 water is spilled away in this case.

It can be seen that the operation with optimizer is more flexible with assuring power production and handling flood. More water can be utilized for production with the optimizer. As a result, this optimization with PA can use the stored water as much as possible. In other words, it can realize a higher utilization efficiency of water and then increase the efficiency of hydropower plant.

4.3.2 Scenario two: dry situation

Another simulation is demonstrated under a circumstance of a dry situation. The best operation zone of reservoir level is decided as from 58.85m to 59.85m, which is the same with last simulation. The estimated inflow by UKF is shown in Figure 34, resulting reservoir level and production flow are presented in Figure 35, and floodgate control result is in Figure 36. It is initialized with 12 m^3/s for production flow and 59 m for reservoir level. On the first day, the inflow is only around 10 m^3/s, and the level is near LRV. Towards the purpose to avoid being out of the specified operation zone, the optimal controller of production flow reduced it to the minimum 5 m^3/s as in Figure 35.

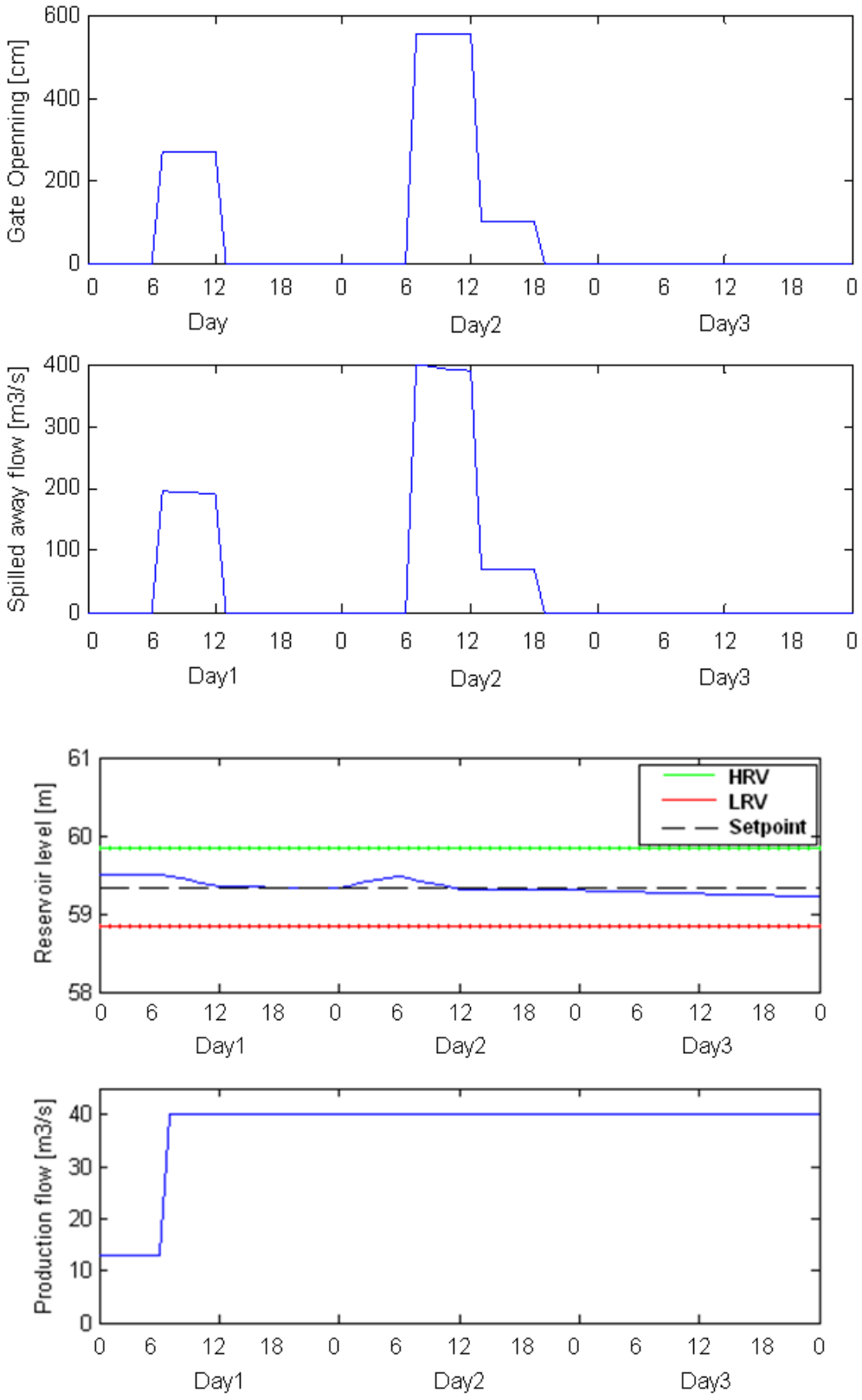

Figure 33. Operation with a fix setpoint

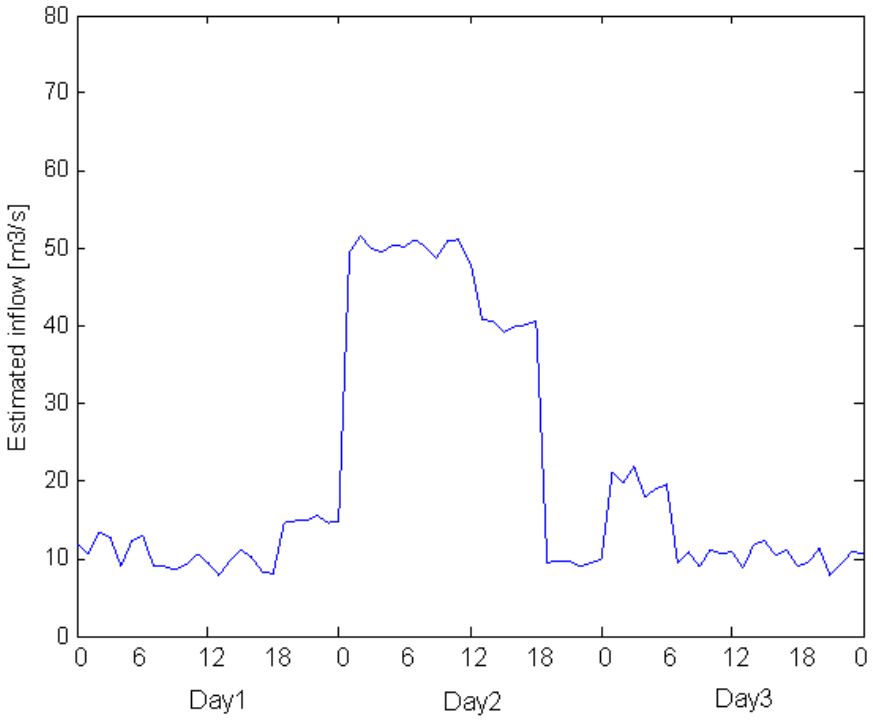

Figure 34. Estimated inflow of reservoir for scenario two: dry situation

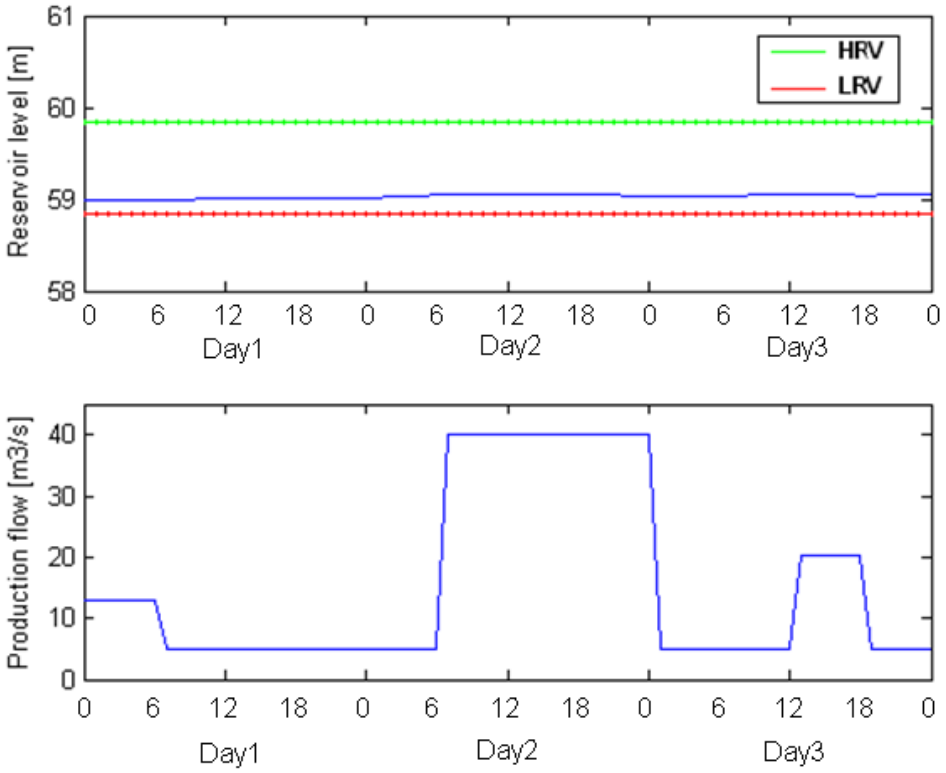

Figure 35. Optimized reservoir level and production flow of scenario two: dry situation

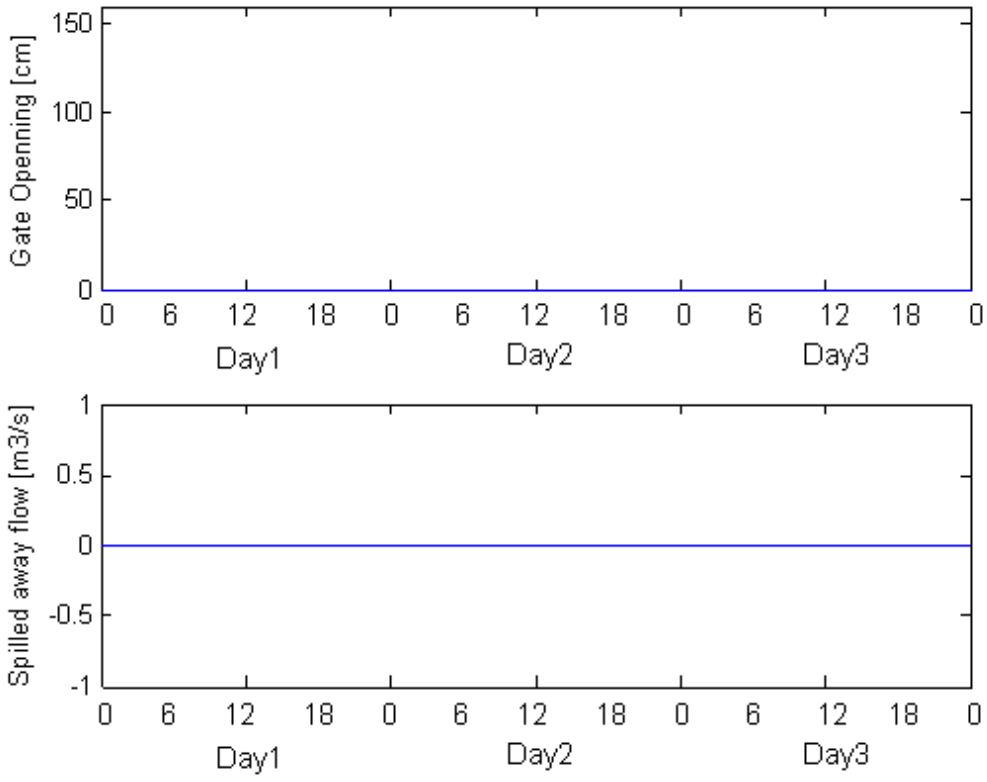

Figure 36. Floodgate opening and spilled away flow of scenario two: dry situation

On second day, there is more inflow and correspondingly reservoir level raised little, and then the production flow is manipulated to offer more water to hydraulic turbine. The production flow is made to its maxima during this day. On the third day, because it was maintained with maximum capacity on previous day, less water available in reservoir. but in the period from clock 0:00 to 06:00, water flew into reservoir with a rate of around 20 m^3/s, thus production flow was decided to be 20 m^3/s in control interval from 12:00 to 18:00.

Throughout these three days, floodgate is always kept closed because of seldom water can be available for production, shown in Figure 36. If floodgate is opened any, it definitely will make lower utilization efficiency of water.

In this simulation, it can be seen that the production flow has been manipulated according to the requirement of keeping the reservoir level in the specified zone and response to various inflow. It also has shown floodgate does not open in dry situation.

This scenario has also presented the work procedure of PA. When there is any inflow, production flow is enhanced first of all. If it is without a priority assignment, it could have maintained production flow and let the reservoir level increased which is contrast with the simulation of day one. But the risk to do so is from the uncertainties on the level of downstream reservoir. It may happen that even increased upstream reservoir level would not help to increase power production, because downstream reservoir level was also increased. To maximize production flow skips those uncertainties and is more straightforward.

4.3.3 Comparison with historical data

In the interest to see the achievements of the optimizer, simulations are made to compare the optimization results and the historical operation record under the same circumstance. The inflow input to optimizer is from the historical data, not necessarily estimated from the weather forecast, but the weather prediction step is still six hours forward. The assumption of the downstream reservoir level and all the other parameters are applied with exactly the same values in both two cases. In this way, all the conditions are set to be identical for the calculation of power generation for the simulation with optimizer and history without optimizer so as to make them comparable. Moreover, the initializations of them are also set to be identical. Only the operation of reservoir, which includes discharging production flow and regulation of reservoir level, would make different effects to provide the mechanical power for electrical power generation.

- Normal operation

The August in year 2009 is selected as the comparing object, because it was in summer when the hydropower plant normally keeps the maximum production. Furthermore, there is no big flood in this month. Therefore, it can distinguish scheduling function of the optimizer.

Sequential operation throughout the month is show in Figure 37. The resulted reservoir level and discharged production flow are presented. The general operation trend of the

simulation with optimizer is similar with historical record, but more flexible. It can be seen that with optimizer, when the reservoir is not to approach to the LRV, the production flow keeps its possible maxima. Whereas, when it is going to be close to LRV, the optimizer outputs a minimal production flow. Even though sometimes the production flow or reservoir level is lower than historic, it can acquire a relatively high level or big production flow later.

Daily electrical power production is calculated with same turbine efficiency for both two cases and presented in Figure 38. During the first 10 days, because of a comparatively small production flow under the purpose of avoiding too low reservoir level, the generated power is less than the historical operation. But from the 11th of August, more water flew in, which can be seen from the inflow information in Figure 39, and correspondingly more water is discharged for power production. In addition, because operation with optimizer released less water and stored more before, it maintained a higher level than historical operation. Thus, during period from 11th till 20th August, operation with optimizer can offer more electrical power. After 20th August, the operation with optimizer got a rather low reservoir level, however it still can produce comparable electrical power. On the other hand, the historical operation reduced production flow because of less inflow. In this simulation, there is no big inflow that can cause a flood, so floodgate didn't work during the period.

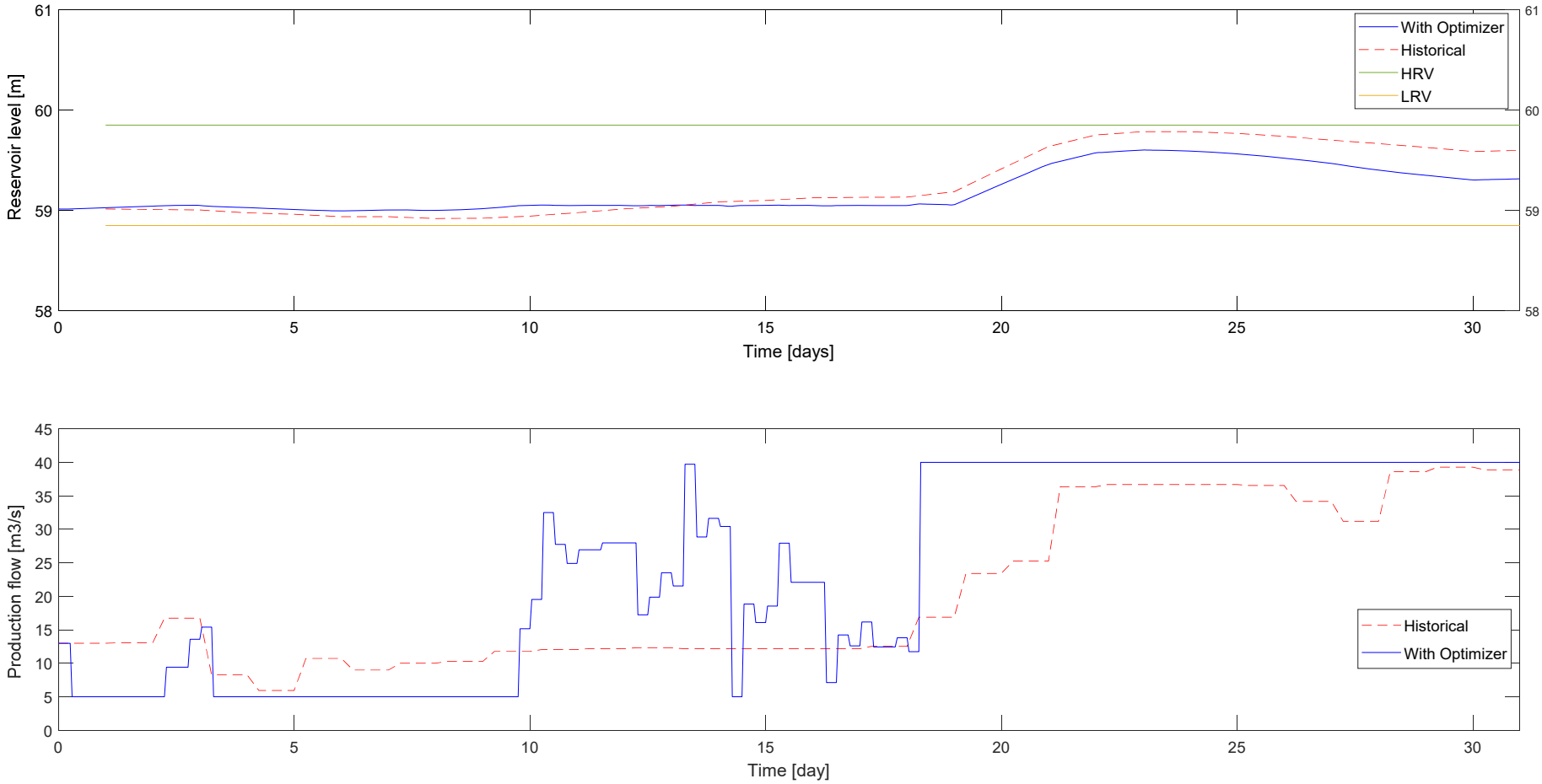

Figure 37. Sequential operation made by optimizer against history record for August 2009

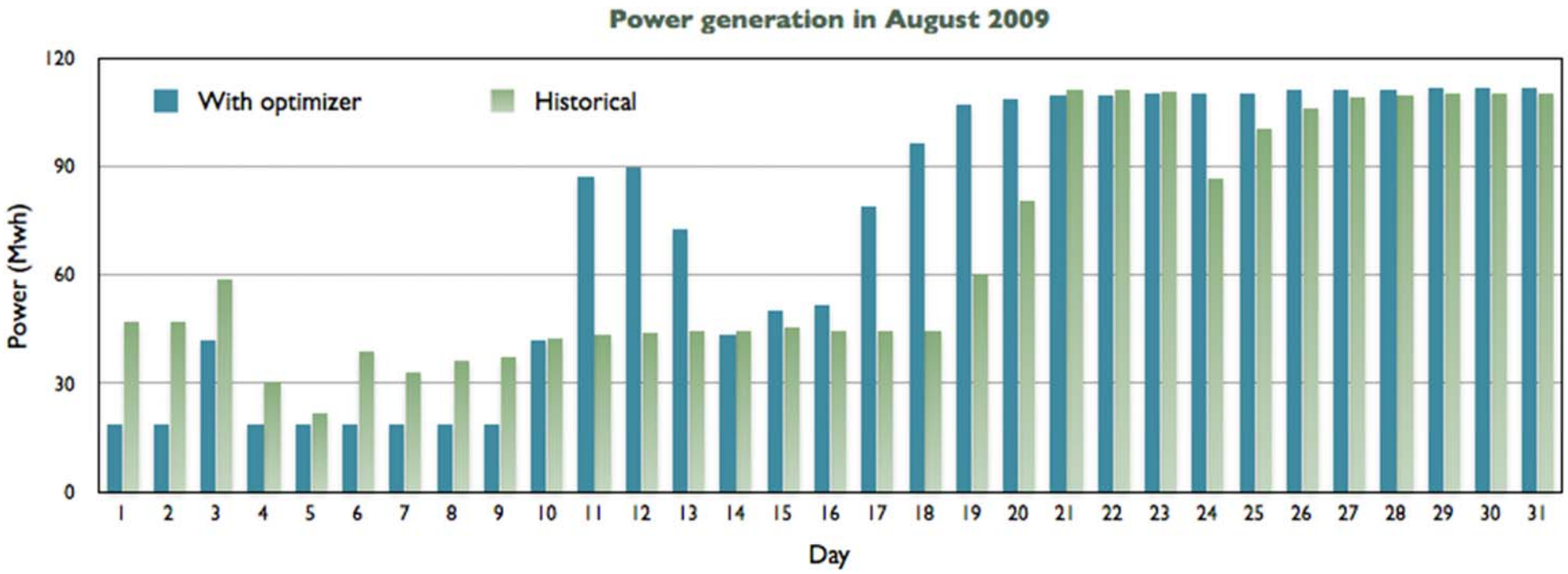

Figure 38 Power generation comparison between with optimizer and history record

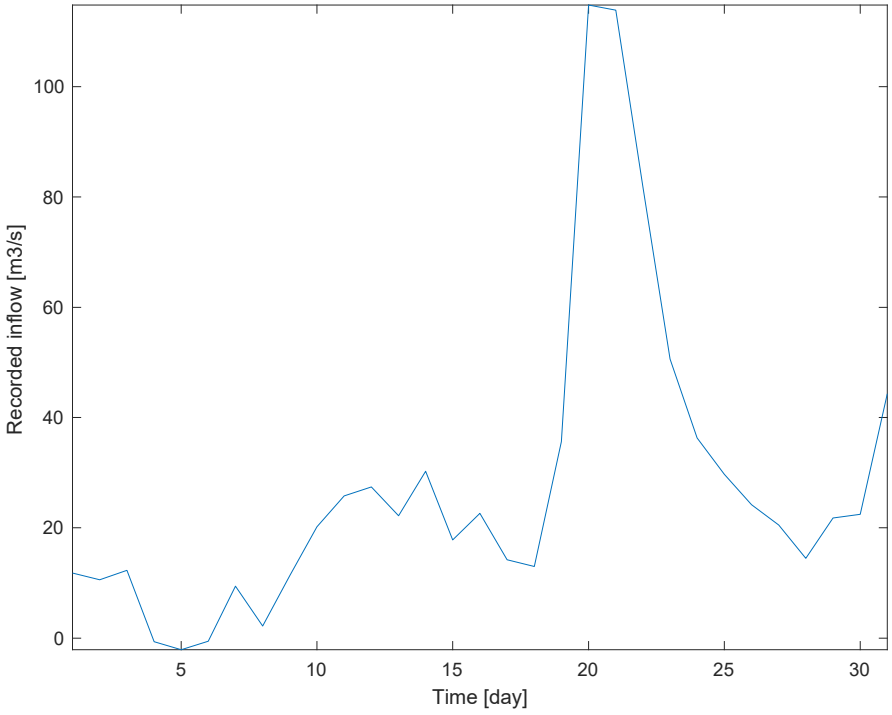

Figure 39. Recorded inflow of August 2009

With Optimizer, total generated electrical power is 2.3159Gwh, and the Historical data is 2.0623Gwh for August in 2009. Because this optimizer does not consider the electricity market, from 10th to 15th August, it indicates there is more power can be generated. However, the historical operation was carried out according to market demand, so there are some differences on the reservoir operations. Since the total energy offered by reservoir for two cases is same, if it transferred less to electricity production before, it will save more energy for later. Therefore, with optimizer, it results in a lower reservoir level at the end of this period. Without further weather prediction, it probably left less energy. But paradoxically, it also left more space to store floodwater for next month. The importance of preparing for flood and saving energy for future depends on season and inflow. A more varied level constraint decided by temporal predicted inflow can help with better operation with different purposes. This simulation can only say the optimizer can give an effective reference reservoir operation for power generation satisfying the level restrictions. Final operation should take electricity market into account.

- Flood regulation

Another historical operation is introduced for comparing with optimized operation under a flood situation. The comparison duration is also extended so as to see the responses of operations when there is a step change of constraint. A hundred days from 10th of March to 18th of June in 2009 are selected as the study objective, which presented an ordinary condition during spring and summer. The constraints are shifted from [55.75, 60.35] to [58.85, 59.85] on 1st April. It has shown in Figure 40 that the optimizer can bring the reservoir level back to best operation region two or three days earlier than historical operation when the constraints are changed. It should be mentioned that how fast the reservoir level track the operation region also depends on the weather condition, not merely related with reservoir operation.

Besides, it can be seen that the operation with optimizer abides by the best operation zone more strictly. According to the requirement of rejecting flood to surroundings, it is better to keep the reservoir level in target operation region, even though higher reservoir level implies more power production. As a result, the optimizer made decision that floodgate spilled away some water to avoiding flood, when the water level is approaching HRV, as it is shown in Figure 41.

Because the historical operation accumulated more water for production, which exceeded the level constraints, more electricity can be generated. There is no comparison for power production between historical and optimized operation, since the two cases are under unequal conditions. This simulation has shown, if there is any risky flood, the optimization will abide by the operation region better than the history record and reduced the possibilities of experiencing flood.

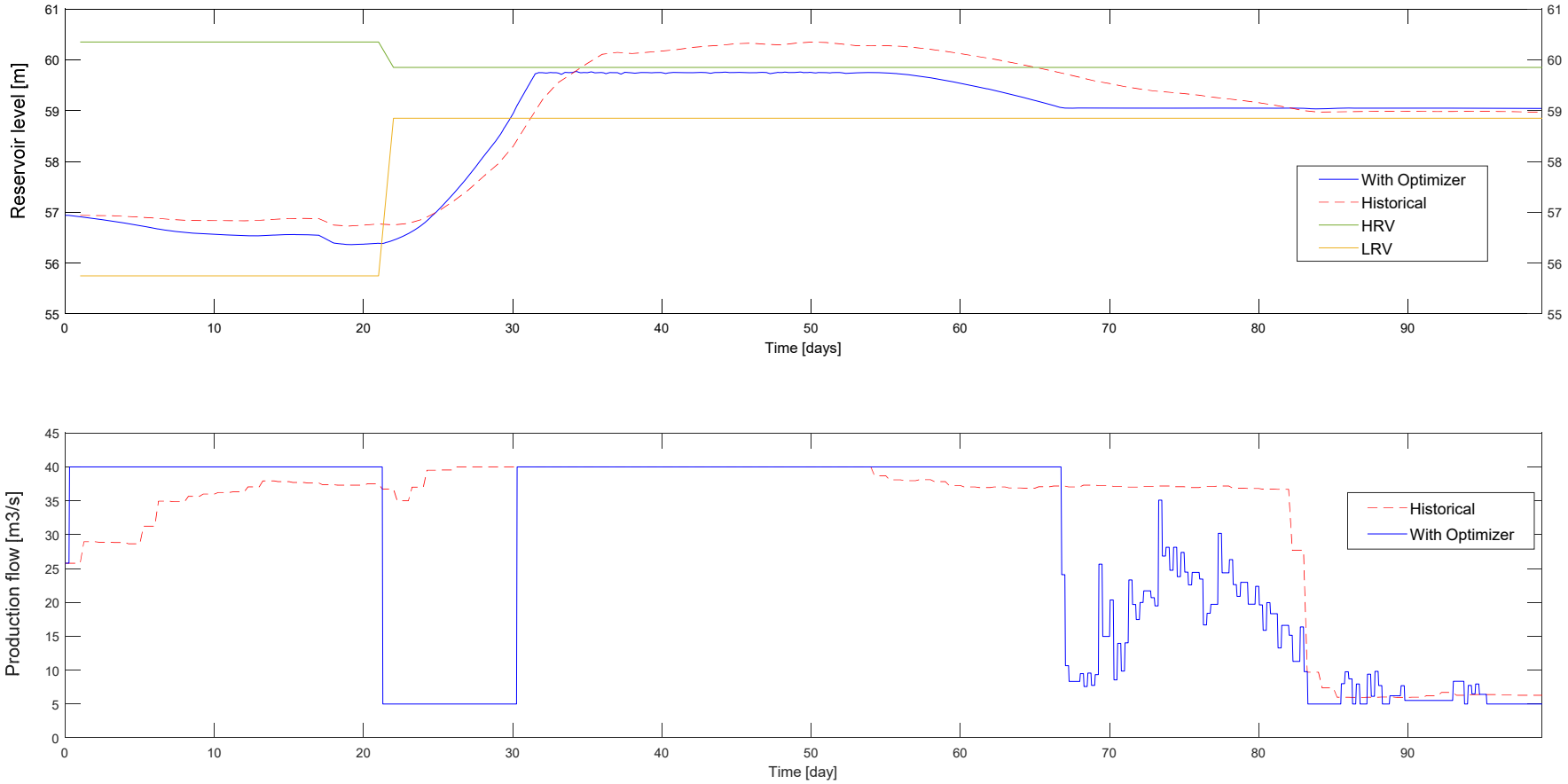

Figure 40. Sequential operation made by optimizer against history record for 10th March to 18th June 2009

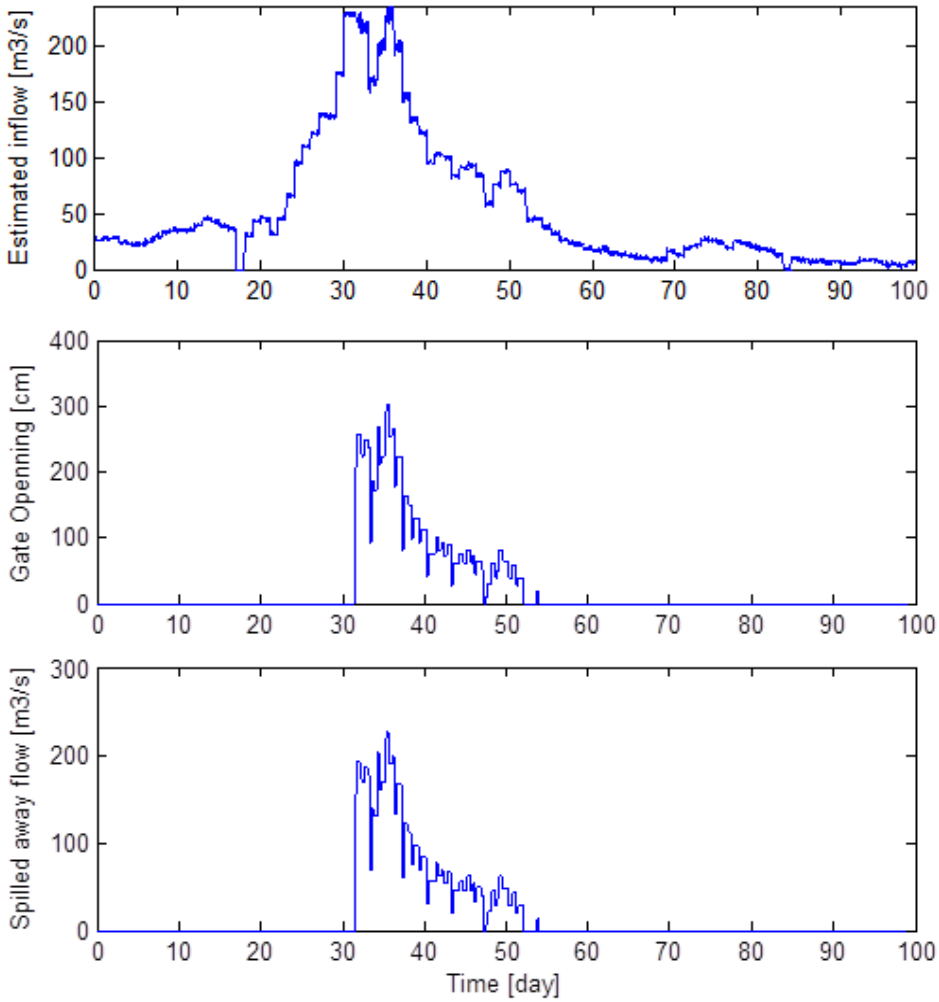

Figure 41. Estimated inflow (Top) and optimal floodgate control results on gate opening (Middle) and its corresponding spilled flow (Bottom)

4.4 Conclusion

This work has presented an optimizer that can simultaneously manage to handle flood effectively and utilize floodwater for power production as much as possible through an optimal reservoir operation. This optimizer is made as simulation based and comprises of optimal control with priority assignment for reservoir level and production flow, floodgate control. A nonlinear constrained optimization process with the optimizer is implemented and solved by SQP method. Dry and flood scenario are simulated to clarify the optimization process, which has shown the abilities of the optimizer to keep reservoir level in feasible and predefined operation zone, to maximize and maintain

discharging production flow, and to avoid flood. Furthermore, the optimizer is also carried out to historical data to compare the operation results. It has presented that, operation with optimizer can give an effective reference reservoir operation which should also consider electricity market, can track reservoir level operation zone faster when it changes with different seasons, and can manage the reservoir level abide by the variation limitations more strictly. Even though the electricity market is not considered, the optimizer still can give a reference operation that is better for avoiding flood and optimizing power production.

5 Conclusion

This study has focused on exploring new technical applications on a traditional industry. Diverse mathematical models, state estimations, nonlinear model predictive control and optimizations have been applied and illustrated their benefits for hydropower generation.

When modelling a hydropower plant, a simple model has been developed as a basis throughout this PhD work. However, as concerning its simplification of PDE equations of penstock that may distort the overall modelling result, other advanced methods, such as FVM, MOC, EEC are introduced to examine the impacts of its deficiency. How to resolute the PDE model of penstock using these methods are detail deduced and demonstrated in this thesis. From the comparison, we can see, even neglecting certain amount of pressure loss over the whole penstock, simple method still represents similar water behaviour when operating turbines as the other methods, which means the simulation result of simple method can catch significant effects that are caused by any action been taken in hydropower plant. The simulation results of MOC, EEC and FVM are comparable, but with lower pressure rise from simple method because of the friction is detailed to each segment while their modeling. However, since MOC using linear approximates rather than ODE solver, its result behavior is more like a straight line, which also makes its difference from other methods. EEC and FVM result in similar pattern. EEC has relatively economic computation cost from FVM and more straightforward to understand. However, FVM is an alternative of FEM which is the most popular computational method for analysis any process. How to or to use which modelling for a process is quite depending on the intention. For this study, to develop an advanced controller for hydropower production is driving the candidate to choose simple method, due to the convenience to add a mathematic based controller.

Most of industry process are nonlinear, NMPC is then decided to be implemented for a hydropower plant. In general, hydropower plant can be considered as a MIMO system with mechanical power and excitation voltage as inputs, where the power frequency

and terminal voltage as outputs. The developed NMPC performs better results than conventional PI controller, which is illustrated in Chapter 3 that the variation of frequency and generated power by NMPC is smaller than PI. Aside of NMPC make the process more stable, Traditional PI controller also has its constraints for handling nonlinear process and the drawback of requiring tuning PI parameters, which make it less adaptive for extreme condition. Hydropower production process could be occasionally experiencing harsh weather, e.g. devastating storm, frozen. Considering this aspect, NMPC has its advantage with a prediction function.

In further, this study has examined the possibility to improve water utilization with a limitation of water reservoir geographical size. This part is to optimize the water inputs for power generation. To achieve the purposes of avoiding flood and reservoir drained out, an optimizer with upper and lower constraints has been developed. Compared its function against historical data. The results showed the optimizer used the water more efficiently. Even in dry season, the water still can be flow for power generation, in rain season, with manipulating flood gate more sensible, power generation is much more than reality.

6 Future Work

Suggestion for Modeling. Due to lacking data from an actual power plant, the developed mathematic models are only theoretically discussed and mutually compared. Future work would be use the real data to verify the models. Model fitting technics can be carried out for improvements.

Suggestion for NMPC. Even the NMPC has been implemented for power plant connecting to an infinite bus and small grid, the complexity of a large-scale grid is not studied in this work. How NMPC handling the start-up multi-units power generation after a large-scale black out would be interesting to see. Besides, same issue as modeling, NMPC is developed on a theoretical level and should be verified with physical power plant.

Suggestion for the nonlinear optimizer. Metrology data can be introduced for predicating the reservoir water amount further and better. Moreover, the power market and price can help the optimizer to output a commercial sensible power generation schedule. In this work, data treatment is quite rough, since there were very few historical data obtained. However, for future work, data science techniques would be beneficial for power generation scheduling study.

References

A. Faina, B. R. (2002). Tracking a ballistic target comparision of several nonlinear filters. *IEEE Transactions on Aerospace and Electronic Systems, 38*(3), 854-867.

A. Rahideh, M. S. (2012). Constrained output feedback model predictive control for nonlinear systems. *Control Engineering Practice, 18*, 431-443.

A. Ramírez-Arias, F. R. (2012). Multiobjective hierarchical control architecture for greenhouse crop growth. *Automatica, 48*, 490-498.

A. Romanenko, J. C. (2004). The unscented Kalman filter as an alternative to EKF for nonlinear state estimation: a simulation case study. *Computers and Chemical Engineering*, 347-355.

A. Tilmant, E. F. (2002). "Optimal operation of multipurpose reservoirs using flexible stochastic dynamic programming". *Applied Soft Computing, 2*, pp.61-74.

A.H. Grattfelder. L. Huser, P. D. (n.d.). Automatic control for hydroelectric power plants. *Control systems, Robotics and Automation, XVIII*.

Adetola V, D. D. (2009). Adaptive model predictive control for constrained nonlinear systems. *Systems & Control Letters, 11*, 320-326.

B. Aufderheide, V. Prasad, B. W. Bequette. (2001). A Comparison of Fundamental Model-Based and Multiple Model Predictive Control. *IEEE conference on decision and control*, (pp. 4836-4868).

B. Aufderheide, V. Prasad, B. W. Bequette. (2001). A Comparison of Fundamental Model-Based and Multiple Model Predictive Control. *IEEE conference on decision and control*, (pp. 4853-4868).

B. R. Maner, F. J. (1996). Nonlinear model predictive control of a simulated multivariable polymerization reactor using second-order Volterra models. *Automatica, 32*(9), 1285-1301.

B. R. Sharefi, W. B. (2010). The effect of compressibility of water and elasticity of penstock walls on the behavior of a high head hydropower station. *52th Int. Conference SIMS.*

B.Strah, O. Z. (2005). Speed and Actie Power Control of Hydro Turbine Unit. *IEEE Transactions on Energy Conversion*, 424 - 434 .

C. Buskens, H. M. (2000). SQP-method for solving optimal control problems with control and state constraints: adjoint variables, sensitivity analysis and real-time control. *Journal of Computational and Applied Mathematics, 120*(1-2).

Chung, T. J. (2002). *Computational Fluid Dynamics.* Cambridge, UK: Cambridge University Press.

D. Dougherty, D. Cooper. (2003). A practical multiple model adaptive strategy for multivariable model predictive control. *Control Engineering Practice, 11*, 649-664.

D. Dougherty, D. Cooper. (2003). A practical multiple model adaptive strategy for multivariable model predictive control. *Control Engineering Practice, 11*, 649-664.

D. Edouard, P. D. (2005). Observer based multivariable control of a catalytic reverse flow reactor: comparison between LQR and MPC approaches. *Computers and Chemical Engineering, 29*, 851-865.

D.W. Watkins Jr., L. M. (2000). “A scenario-based stochastic programming model for water supplies from the highland lakes”. *International Transactions in Operational Research,, 7*(3), pp. 211–230.

E. Ghamahermani, I. K. (2011). Online State Estimation of a Synchronous Generator Using Unscented Kalman Filter From Phasor Measurements Units. *IEEE Transaction on energy conversion, 26*(4), 1099-1108.

E.A. Wan, R. V. (2000). The unscented Kalman filter for nonliear estimation. *Adaptive Systems for Signal Processing, Communications, and Control Symposium*, (pp. 153-158).

Farkas, I. (2005). Modelling and control in agricultural processes. *Computers and Electronics in Agriculture, 49*(3), 315-316.

G. Chowdhary, R. J. (2010). Aerodynamic parameter estimation from flight data applying extended and unscented Kalman filter. *Aerospace Science and Technology, 14*, 106-117.

H. K. Versteeg, W. M. (1995). *An Introduction to Computational Fluid Dynamics: The Finite Volume Method.* Longman.

H.L.Zeynelgi, A. (2002). Modelling and Simulation of synchronous machine transient analysis using Simulink. *International Journal of Electrical Engineering Education, 39*(4).

Hannett, L., Feltes, J., Fardanesh, B., & Crean, W. (1999). Modeling and control tuning of a hydro station with units sharing a common penstock section. *Power Systems, IEEE Transactions, 14*(4), pp.1407-1414.

IEEE Power & Energy Society. (1992). Hydraulic turbine and turbine control models for system dynamic studies. *IEEE Transactions on Power Systems, 7*(1), 167-179.

J. K. Gruber, D. R. (2009). Control of a pilot plant using QP based min–max predictive control. *Control Engineering Practice, 17*, 1358-1366.

J. Robert Eaton, E. C. (1983). *Electric Power Transmission Systems.* Englewood Cliffs: Prentice-Hall.

J. Z. Wan, M. V. (2004). Efficient scheduled stabilizing output feedback model predictive control for constrained nonlinear systems. *IEEE Transaction on Automatic Control, 49*(7), 1172-1177.

J.T. Needham, D. W. (2000). Linear Programming for Flood Control on the Iowa and Des Moines Rivers. *Journal of Water Resources Planning and Management, 126*(3), pp.118-127.

Jan Machowski, J. J. (2008). *Power System Dynamics, Stability and Control.* UK: John Wiley & Sons, Ltd. 455.

K. Reznicek, C. C. (1991). "Stochastic modeling of reservoir operations". *European Journal of Operational Research,, 50*(3).

K. Xiong, H. Z. (2006). Performance evaluation of UKF-based onlinear filtering. *Automatica, 42*, 261-270.

K. Xiong, L. L. (2009). Modified unscented Kalman filter and its application in autonomous satellite navigation. *Aerospace Science and Technology, 13*, 238-246.

Kjølle, A. (2001). *Hydropower in Norway, Mechanical Equaipment* (Vol. Chapter 1.7). Norwegian University of Science and Technology.

L. Grüne, J. P. (2011). *Nonlinear Model Predictive Control: Theory and Algorithms.* Spriner.

Lewin, J. (2001). *"Hydraulic Gates and Valves in Free Surface Flow and Submerged Outlets".* London: Thomas Telford Ltd.

Lu JZ. (2003). Challenging control problems and emerging technologies in enterprise optimization. *Control Engineering Practice, 11*, 847-858.

M. Boutayeb, D. A. (1999). A strong tracking extended Kalman observer for nonlinear discrete-time systems. *IEEE Transactions on Automatic Control, 44*(8), 1550-1556.

M. Kadowaki, T. O. (2009). “Short-term hydropower scheduling via an optimization-simulation decomposition approach”. *IEEE Bucharest Power Tech Conference proceedings.* Bucharest.

M.Aasen, H. W. (2010). The EU electricity disclosure from the business perspective-A study from Norway. *38*, 7923.

M.H. Afshar, M. R. (2009). Simulation of transient flow in pipeline systems due to load rejection and load acceptance by hydroelectric power plants. *International Journal of Mechanical Sciences*.

M.R. Piekutowski, T. L. (1994). Optimal short-term scheduling for a large-scale cascaded hydro system. *IEEE Transaction on power system, 9*, pp.805-811.

Milano, F. (2010). *Power System Modelling and Scripting.* Springer.

N. Daraoui, P. D. (2010). Model predictive control during drying stage of lyophilisation. *Control Engineering Practice, 18*, 483-494.

Otnes.J, R. (1978). ”Hydrologi i praksis”. *Ingeniørforlaget*.

P. Potocnik, I. G. (2002). Nonlinear model predictive control of a cutting process. *Neurocomputing, 43*, 107-126.

Park, R. (1929). Two-reaction theory of synchronous machines generalized method of analysis-part I . *AIEE Transactions, 48*, 716-727.

R. Kandepu, B. F. (2008). Applying the unscented Kalman filter for nonlinear state estimation. *Journal of Process Control, 18*, 753-768.

R. Turner, C. R. (2012). Model based learning of sigma points in unscented Kalman filtering. *Neurocomputing, 80*, 47-53.

R. Van der Merwe, E. W. (2004). Sigma-point Kalman filters for intergrated navigation. *60th Annual metting, Inst. of Navig*, (p. 56). Ohio.

S.J Qin, &. T. (2003). A survey of industrial model predictive control technology. *Control Engineering Practice, 11*(7), 733-764.

S.J. Julier, J. U. (2004). Unscented Kalman filter and nonlinear estimation. *Proceedings of IEEE* (pp. 401-422). IEEE.

S.J. Julier, J. U.-W. (2000). A new method for the nonlinear transformation of means and covariances in filters and estimators. *IEEE Transaction on Automatic Control, 45*(3), 477-482.

S.J.Qin, T. (2000). An overview of nonlinear model predictive control applications. *Nonlinear Model Predictive Control*, 369-392.

Sluis, P. (2008). *Electrical Power System Essentials.* John Wiley&Sons.

Tri C.S. W, N. S. (2010). MIMO model of an interacting series process for Robust MPC via System Identification. *ISA transactions, 49*, 335-347.

Vournas, C., & Zaharakis, A. (1993). Hydro turbine transfer functions with hydraulic coupling. *Energy Conversion, IEEE Transactions, vol.8*(3), pp.527-532.

W. Jiekang, Z. J. (2008). "A hybrid method for optimal scheduling of short-term electric power generation of cascaded hydroelectric plants based on particle swarm optimization and chance-constrained programming". *IEEE Transactions on power systems,, 23*, pp.1570-1569.

W. Zhou, B. G. (2012). Implementation of unscented Kalman filter for nonlinear state estimation in hydropower plant. *IEEE Powercon 2012.*

W. Zhou, H. B. (2012 IEEE Power and Energy Society General Meeting). "Application of Kalman filter based nonlinear MPC for Flood Gate control of Hydropower plant". *IEEE Power and Energy Society.* San Diego.

Wahba, E. (2009). Turbulence modeling for two-dimensional water hammer simulations in the low Reynolds number range. *Computers & Fluids, 38*, 1763–1770.

Wenjing Zhou, Bernt Lie, Bjorn Glemmestad. (2011). Modeling of a Typical High Head Power Plant. *World Congress on Engineering and Technology, IEEE, 2011.* Shanghai.

X. Liu, C. L. (2002). Analysis on oscillations between two generators in a hydro power plant and development of math model for a compound excitation sys. *Proc. 2002 Int. Conf. Power System Technology*, (pp. 1259–1263). Kunming, China.

Y. Cheng, Z. L. (2011). Optimized Selection of Sigma Points in the Unscented Kalman Filter. *Electrical and Control Engineering Conference*, (pp. 3073-3075).

Y. Xiang, Y. S. (2006). Optimization Theory and Methods- Nonlinear programming,. *Optimization and Its Applications, 1*.

Yoo, J.-H. (2009). “Maximization of hydropower generation through the application of a linear programming model”. *Journal of Hydrology, 379*, pp. 182–187.

Z. Wan, M. V. (2004). Efficient scheduled stabilizing output feedback model predictive control for constrained nonlinear systems. *IEEE Transaction on Automatic Control, 49*(7), 1172-1177.

Appendix A: Selected published papers

Paper A1

Modeling and Control of a Typical High Head Power Plant.

(World Congress on Engineering and Technology, IEEE, 2011)

Modelling and control of a typical high head hydropower plant

Wenjing Zhou, Behzad Rahimi Sharefi, Bernt Lie, Bjørn Glemmstad
Faculty of Technology, Department of Electrical Engineering, Information Technology and Cybernetics
Telemark University College, P. O. Box 203, N-3901
Porsgrunn, Norway

***Abstract*—This paper describes an effective mathematical model of a hydropower plant and how a decentralized control strategy for frequency and terminal voltage can be simulated. Several dynamic equations are presented for each hydraulic element of a typical high head hydropower with ODEs (ordinary differential equations), as well as a fourth order model of synchronous generator with exciter is proposed for the modelling of generated electrical power and terminal voltage. This paper merged these two models and eventually results in a MIMO system. The frequency and terminal voltage were chosen as the control objectives according to the quality of power. For the control strategy, a PI controller coupled with droop characteristics was implemented for the frequency, and a decentralized controller with stabilizer was applied to terminal voltage control. The interactions of these two controllers are simulated and analyzed. The simulation results are presented and discussed.**

I. INTRODUCTION

Hydropower is a renewable and safe energy compared to thermal and nuclear power. In Norway, hydropower covers close to 100% of the electricity production, so it is of interest to utilize this energy as efficiency as possible. With this purpose, it is important to develop models for hydropower system in a way suitable for developing modern control strategy. Such a modelling work is normally done separately either for mechanical power or the synchronous generator in the plant at present. Few simulations of their interactions have been carried out, and this is another purpose of modelling.

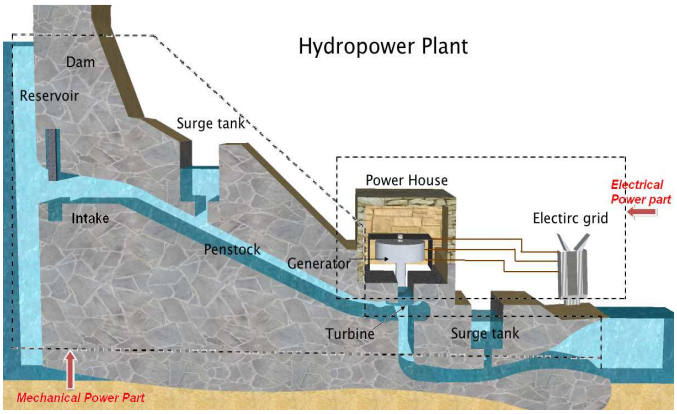

Figure1. Overview of a typical hydropower plant.

The plant in Figure 1 is a typical high head hydropower plant in Norway and also the modelling and control object of this paper. Normally, a dam is built after the water reservoir to accumulate water. At the intake, there always is a gate to control water flows from the reservoir to water conduits. This gate has been assumed opened with a constant value and ignored in modeling. The function of the surge tank is briefly to reduce water hammer pressure variations and keep the mass oscillations, caused by load changes, within acceptable limits and decrease the oscillations to stable operation as soon as possible [1]. There is an upstream surge tank and a downstream surge tank has been included in this paper. A water conduit after dam and a penstock after upstream surge tank guide the water flowing to the hydraulic turbine. There is another water conduit connecting downstream surge tank and downstream water reservoir. The hydraulic turbine is the mechanical part that transfers water kinetic power to mechanical power. There are two main kinds of hydraulic turbine in Norway: Francis turbine and Pelton turbine. For the Francis turbine, the water flows into the runner of the turbine through a guide vane with adjustable opening to control the rotation speed of the runner. For Pelton turbine, the water flows into runner bucket as a jet from a nozzle. The rotation speed is controlled by needle opening. The hydraulic system from reservoir to turbine supplies mechanical power. Modelling of it is called mechanical power modelling in this paper. Furthermore, there are several synchronous generators in the power house to transfer mechanical power to electrical power to the grid for peoples' everyday use. Modelling of them is called electrical power modelling. It is assumed the electrical part is a single machine connected to infinite bus (SMIB) model

II. MODELLING OF MECHANICAL POWER

The modeling process of mechanical power is shown in Figure 2. There are two reservoirs and two surge tanks, which are located respectively in upstream and downstream, a hydraulic turbine, water conduits and penstocks connecting the other elements. The mechanical power is the output from this system, and the gate opening is the manipulated variable. The gate here is an effective opening of the guide vane of Francis turbine or nozzles of Pelton turbine. It was assumed that the water head of the reservoirs are constant.

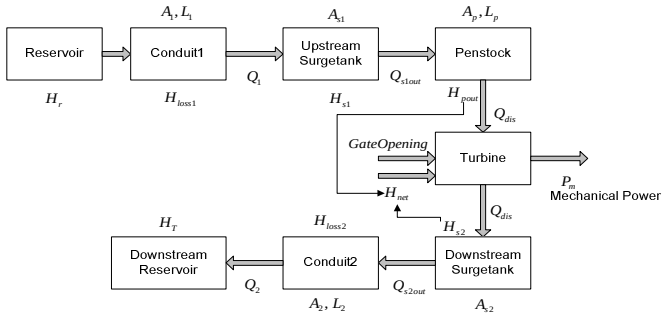

Figure 2. Flowchart for modeling mechanical power of a hydropower plant.

In this paper, the friction term of fluid, in water conduit and penstock model, is expressed as a head loss which is derived from Darcy–Weisbach equation considering that the direction of the flow can be inversed, and then it can be described as:

$$H_{loss} = f_r \cdot \frac{L}{D} \cdot \frac{\bar{v} \cdot |\bar{v}|}{2g} = f_r \cdot \frac{L}{D} \cdot \frac{\bar{Q} \cdot |\bar{Q}|}{2g \cdot A^2} \quad (1)$$

where:

A	Cross sectional area of pipe, m^2
D	Internal diameter of pipe, m
f_r	Friction factor, *dimensionless*
g	Gravity acceleration, m^2/s
L	Length of the pipe, m
$\bar{Q}$	Average volume flow, m^3/s
$\bar{v}$	Average fluid flow, m/s

A. Reservoir

Upstream reservoir is the water resource for the hydropower. After producing power, the water is gathered in downstream reservoir or directly flow into river. It has been assumed here the water levels of reservoirs are constant. In other words, H_r and H_T in Figure 2 are constant.

B. Penstock

Penstock is an enclosed pipe that delivers water to hydraulic turbine. Then Elasticity of water is only included in penstock model, not in all the models which can be an open volume. Penstock construction material can be cerement, plastic or other things, what just make a difference of friction in modelling. Furthermore, it is also assumed there is no water leakage. The dynamics of penstock have been simplified as just one discrete space element from a set of partial differential equations [2], which considered one-dimensional water flow through a chosen plane area [3].

$$\frac{dQ_{pin}}{dt} = \frac{g \cdot A_p}{L_p}(H_{s1} - H_{pout} - H_{lossp}) \quad (2)$$

$$\frac{dH_{pout}}{dt} = \kappa \cdot (Q_{pin} - Q_{pout}) \quad (3)$$

$$\kappa = \frac{a^2}{g \cdot A_p \cdot L_p} \quad (4)$$

where:

A_P	Cross sectional area of penstock, m^2
L_p	Length of the penstock, m
Q_{pin}	Inlet flow of penstock, m^3/s
Q_{pout}	Outlet flow of penstock m^3/s
H_{s1}	Water head of upstream surge tank, m
H_{pout}	Water head at Outlet of penstock, m
H_{lossp}	Head loss along penstock, m
a	Water pressure wave velocity, m/s

C. Surgetank

The surge tanks are open volume in this paper which means there is no air or water compressed when water level increases inside it. The surge tank equations are derived from the continuity of flow at the two junctions. The hydraulic losses at orifices of each surge tank have been neglected [4].

For upstream surge tank:

$$A_{s1} \cdot \frac{dH_{s1}}{dt} = Q_{s1in} - Q_{s1out} \quad (5)$$

For downstream surge tank:

$$A_{s2} \cdot \frac{dH_{s2}}{dt} = Q_{s2in} - Q_{s2out} \quad (6)$$

where:

A_{S1}	Cross sectional area of upstream surge tank, m^2
A_{s2}	Cross sectional area of downstream surge tank, m^2
Q_{s1in}	Inlet flow of upstream surge tank, m^3/s
Q_{s2out}	Outlet flow of upstream surge tank, m^3/s
Q_{s2in}	Inlet flow of downstream surge tank, m^3/s
Q_{s2out}	Outlet flow of downstream surge tank, m^3/s
H_{s2}	Water head of downstream surge tank, m

D. Water Conduits

The model of water conduit has been simply derived from Newton's second law without considering elasticity of water:

$$F = m \cdot a \quad (7)$$

$$\Delta p \cdot A = m \cdot \frac{dv}{dt} \quad (8)$$

The Δp is the pressure difference between inlet and outlet.

Taking the conduit1 as an example, its inlet pressure is from the reservoir, and its outlet pressure is equal to pressure from surge tank. Considering the head loss along the penstock, the Equation (3) can be developed as:

$$m \cdot \frac{dv}{dt} = \rho \cdot g \cdot (H_r - H_{s1} - H_{loss1}) \cdot A_1 \quad (9)$$

with $m = \rho \cdot L_1 \cdot A_1$, $v = \frac{Q_1}{A_1}$

Then the dynamic ODE of flow for conduit1 now can be stated as:

$$\frac{dQ_1}{dt} = \frac{g \cdot A_1}{L_1}(H_r - H_{s1} - H_{loss1}) \quad (10)$$

Correspondingly, the dynamic equation for the conduit2 which joins the downstream surge tank to the tail reservoir is:

$$\frac{dQ_2}{dt} = \frac{g \cdot A_2}{L_2}(H_{s2} - H_T - H_{loss2}) \quad (11)$$

where:

$A_{1,2}$	Cross sectional area of conduit 1,2, m^2
$H_{loss1,2}$	Head loss along conduit 1, 2, m
H_r	Water head of upstream reservoir, m
H_T	Water head of downstream reservoir, m
$L_{1,2}$	Length of the conduit1, 2, m
$Q_{1,2}$	Average volume flow along conduit1, 2 m^3/s

E. Hydraulic Turbine

The general mechanical power from water, no matter which kind of the turbine it is, can be stated as:

$$P_m = \eta \cdot \rho \cdot g \cdot H_{net} \cdot Q_{dis} \quad (12)$$

The net head is identical to the difference of water heads of two surge tanks minus some head loss:

$$H_{net} = H_{pout} - H_{s2} - H_{loss3} \quad (13)$$

The discharged flow into the turbine is related the type of turbine. It is all generally applied as an effective gate opening *OP* [5]. Then, the discharged flow is formulated as

$$Q_{dis} = k \cdot A_p \cdot OP \cdot \sqrt{H_{net}} \tag{14}$$

$$Q_{dis} = Q_{pout} \tag{15}$$

The flow before the turbine and after turbine is assumed identical. The gate opening OP is simulated as a linear function depends on time, every second it can move 1% of full opening.

$$\Delta OP = 1 \cdot \Delta t \tag{16}$$

Symbolist for Equation (12)-(16):

H_{net}	Net head to Turbine, *m*
H_{pout}	Outlet head of penstock, *m*
k	Gate constant, *dimensionless*
OP	Effective gate Opening, *%*
P_m	Mechanical power, *W*
Q_{dis}	Discharge flow to Turbine, m^3/s
η	Turbine efficiency

F. Model testing

A gate close situation is simulated. At time 200sec, the gate is closed from 50% to 35%, ramping down 1% per second. The resulting mechanical power is shown in Figure 3. There is an inverse response of power when gate closed. It is because the flow continuously reduced, but the water head is suddenly increased due to smaller passage. The pressure before turbine and net head across turbine, which is shown in Figure 4, should not be too high that it may damage the turbine or penstock. Therefore, the gate should be controlled very carefully.

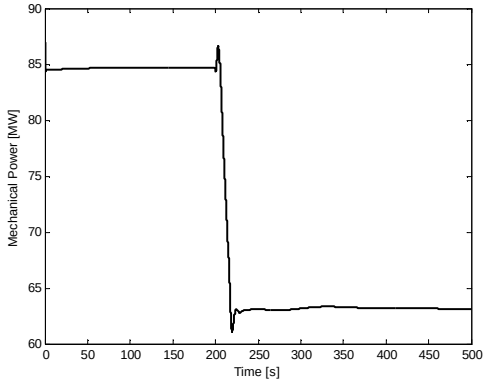

Figure 3. Mechanical power when gate is closed.

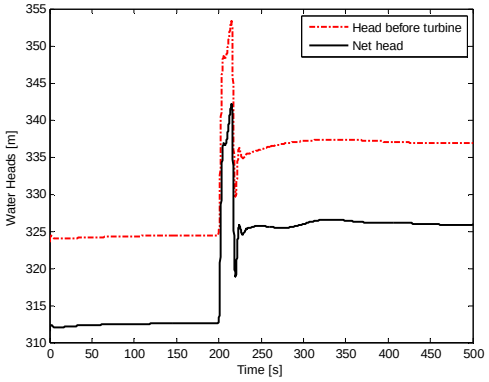

Figure 4. Water heads when gate is closed

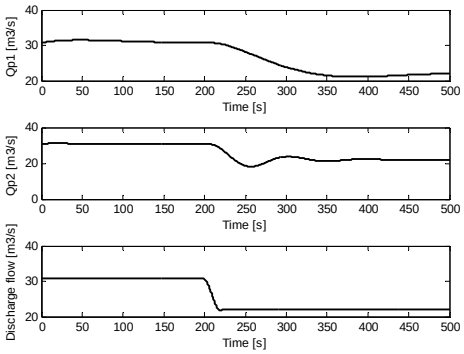

Figure 5. Flow rate when gate is colsed

III. MODELING OF ELECTRICAL POWER

In this paper, a synchronous generator model is presented with simplification of Park transformation [6]. But it is enough to analyze the electrical transient. A fourth order model [7] with ODEs is as below:

Electrical equations:

$$T'_{d0} \cdot \frac{dE'_q}{dt} = (X_d - X'_d) \cdot I_d - E'_q + E_{fd} \tag{17}$$

$$T'_{q0} \cdot \frac{dE'_d}{dt} = (X'_q - X_q) \cdot I_q - E'_d \tag{18}$$

Terminal equations:

$$U_{td} = E'_d - R_a \cdot I_d - X'_q \cdot I_q \tag{19}$$

$$U_{tq} = E'_q - R_a \cdot I_q + X'_d \cdot I_d \tag{20}$$

$$P_e = E'_d \cdot I_d + E'_q \cdot I_q + (X'_d - X'_q) \cdot I_d \cdot I_q \tag{21}$$

$$U_t = \sqrt{U_{td}^2 + U_{tq}^2} \tag{22}$$

Rotor motion equations:

$$\frac{d\delta}{dt} = \omega_0 \cdot (\omega - 1) \tag{23}$$

$$M \cdot \frac{d\omega}{dt} = P_{m,(p,u)} - P_e - Dp \cdot \frac{d\delta}{dt} \tag{24}$$

With δ and consider the voltage from infinite bus, the terminal voltages can also be stated as [8]:

$$U_{td} = -V_0 \cdot \sin\delta + R_e \cdot I_d + X_e \cdot I_q \tag{25}$$

$$U_{tq} = V_0 \cdot \cos\delta + R_e \cdot I_q - X_e \cdot I_d \tag{26}$$

The exciter here is simply treated as a second order [9] dynamic model:

$$T_E \cdot \frac{dE_{fd}}{dt} = K_E \cdot (U_r - U_t - U_s) - E_{fd} \tag{27}$$

$$T_{FE} \frac{dU_s}{dt} = K_F \cdot \frac{dE_{fd}}{dt} - U_s \tag{28}$$

Symbolist for Equation (17)-(28):

D_p	Damping coefficient, *dimensionless*
E'_d	d axis transient voltage, *p.u*
E_{fd}	d axis field voltage, *p.u*

$E_q^{'}$	q axis transient voltage, *p.u*
P_e	Electrical power, *p.u*
$P_{m(p,u)}$	Mechanical power, *p.u*
I_d	d axis armature current, *p.u*
I_q	q axis armature current, *p.u*
J	Generator inertia constant, *dimensionless*
K_E	Exciter gain, *dimensionless*
K_F	Stabilizer gain, *dimensionless*
R_a	Armature resistance, *p.u*
R_e	Equivalent resistance of transmission lines, *p.u*
$T_{d0}^{'}$	d axis open circuit time constant, *second*
$T_{q0}^{'}$	q axis open circuit time constant, *second*
T_E	Exciter time constant
T_{FE}	Stabilizer circuit time constant
U_t	Generator terminal voltage, *p.u*
U_{td}	d axis component of terminal voltage, *p.u*
U_{tq}	q axis component of terminal voltage, *p.u*
U_r	Reference voltage, *p.u*
U_s	Stabilizer voltage, *p.u*
V_0	Infinitive bus voltage, *p.u*
X_d	Synchronous reactance, *p.u*
$X_d^{'}$	d axis transient reactance, *p.u*
X_q	q axis synchronous reactance, *p.u*
$X_q^{'}$	q aixs transient reactance, *p.u*
X_e	Equivalent reactance of transient line, *p.u*

A. *Model Testing*

For testing this model, a short circuit error situation is simulated at 1.1s and recovered at 1.2s, results shown in Figure 6 and Figure 7. Notice that the voltage control is in closed-loop during the simulation. The terminal voltage was suddenly set to zero because of the short circuit, and it leaded to unexpected oscillations of electrical power. In the meanwhile, the excitation voltage, the manipulated variable for terminal voltage, went up to increase the voltage to reference point again. Apparently, the change of terminal voltage has caused oscillation of electrical power. From Equation (24), it will result in oscillation of angular speed, equilibrium to oscillation of frequency which should be as stable as possible. To obtain a constant frequency normally requires control actions for mechanical power. Therefore, the voltage control and frequency control sequentially should be implemented simultaneously for the hydropower system. This paper only presented a decentralized control with two separate controllers, which was discussed in next section. The generated electrical power was assumed thoroughly consumed. There is no mathematical modeling of detailed electric grid with load included.

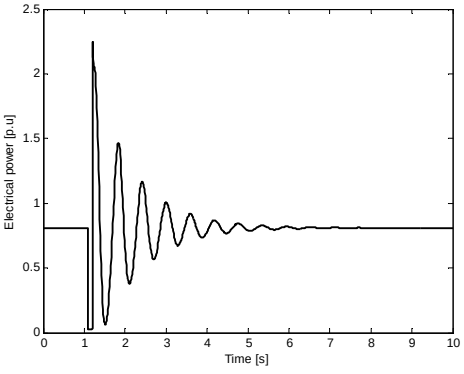

Figure 6. Simulated electrical power with a short circuit error

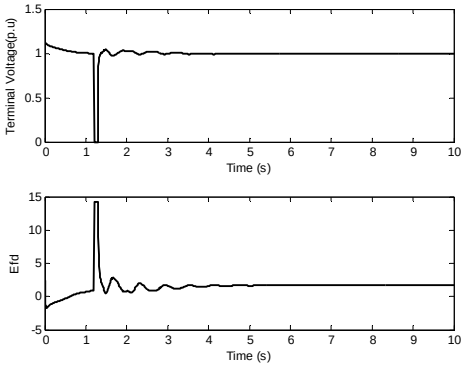

Figure 7. Simulated terminal voltage of excitation voltage with a short circuit error

IV. CONTROL STRUCTURE

The modeling results in a MIMO system, the mechanical power from water and excitation voltage of synchronous machine are the inputs, while the frequency and voltage are the outputs in this system. A traditional PI controller was implemented with this model for frequency and another controller for voltage. This interacted and controlled MIMO system working process is shown in Figure 8.

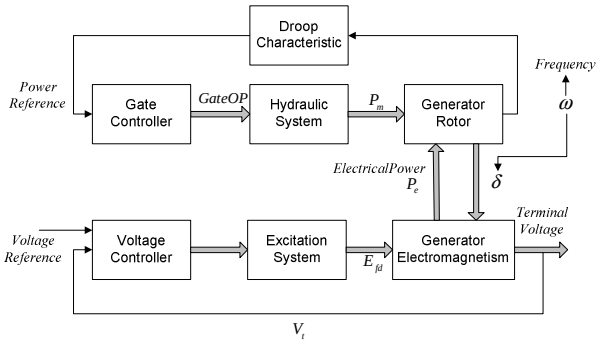

Figure 8. Flow chart of controlled MIMO hydropower system

A. *Frequency Control*

The frequency control is equal to the speed control or the active power control of the hydraulic turbine. The controller should comply with the main purpose, which is to keep the rotational speed stable and constant of the turbine-generator unit at any grid load. In other words, it should respond to any change of electrical power.

When a real hydropower plant is connected to an isolated load, in case of a load decrease, the excess power will accelerate the rotation of the turbine. Then the controller should reduce turbine speed that means deceleration of the water in the penstock and corresponding pressure rise and oscillations. However, to avoid it approaching to bearable pressure for turbine and penstock, closing rate should be limited. To fulfill and balance these two opposite demands, a PI controller has been implemented. Since the SMIB assumption, this PI controller was implemented with a droop characteristic, which is a traditional control method to decide how much a single machine should contribute to the network at present, for active power and frequency. The droop relationship [10] for them is described as:

$$\frac{\Delta f}{f_{nom}} = -Dr \cdot \frac{\Delta P}{P_{nom}} \tag{29}$$

Every simulation control interval, the function of droop characteristic will calculate deviation of frequency and obtain a reference power for PI controller as

$$P_{new} = -\frac{1}{Dr} \cdot \frac{f_{new} - f_{old}}{f_{nom}} \cdot P_{nom} + P_{old}, \qquad P_{ref} = P_{new} \qquad (30)$$

B. Voltage Control

The voltage control was carried out with the generator excitation control using a controller with a stabilizer. The controller was embedded in the second order model of exciter, which is shown in Equation (27), (28). The purpose of the controller is to hold the terminal voltage magnitude of a synchronous generator at a specific value. An increase in reactive power load of the generator should be accompanied by a drop in the terminal voltage magnitude. This voltage is rectified and compared to a set point signal. The difference of them input into a controller and then it controls the exciter field and increases the exciter voltage. Thus, the generator field current is increased, which results in an increase in the generated voltage [11].

V. RESULTS AND DISCUSSION

From Figure 8, it can be seen that the mechanical power, electrical power, frequency, phase angle and terminal voltage are interacting with each other. These mutual effects also can be seen from Equation (17) to Equation (26). Even with these effects, two decentralized controllers still perform working effectively with disturbances. Because this paper presumed it is a single machine to infinite bus system, the disturbances have been simulated as a suddenly frequency step change and voltage change in the infinite bus. These disturbances were added to the process compulsorily, not simulated as mathematical functions. That means during simulation process, when these disturbances happen, they would last for several seconds. In such a period, how a single machine in a hydropower plant response to the disturbance can be observed.

In all simulations with controllers, what should mention are the oscillations in the beginning, it is because when combining the electrical power model and mechanical power part, the system needs some time to be initialized. The physical meaning of this situation can be explained like what happens when a generator injects to the electrical grid.

- Simulation results with a frequency disturbance of 51Hz at period 25s to 35s.

As it can be seen in Figure 9, when the system got this disturbance, the gate moved towards to a smaller opening with its characteristic steps to get a smaller mechanical to reduce the rotation speed. In other words, it was to reduce the frequency. After the disturbance ends, the gate moved back to its working point when it was at 50 Hz. And consequently, the mechanical power was also raised up. After the gate finished its movements, the mechanical power got some waves. It is because of the dynamics of the hydraulic system.

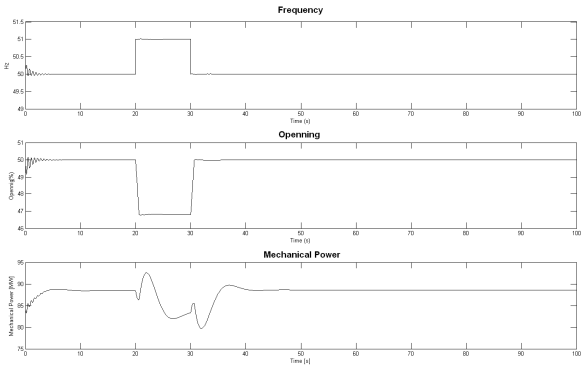

Figure 9. Simulation results of gate controller with a frequency disturbance

When the disturbance happened, there was a small effect to terminal voltage what is shown in Figure 10. The exciter maintained the terminal voltage quite well. It reduced to a smaller value, when got a disturbance. This is because the when the mechanical power is decreased, the electrical power will correspondingly should be reduced. Then, the excitation voltage should be smaller to keep the terminal voltage at its reference point. The control response of exciter can be seen rather faster than the gate. This is reasonable and practical. A turbine is mechanical equipment bearing high pressure and tons of water. Its movement is certainly slower than the electrical voltage generation with several windings.

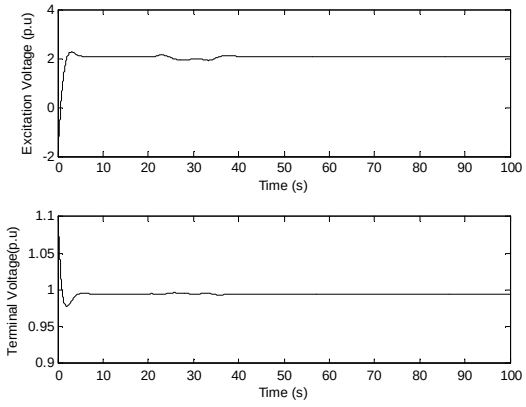

Figure 10. Simulation results of voltage controller with a frequency disturbance

- Simulation results with a voltage disturbance of 0.9 p.u at period 20s to 25s.

Firstly, the controlling of excitation voltage can be seen in Figure 11. It responded very quickly, and it went up to get a higher terminal voltage. Due to its quick response, the voltage also got a deviation after the disturbance ended. But again, the exciter forced it back to its nominal working point. This control result is acceptable.

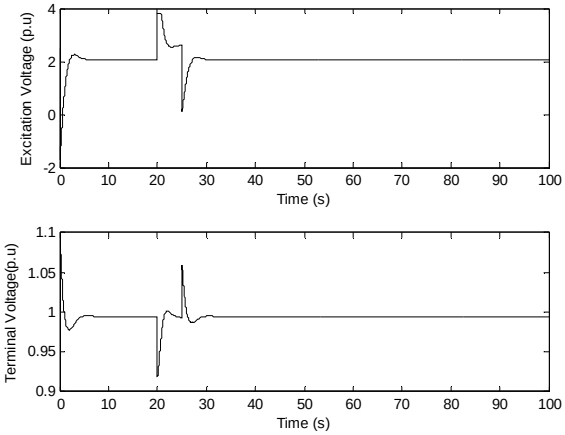

Figure11.Simulation results of voltage controller with a voltage disturbance

However, when there was voltage disturbance, it caused some oscillations on the mechanical power control that can be seen in Figure 12. Terminal voltage changed means the electrical power changed, which is also presented in Figure 6; the frequency sequentially got a deviation from its nominal point. To control the frequency, the gate started to act. But because of interactions between electrical power control and mechanical power control, it caused some oscillations till the system went stable again.

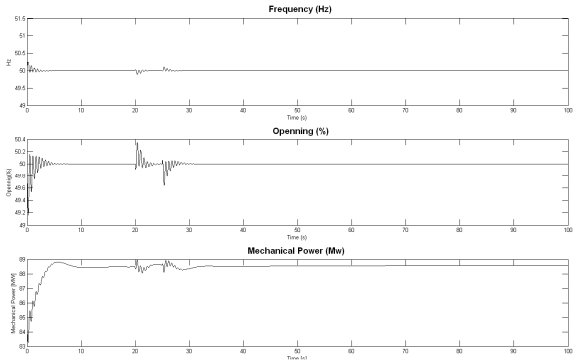

Figure12. Simulation results of gate controller with a voltage disturbance

These simulations presented a simple model with a traditional and most common controller for power system. It shows there are still some interacting effects with two decentralized controllers. By this model, it can be analyzed why oscillations happen. Furthermore, since there are thousands of generators in the system and many different hydropower plants in the electrical net, to reduce oscillation in the electrical grid, to use less water make more power, a more advanced modern control strategy can be figured out with this modelling work.

VI. REFERENCES

[1] Arne Kjølle, "Hydropower in Norway,Mechanical Equaipment", Norwegian University of Science and Technology, 2001, Chapter 1.7.

[2] "Hydraulic turbine and turbine control models for system dynamic studies", IEEE Trans. Power Syst, vol.7, pp.1167-179, Feb. 1992.

[3] B.Strah, O.Kuljaca, Z.Vukic, "Speed and Actie Power Control of Hydro Turbine Unit", IEEE Trans.Energy Conv,vol.20,No.2,June,2005.

[4] H. Fang, L.C., N. Dlakavu, Z. Shen, "Basic Modeling and Simulation Tool for Analysis of Hydraulic Transients in Hydroelectric Power Plant". IEEE Transactions on energy conversion. Vol. 23, pp.834-841, (2008).

[5] Juan Garrido, A.Z., Francisco Vazquez, "Object oriented modelling and simulation of hydropower plants with run-of-river shceme: A new simulation tool". Simulation Modelling Practice and Theory, 2009. Vol. 17: pp. 1751-1752.

[6] Park, R.H., "Two-reaction Theory of Synchronous Machines, Generalized Method of Analysis". Part I. AIEE Transactions 1929.Vol.48: pp. 716-727

[7] Milano, F., Power System Modelling and Scripting. 2010: Springer, p. 325-326.

[8] Jan Machowski, J.W.B., James R. Bumby, Power System Dynamics. Stability and Control. 2008, UK: John Wiley & Sons, Ltd. 455.

[9] H.L.Zeynelgi, A.D., "Modelling and Simulation of synchronous machine transient analysis using SIMULINK". International Journal of Electrical Engineering Education. Vol.4, pp. 39.

[10] Saadat, H., Power System Analysis. 2nd ed. 2002: McGraw-Hill Primis Custom Publishi. pp. 555-562

[11] Sluis, P.S.a.L.v.d., Electrical Power System Essentials. 2008: John Wiley&Sons pp. 144.

Paper A2

Application of Kalman Filter Based Nonlinear MPC for Flood Gate Control of Hydropower Plant

(IEEE Power & Energy Society General Meeting, 2012)

Application of Kalman filter based nonlinear MPC for Flood Gate control of Water Reservoir

Wenjing Zhou, Bjørn Glemmstad
Faculty of Technology, Department of Electrical Engineering, Information Technology and Cybernetics
Telemark University College, P. O. Box 203, N-3901
Porsgrunn, Norway

***Abstract*—This paper addresses the issue of regulating the water level of a reservoir in a hydropower plant with nonlinear predictive control (NMPC). Besides, according to pre-specified water level variant limits, an error tolerance NMPC (ET-NMPC) was extended from a regular NMPC. A nonlinear mathematical model was developed for dynamics of water reservoir level. A theoretical hydrology model was included to calculate inflow of reservoir. Extended Kalman Filter (EKF) was applied to estimate the inflow depends on various weather conditions and help to predict future water level. Closed loop simulations with ET-NMPC were demonstrated.**

I. INTRODUCTION

There is abundant water resource in Norway. Therefore lots of hydropower plants utilize this resource to produce electricity. Water reservoirs are the origins of those plants. As well as to ensure power supply, to be safe for the neighbourhood is also crucial. Generally, water reservoirs experience floods almost one third of a whole year on average in Norway. To avoid water exceeding the danger level and overflowing to the neighbourhood people or environment, there is usually a floodgate to draw off expected quantity of water to downstream from time to time to maintain reservoir's level in a safe range. At present, this floodgate is normally operated manually with knowledge of weather and season conditions. But because of frequent heavy rainfall or snow melting in Norway, it is not easy for operators to achieve this scope. In nowadays, advanced controllers and soft sensors are implemented for industry in various ways and it is possible to replace manual control of floodgate, what is one aim of this research work. From the electricity producer's view, it is in fact significant to guarantee surrounding safe and also to use as much as possible available water for power production without any unnecessary release of water, what is another purpose of this work.

II. MODELLING

A. Reservoir model

This paper took the water reservoir Tokevatn in Norway as a study case, which is a shared main reservoir for five downstream hydropower plants. It is with 150 million m^3 storage of water and a regulation height around 4.6 m. The reservoir model is gained from continuity equation which is with the assumptions that the water is inelastic. Geometry of reservoir was included in the term *A[H(t)]*, which means the surface area of water depends on current water level. Because of complex geometry, some nonlinearity is involved in this model.

$$\frac{dH}{dt} = \frac{1}{A[H(t)]} \cdot (Q_{in} - Q_{out}) \tag{1}$$

$$Q_{out} = Q_p + Q_G \tag{2}$$

where:

H	Water level of reservoir, m
A	Surface area of top of water, m^2
Q_{in}	Inflow rate to reservoir, m^3/s
Q_{out}	Outflow rate of reservoir, m^3/s
Q_p	Discharge flow rate for production, m^3/s
Q_G	Flow rate of water pass through gate, m^3/s

B. Floodgate model

A floodgate is used to control water level in safe range in Tokevatn. The flow through such a gate can either be free or submerged, depending on the water level difference through the gate. In this paper, the flow discharged is considered to be "Free Flow" with assumption of Z_D in Figure 1 is not that high to cause an increase in the upstream headwater. A simplified common formula was introduced for floodgate, which is also a nonlinear model.

$$Q_G = \varepsilon \cdot OP \cdot A_G \cdot \sqrt{2 \cdot g \cdot \Delta H} \tag{3}$$

$$\Delta H = H - Z_D \tag{4}$$

where:

A_G	Total gate passage area, m^2
OP	Gtae opening, $\%$
Z_D	Downstream river level, m
g	Gravity acceleration, m^2/s
ε	Discharge coefficient, *dimensionless*

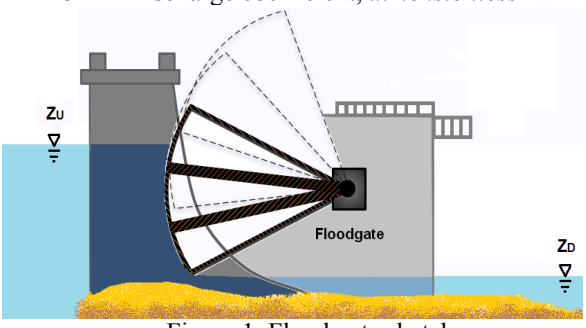

Figure 1. Flood gate sketch

Among the hydraulic characteristics, discharge coefficient ε is a parameter can be varied and estimated to fit gate model to real gate movements. For submerged gate it will be in the range 0.3 -0.6 and for free discharge it is in the range 0.5 –0.7 [1]. Maximum capacity of flood gate is 400 m3/s. Take the biggest and smallest level difference into account.

$$\varepsilon \quad [\frac{400}{A_G \cdot \sqrt{2g \cdot 6.3}}, \frac{400}{A_G \cdot \sqrt{2g \cdot 3.75}}] \tag{5}$$

C. Hydrology model

There is a so called HBV model [2], a rainfall - runoff model, which includes conceptual numerical descriptions of hydrological processes in catchment scale. The general water balance is with consideration of water precipitation, evapotranspiration, snow pack melting and etc. By this model, inflow to reservoir can be briefly calculated. However, this paper only includes rainfall broadcasted by weather report and consideration of different seasons, for example, later in spring, inflow is combined of rainfall and extra value from snow smelting. Even with HBV model, there are still too many uncertainties about inflow, like the smelted water is hard to measure, or too many branches to reservoir, so a Kalman filter was implemented to estimate inflow to reservoir and predict future water level.

III. ALGORITHM

A. Discretized NMPC

Nonlinear model predictive control (NMPC) is an optimization based method for the feedback control of nonlinear systems [3]. NMPC inherits many advantages of linear MPC, such as handling constraints. Moreover it uses nonlinear representation of dynamic systems. Implement NMPC, it is not necessary to linearization system which might lead to lose accuracy of modelling. Since the nonlinear mathematic model and online controllers for industry usually is in discretion form, discretized NMPC was employed for control in this work. As a common scheme of MPC, only the first of calculated gate opening sequence was input to system, and optimization work repeated at every control interval. Cost function of this NMPC is

$$J = \sum_{k=1}^{h_p} e^2(k) + \lambda \cdot \sum_{k=1}^{h_c} \Delta OP^2(k) \tag{6}$$

$$e(k) = H_{set}(k) - H(k) \tag{7}$$

$$\Delta OP(k) = OP(k) - OP(k-1) \tag{8}$$

$$H(k) = \frac{1}{A[H(k)]} \cdot (Q_{in}(k) - Q_p(k) - \varepsilon \cdot OP(k) \cdot A_G \cdot \sqrt{2 \cdot g \cdot (H(k) - Z_D)}) + H(k-1) \tag{9}$$

where:

J	Cost function, *dimensionless*
H_{ref}	Reference level, *m*
λ	Optimization parameter, *dimensionless*
k	Time index, *dimensionless*

Calculate gate opening in control horizon to minimize cost. The algorithm became as

$$\min J(OP(\cdot)) = \sum_{k=1}^{h_p} e^2(k) + \lambda \cdot \sum_{k=1}^{h_c} \Delta OP^2(k) \tag{10}$$

As an industry process, there are some inequality constraints for manipulate variable and output.

$$0 \le OP(k) \le 100 \tag{11}$$

$$Z_D \le H(k) \le H_{edge} \tag{12}$$

where:

H_{edge}	Edge level of reservoir, *m*

B. Error tolerance NMPC

For the purpose of protection of people and environment, all of the waterways in Norway are subject to the laws and regulations given by NVE – The Norwegian Water Resources and Energy Directorate. Their mandate is to ensure an integrated and eco – friendly management of the country's water resources, promote efficient energy markets and cost-effective energy systems and contribute to an efficient energy use. The directorate plays a central role in the national flood contingency planning and bears overall responsibility for maintaining national power supplies. In 2001, NVE introduced minimum and maximum water levels during summer and autumn in addition to existing regulations regarding water level limits, which is shown in Figure 2.

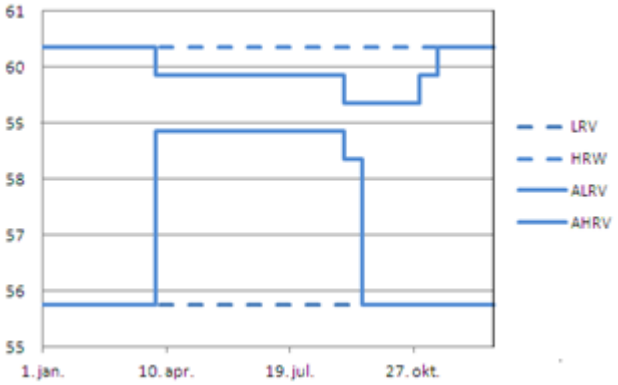

Figure 2. Prescribed water level limits by NVE

According to these water level limits, an error tolerance control method was introduced to couple with NMPC. Error tolerance MPC (ETMPC) was first mentioned by Ilchmann and Ryan (1994) for designing an adaptive controller of a bioreactor into a pre-specified and allowed small deviation around reference value. With similar purpose, this idea can be addressed to solve the problem of stated tolerant error of water level limits by NVE. Then the performance index now is

$$OP(k) = \begin{cases} OP : \min J(OP(\cdot)) = \sum_{k=1}^{h_p} e^2(k) + \lambda \cdot \sum_{k=1}^{h_c} \Delta OP^2(k), \ \ if \ \ |E_t| \le \partial \\ OP_1^*, \ \ if \ \ E_t > \partial; \ \ OP_2^*, \ \ if \ \ E_t < -\partial \end{cases} \tag{13}$$

$$E_t = H(k) - H_{ref}(k) \tag{14}$$

where:

E_t Tolerance error, *dimensionless*

α Pre-specified acceptable error, *m*

The tolerance error term is an instantaneous error. However it can be in different forms, such as the mean of errors between reference and predicted outputs along the prediction horizontal. There are other choices of Et, what depends on practical requirements of process.

C. *Kalman filter*

Hydrology model can help to calculate inflow to reservoir, but because of uncertainties of measurements, inflow was estimated by an extended Kalman filter. Then, future reservoir level can be predicted. EKF utilize derivatives of the process and measurement functions to compute estimates. Algorithm of EKF is [4]:

a) Project state ahead:

$$\hat{x}_k^- = f(\hat{x}_{k-1}, u_{k-1}) \quad (15)$$

b) Project the error covariance ahead:

$$P_k^- = A_k P_{k-1} A_k^T + W_k Q_k W_k^T \quad (16)$$

$$A_{[i,j]} = \frac{\partial f_{[i]}}{\partial x_{[j]}}(\hat{x}_{k-1}, u_{k-1}) \quad (17)$$

c) Compute the Kalman gain:

$$\mathrm{K_k} = \mathrm{P_k^- H_k^T (H_k P_k^- H_k^T + V_k R_k V_k^T)^{-1}} \quad (18)$$

d) Update estimate with measurement zk

$$\hat{x}_k = \hat{x}_k^- + K_k\left(z_k - h(\hat{x}_k^-, 0)\right) \quad (19)$$

e) Update the error covariance

$$\mathrm{P_k = (I - K_k H_k) P_k^-} \quad (20)$$

where:

x State

u Control variable

K Kalman gain

P Error covariance

z measurement

u Control variable

Q measurement error

IV. CONTROL PROCEDURE

The working procedure can be seen in Figure 3. Start point is updating weather information from weather report, which can be done by operators every day. Measured level can be acquired by sensors. With interface communication between sensors and computer, it is possible for these on-line data input to MATLAB in real-time, which is the developing environment of this paper. Then, with EKF and ET-NMPC, output can be obtained and command to floodgate.

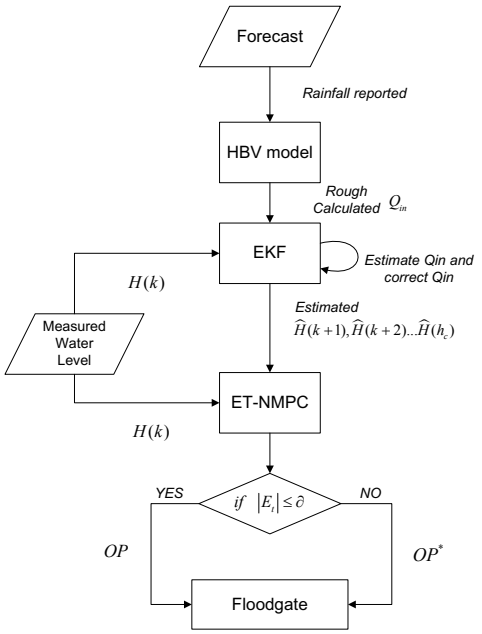

Figure 3. Flow chart of control process

V. RESULTS

Study case: Rainy season in May.

- Simulation interval: 0.1 hour
- Control interval: 2 hours
- Simulation time: 3 days
- Pre-specified water level limits:58.8-60.3m
- Initial opening: 30%
- Q_p=40 m^3/s

In this case, Floodgate will work in every two hours. The work frequency can be decided by seasons. In rainy season, floodgate could work more. In dry season, floodgate can be ennui till approaching to danger level. Otherwise, simulation time step is smaller than control interval. It is more realistic to make it in this way. Measurements are simulated in every 0.1 hour. Consequently, EKF is working in every simulation time step, while ET-NMPC is in function in every control interval. OP_1^* in equation (14) is simply treated as fully open and OP_2^* is treated as fully closed.

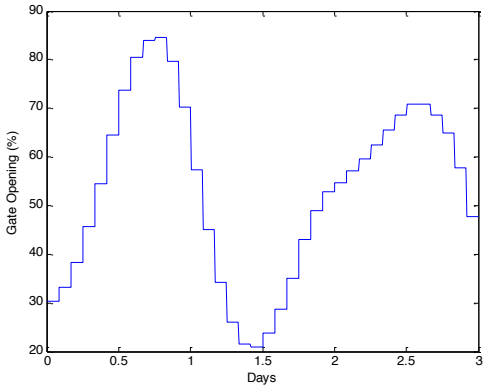

Figure 4. Gate opening

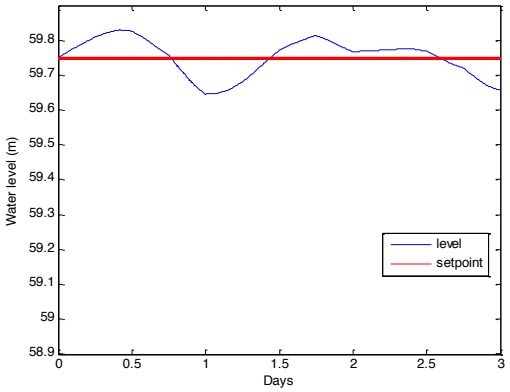

Figure 5. Reservoir level

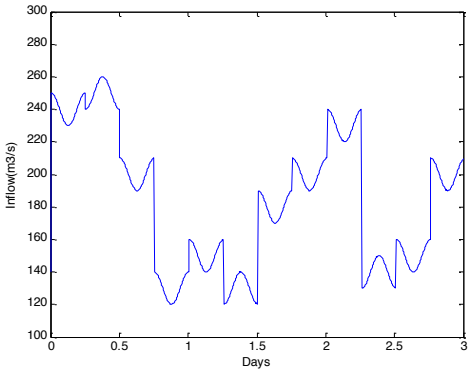

Figure 6. Inflow to reservoir

It simulated a situation that experiences a heavy rain in continuous three days. Inflow information can be seen in Figure 6. Compare with it, when there was much water pouring into reservoir, floodgate tried to discharge water and maintain the level at reference point. When there is a smaller inflow, floodgate closed to a smaller opening to lift level.

VI. CONCLUSION

Nowadays' advance control and soft sensor technology have been implemented in many ways of industry. It is time to replace manual control into NMPC or other advance controllers for floodgate to security people and environment from floods. This paper just showed it can be realized. But, considering the economic aspects, to produce more power which also means discharge less water, more optimization work should carry out.

VII. REFERENCES

[1] Lewin, Jack, 2001, "Hydraulic Gates and Valves in Free Surface Flow and Submerged Outlets", 2nd Edition, Thomas Telford Ltd, Heron Quay, London.

[2] Otnes. J and Ræstad.E, 1978, "Hydrologi i praksis", 2nd Edition, Ingeniørforlaget, Oslo, 1978

[3] L.Grune, J.Pannek, "Nonlinear Model Predictive Control,Theory and Algorithms", Springer,p1, London,2011.

[4] G.Welch, G.Bishop, "An introduction to Kalman Filter",TR95-041, p7, Chapel Hill, 2004

Paper A3

Implementation Unscented Kalman Filter for Nonlinear States Estimation of a Hydropower Plant

(IEEE Power & Energy Society, Powercon, 2012)

Implementation Unscented Kalman Filter for Nonlinear State Estimation of Hydropower plant

Wenjing Zhou, *Associate Member, IEEE*, and Bjørn Glemmestad

***Abstract*-- As it is known that there is an inverse response of the pressure in the penstock when manipulating the guide vane of a hydraulic turbine in hydropower plant, considering safety issues, it is of interest to estimate this dynamic state to compensate the uncertainties in the pressure measurements. Besides, the mathematical model of a hydro power plant is highly nonlinear, which may make classic extended Kalman filter (EKF) theoretically lose accuracy or not capable of estimation due to its linear approximation way. The purpose of this paper is to achieve fast predictions and more precise estimations by introducing an unscented Kalman filter (UKF) to a hydropower system. The derivation of the UKF is presented. Different scenarios with real measurements are introduced to see the effects of UKF.**

***Index Terms*--Hydropower; Inverse response of pressure in penstock; Nonlinear state estimation; Unscented Kalman Filter**

I. Nomenclature

List of symbols from (1) to (17):	
x	State
$\bar{x}$	Average of x
χ	Sigma point
w^m	Mean weights of sigma
w^c	Covariance weights of sigma
P	Covariance
n	Number of states
k	Time step index
f	Process equation
h	Measurement equation
Q	Process noise covariance matrix
R	System noise covariance matrix
List of symbols from (18) to (28):	
A	Cross sectional area, m^2
a	Water pressure wave velocity, *m/s*
D	Internal diameter of pipe, *m*
f_r	Friction factor, *dimensionless*
g	Gravity acceleration, m^2/s
H	Water head, *m*
k	Gate constant, *dimensionless*
L	Length of the pipe, *m*
OP	Effective gate Opening of hydraulic turbine, *%*
P_m	Mechanical power, *W*
Q	Flow rate, m^3/s
η	Turbine efficiency,%
Subscripts for (18) to (28)	
C	Water conduit
P	Penstock
R	Water reservoir
S	Surge shaft
T	Tailor water reservoir
loss	Head loss
dis	Discharged flow to hydraulic turbine

This work is part of a project supported by the Research Council of Norway.

W. Zhou is with Faculty of Technology, Department of Electrical Engineering, Information Technology, Telemark University College, P.O. Box 203, N-3901, Porsgrunn, Norway (e-mail: wenjing.zhou@hit.no)

B. Glemmestad is with Department of Process, Energy and Environmental Technology, Telemark University College.

II. Introduction

It is crucial to detect some states of industry processes to ensure the safety, e.g in case of an abnormal situation like a sudden controller failure. However, monitoring the process is impossible when the states cannot be directly measured or too infrequently measured to capture instantaneous dynamics [1]. Under these circumstances, state estimation can be utilized for additional supervision. Likewise, when it refers to process control, state estimation also plays an important role in order to make a more reliable controller, because it can help to overcome measurement uncertainties due to sensor failure or noise. According to the working condition at a hydro power plant, the pressure in the penstock is most critical state to estimate and predict. The reason is that if the hydraulic turbine is shut down suddenly, the pressure will rise to a very high value that may damage the hydraulic turbine or penstock. This situation can happen too quickly to response, thus monitoring and prediction of it are required to secure the plant. However there is no back up monitor in the specific power plant in this work (Fjone in Norway), if the pressure meter of it failed working, what is also why the state estimation is with significant requirement.

In recent, the most popular nonlinear estimators are EKF and UKF. It is claimed that they have comparable computation complexity [2]. Different comparison works have been presented in some papers [3, 4]. They are also tested in some industry area, and found there is no big estimation difference between them [5]. But EKF approximate nonlinearities by linearization, it needs Jacobian matrix to do so at every update

time step, which is hard to be calculated for high order system models. Hydro-electricity system is well known with its high nonlinearities, thus it is not easy to acquire the Jacobian matrix, especially in its hydraulic part. The geometry structure, hydraulic friction, characteristic movement of hydraulic turbine etc are the factors that make the mathematical model of hydro-electricity very nonlinear. Furthermore, EKF may involve some errors through linearization of them. In order to have an effective and accurate estimation of hydropower system, it is with sense to utilize UKF.

III. ALGORITHM

Probability distribution function (pdf) is with superiorities for representing process, model state and measurement noise. Filtering technique, e.g. Kalman filters, EKF, UKF, propagate mean and covariance of pdf with some optimizations to estimate process or system parameters. EKF uses linear approximation to propagate pdf for nonlinear system, whereas UKF propagates the pdf in a rather simple and effective way [6].

UKF is based on unscented transformation (UT) introduced by Julier and Uhlman [2]. It uses a set of sigma points to approximate the probability distribution of the random variable. The parameterized sets of sigma points are propagated through the nonlinear transformation and the mean and covariance of the transformed variables is used to approximate the mean and covariance of sample space [5]. The main motivation for UT was to address the shortcomings of EKF linearization approach and was developed further to incorporate higher order moments of distribution [7].

A. Sigma points selection

Otherwise than EKF, UKF has the freedom to select parameters, e.g the sigma points. Better placement of sigma points can contribute to improve performance of UKF. Several previous research works have been carried out to determine the location of sigma points [7]. A model based learning method for sigma points is also presented with a lower computation complexity UKF by Ryan and Carl in [8]. An n+1 sigma points' placement method in a spherical simplex UKF shows satisfactory in implementation in [9]. In this paper, it is simply introduced modifications for UT done by [10], which allows determine location and scaling of sigma points at every update step. Sigma points are calculated as:

$$
\begin{aligned}
&\chi_0 = \bar{x} \\
&\chi_i = \bar{x} + (\sqrt{(n+\lambda)\cdot P_x})_i \qquad i = 1,\ldots,n \\
&\chi_i = \bar{x} - (\sqrt{(n+\lambda)\cdot P_x})_{i-n} \qquad i = n+1,\ldots,2n \\
&w_0^m = \frac{\lambda}{n+\lambda} \qquad i = 0 \\
&w_0^c = \frac{\lambda}{n+\lambda} + (1-\partial^2+\beta) \qquad i = 0 \\
&w_i^m = w_i^c = \frac{1}{2(n+\lambda)} \qquad i = 1,\ldots 2n
\end{aligned}
\tag{1}
$$

where $\lambda = \alpha^2(n+\kappa) - n$. For α, the smaller of it the smaller the sigma point spread and the less likely to pick up anomalous, normally it is set as $0 \le \alpha \le 1$. For Gaussian distributions, $\beta=2$ is optimal [7]. κ is not critical and set to zero here. [11]. In order to avoid sigma point with complex value, square root is recommended done by Cholesky decomposition.

B. Kalman filter work procedure

The system model is considered as:

$$
\begin{aligned}
x_k &= f(x_{k-1}, v_{k-1}) \\
y_k &= h(x_k, \eta_k)
\end{aligned}
\tag{2}
$$

The general procedure of UKF is

a) Initialize UKF with:

Let $x_k^a = [x_k^T \quad v_k^T \quad \eta_k^T]^T$, $\chi_k^a = [(\chi^x)_k^T \quad (\chi^v)_k^T \quad (\chi^\eta)_k^T]^T$

$$\hat{x}_0 = E[x_0] \tag{3}$$

$$\hat{x}_0^a = E[x^a] = [\hat{x}_0^T \quad 0 \quad 0]^T \tag{4}$$

$$P_0^a = E[(x_0^a - \hat{x}_0^a)(x_0^a - \hat{x}_0^a)^T] = \begin{bmatrix} P_0 & 0 & 0 \\ 0 & P_v & 0 \\ 0 & 0 & P_\eta \end{bmatrix} \tag{5}$$

b) Calculate sigma weights shown in (1)

c) Start repeating next three steps every prediction step:

- Calculate sigma points:

$$\chi_{k-1}^a = \left[\hat{x}_{k-1}^a \quad \hat{x}_{k-1}^a + \sqrt{(n+\lambda)\cdot P_{k-1}^a} \quad \hat{x}_{k-1}^a - \sqrt{(n+\lambda)\cdot P_{k-1}^a}\right] \tag{6}$$

- Time update:

$$\chi_{k|k-1}^x = f(\chi_{k-1}^x, \chi_{k-1}^v) \tag{7}$$

$$\hat{x}_k^- = \sum_{i=0}^{2n} w_i^m \cdot \chi_{i,k|k-1}^x \tag{8}$$

$$P_k^- = \sum_{i=0}^{2n} w_i^c \left[\chi_{i,k|k-1}^x - \hat{x}_k^-\right]\left[\chi_{i,k|k-1}^x - \hat{x}_k^-\right]^T + Q_k \tag{9}$$

$$Y_{k|k-1} = h(\chi_{k|k-1}^x, \chi_{k-1}^\eta) \tag{10}$$

$$\hat{y}_k^- = \sum_{i=0}^{2n} w_i^m \cdot Y_{i,k|k-1} \tag{11}$$

- Measurement update:

$$P_{y_k} = \sum_{i=0}^{2n} w_i^c \left[Y_{i,k|k-1} - \hat{y}_{k|k-1}\right]\left[Y_{i,k|k-1} - \hat{y}_{k|k-1}\right]^T + R_k \tag{12}$$

$$P_{x_k y_k} = \sum_{i=0}^{2n} w_i^c \left[\chi_{i,k|k-1} - \hat{x}_{k|k-1}\right]\left[Y_{i,k|k-1} - \hat{y}_{k|k-1}\right]^T \tag{13}$$

$$\mathrm{K}_k = P_{x_k y_k} \cdot P_{y_k}^{-1} \tag{14}$$

$$\hat{x}_k = \hat{x}_k^- + \mathrm{K}_k \cdot (y_k - \hat{y}_k^-) \tag{15}$$

$$P_k = P_k^- - \mathrm{K}_k \cdot P_{y_k} \cdot \mathrm{K}_k^T \tag{16}$$

C. Initial estimation error

Use a proportional serif typeface such as Times Roman or Times New Roman and embed all fonts. Table I provides samples of the appropriate type sizes and styles to use.

Another important aspect concerning to performance of UKF is the initial estimation error. It is said that the nonlinear filters may diverge if it is not initialized closely enough to actual states [12]. Some research has been developed to cope with this problem. Modification of noise covariance can ensure UKF stability for nonlinear systems with linear

measurements [13]. Another modified UKF has also been proposed and analyzed stability for nonlinear systems with nonlinear measurements [14]. In their work, the noise covariance matrix is altered to:

$$\hat{Q}_k = Q_k + \gamma \cdot P_{k-1} \cdot e^{-(k-1)} \tag{17}$$

where γ represents a positive scalar to be determined. In this way, when the algorithm starts, the covariance matrix will be enlarged to satisfy a specific condition [14].

IV. Process Model

Predication precision of Kalman filter also depends on the precision of its underlying dynamic mathematical model. A fairly simple and reasonable model made in [15] is employed for UKF in this paper. Because the estimation of states is addressed to pressure safety problem, and that only hydraulic elements of hydropower plant are related to this issue, only mechanical power model is used for developing UKF. The synchronous generator model is not included in this paper. Parameters of that model are estimated before for a specific plant called Fjone power plant in Norway. The mathematical model is:

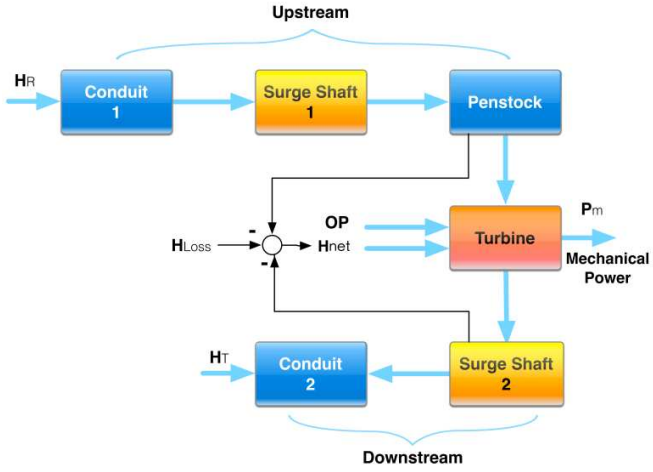

Fig. 1. Flowchart for process model of the hydropower plant.

Conduit 1:
$$\frac{dQ_{C1}}{dt} = \frac{g \cdot A_{C1}}{L_{C1}}(H_R - H_{S1} - H_{loss\_C1}) \tag{18}$$

Conduit 2:
$$\frac{dQ_{C2}}{dt} = \frac{g \cdot A_{C2}}{L_{C2}}(H_{C2} - H_T - H_{loss\_C2}) \tag{19}$$

Surge shaft 1:
$$A_{S1} \cdot \frac{dH_{S1}}{dt} = Q_{S1\_in} - Q_{S1\_out} \tag{20}$$

Penstock:
$$\frac{dQ_{p\_in}}{dt} = \frac{g \cdot A_p}{L_p}(H_{S1} - H_{p\_out} - H_{loss\_p}) \tag{21}$$

$$\frac{dH_{p\_out}}{dt} = \kappa \cdot (Q_{p\_in} - Q_{p\_out}) \tag{23}$$

where
$$\kappa = \frac{a^2}{g \cdot A_p \cdot L_p} \tag{24}$$

Surge shaft 2:
$$A_{S2} \cdot \frac{dH_{S2}}{dt} = (Q_{p\_out} - Q_{C2}) \tag{25}$$

Head loss:
$$H_{loss} = f_r \cdot \frac{L}{D} \cdot \frac{\bar{Q} \cdot |\bar{Q}|}{2g \cdot A^2} \tag{26}$$

Hydraulic turbine:
$$Q_{p\_out} = Q_{dis} = k \cdot A_p \cdot OP \cdot \sqrt{H_{net}} \tag{27}$$

$$H_{net} = H_{p\_out} - H_{S2} - H_{loss\_turbine} \tag{28}$$

and
$$Q_{T1} = Q_{S1\_in},\ Q_{S1\_out} = Q_{p\_in} \tag{29}$$

The final mechanical power available for electrical power generation, which is also the output equation, is

$$P_m = \eta \cdot \rho \cdot g \cdot H_{net} \cdot Q_{dis} \tag{28}$$

V. Results

Simulation results are presented with two scenarios. One is with normal operation points and the other is with abnormal operation that should not happen during production, since it may be risk to hydropower plant, affect quality of electricity and working efficiency. For verifying UKF estimation results and other purposes, an experiment was arranged and done with close control loop and open loop in Fjone power plant of Norway. Experiment data are acquired with sampling time 0.1 second. A digital pressure sensor was set up in penstock before hydraulic turbine, which is not in use in daily production. UKF is configured to predict one minute forward and prediction step is 0.1 second. The parameters of process model were estimated form previous work, not by UKF.

A. Normal operation scenario

A normal operation point is simulated with effective gate opening 58% of hydraulic turbine. It can be seen in Fig.2 that after UKF got the measured pressure and initialized, it predicted all states. From comparison between estimation and measurements, it seems that UKF eliminates some uncertainties or noise of measurements. The prediction for one minute forward costs UKF less than 1.5 seconds and the average error is 0.0908 bar. RMSE is 0.2246. Furthermore, the states that not measured are also estimated. In Fig.3, the predicted surge tank water level and downstream water head are reasonable according to the knowledge of Fjone power plant.

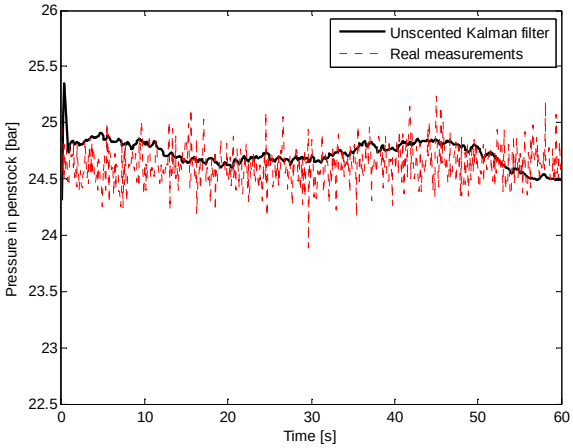

Fig. 2. Estimated pressure with normal operation

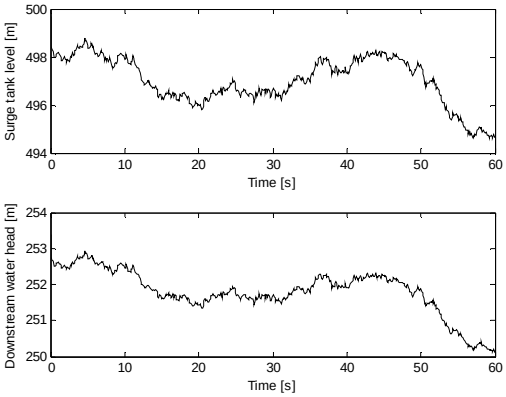

Fig. 3. Estimated water level with normal operation

Estimated flow rates are shown in Fig .4. They are around 18 m^3/s, what is also rational. However what must be noticed, the flow rate should never exceed to the total production flow discharged by head water reservoir. That means constraints should be configured to these states when doing estimation. However, EKF may have problems to accomplish this goal, since that when projecting EKF estimation, the covariance of EKF will not add the information of constraints [16]. Nevertheless, UKF can manage to set the constraints when it projects sigma points. Afterwards, the covariance of UKF still includes the information of constraints. UKF shows its dominant position again here for estimation hydropower system. Handling constrains should also be implemented to the surge tank water level due to its geometry limitations.

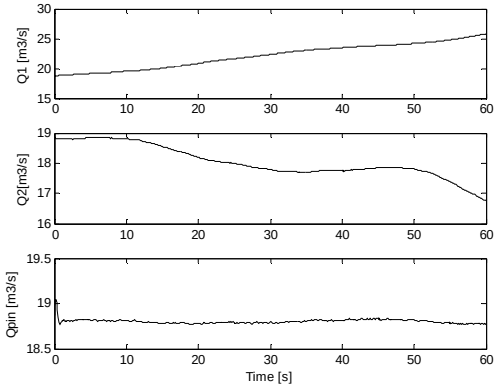

Fig. 4. Estimated flow rates with normal operation

B. Abnormal operation scenario

In the cause of obtain inverse response of pressure in penstock, an abnormal operation was set up in experiment in Fjone hydropower plant. A sudden and fast closure of hydraulic turbine gate was made intentionally from 90% to 80% in 1.5 seconds.

When fast gate closure happen, the pressure can increase to high value that may damage hydraulic turbine or penstock. It is due to a sudden smaller passage into hydraulic turbine. This situation is called inverse response or affect can cause water hammer in some area. Therefore, it is meaningful to estimate consequences when turbine gate is going to close. Usually, the gate closure is limited and divided into several steps, what is implemented into controllers of hydropower plant. Thus, the experiment is done with an open loop and manual control of gate opening of turbine.

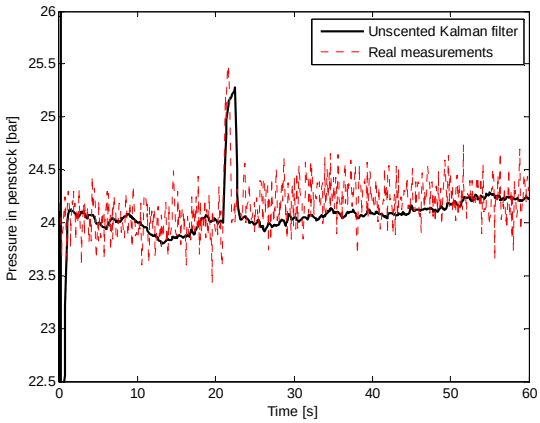

Fig. 5. Estimated pressure with abnormal operation

It is shown in Fig.5 that UKF behaved this specific response exactly like the measurements. In this case, UKF spent 2.2 seconds to predict one minute ahead. And the RMSE is 0.9101. It is probably due to UKF initialized worse with very large estimation errors. And the highest pressure of UKF estimated is little lower than that detected, what could because of uncertainties of measurements or the model errors.

VI. Conclusion

An unscented Kalman filter with modified sigma points projection and noise covariance matrix is applied to hydropower system in this work, which is with realistic and specific constraints are. Normal and abnormal operation scenario are simulated with this UKF and compared with measurement data. Eventually, estimation results of it are close to the real hydro system behaviour, but with not good initialization. Further work is required for modification of initialization. To achieve more precision, it is better to estimate parameters in a more advanced way like estimation with also UKF. A dual UKF may assist to it. Briefly, this paper shows UKF has many advantages in estimation for dynamic states of hydropower system, and can give a fast and relatively reliable prediction.

VII. Acknowledgments

The measurements data are acquired with help of Skagerak Kraft AS, the owner of Fjone hydropower plant in Norway. We appreciate very much Ingvar Andreassen who set up the experiments and master student Jens Niklas Thalberg in conjunction with experiment assembly.

VIII. References

[1] E. Ghamahermani, I. Kamwa, “Online State Estimation of a Synchronous Generator Using Unscented Kalman Filter From Phasor Measurements Units”, IEEE Transaction on energy conversion, 2011, Vol 26(4). PP.1099-1108

[2] S.J. Julier, J.K, Uhlmann, H.F. Durrant-Whyte, “A new method for the nonlinear transformation of means and covariances in filters and estimatots”, IEEE Transaction on Automatic Control 2000, Vol 45(3). pp.477-482.

[3] A. Faina, B. Ristic, D. Benvenuti, “Tracking a ballistic target comparision of several nonlinear filters”, IEEE Transactions on Aerospace and Electronic Systems 2002, Vol. 38(3). pp.854-867.

[4] A. Romanenko, J.A.A.M. Castro, “The unscented Kalman filter as an alternative to EKF for nonlinear state estimation: a simulation case study”, Computers and Chemical Engineering 2004, Vol. 2004, pp.347-355

[5] G. Chowdhary, R. Jategaokar, “Aerodynamic parameter estimation from flight data applying extended and unscented Kalman filter”, Aerospace Science and Technology 2010, Vol 14. pp. 106-117

[6] R. Van der Merwe, “Sigma-Point Kalman Filter for probablity inference in dynamic state-space models”, Ph.D Thesis, Oregon Health and Science University, 2004.

[7] S.J. Julier, J.K, Uhlmann, ” Unscented Kalman filter and nonlinear estimation”, Proceedings of IEEE 2004, Vol. 92(3), pp.401-422

[8] R. Turner, C.E. Rasmussen, “Model based learning of sigma points in unscented Kalman filtering”, Neurocomputing 2012, Vol. 80, pp. 47-53

[9] Y. Cheng, Z. Liu, “Optimized Selection of Sigma Points in the Unscented Kalman Filter”, in Proc. Electrical and Control Engineering Conf. 2011, pp. 3073-3075

[10] E.A. Wan, R. Van der Merwe, ”The unscented Kalman filter for nonliear estimation”, in Pro. Adaptive Systems for Signal Processing, Communications, and Control Symposium 2000. pp.153-158

[11] R. Van der Merwe, E.A. Wan ”Sigma-point Kalman filters for intergrated navigation”, presented in 60th Annual metting, Inst. of Navig, 2004, Ohio. p.56

[12] M. Boutayeb, D. Aubry, “A strong tracking extended Kalman observer for nonlinear discrete-time systems”, IEEE Transactions on Automatic Control 1999, Vol. 44(8), pp. 1550-1556

[13] K. Xiong, H.Y. Zhang, C.W. Chan, “Performance evaluation of UKF-based onlinear filtering”. Automatica 2006, Vol.(42), pp.261-270

[14] K. Xiong, L.D Liu, H.Y. Zhang “Modified unscented Kalman filter and its application in autonomous satellite navigation”, Aerospace Science and Technology, 2009, Vol.13, pp.238-246

[15] W. Zhou, B.R. Shrefi, B. Bernt, B. Glemmestad, “Modelling and control of a high head hydropower plant”, paper presented in 52th Int. Conf. SIMS.

[16] R. Kandepu, B. Foss, L. Imsland, ”Applying the unscented Kalman filter for nonlinear state estimation”, Journal of Process Control, 2008. Vol.18, pp. 753-768

Appendix B: Abstract of co-author paper

The Effect of Compressibility of Water and Elasticity of Penstock Walls on the Behavior of a High Head Hydropower Station

(Published in *SIMS Conference 2011*)

Behzad Rahimi Sharefi, Wenjing Zhou, Bjørn Glemmestad, Bernt Lie

Faculty of Technology, Department of Electrical Engineering, Information Technology and Cybernetics, Telemark University College, P. O. Box 203, N-3901 Porsgrunn, Norway

Abstract: This paper considers modeling of a high-head hydropower generation unit when compressibility of the water and elasticity of the penstock walls are taken into account. Finite Volume Method and MATLAB are used to simulate the behavior of the penstock in this model. Various important parameters for simulation such as the number of grid volumes in the spatial discretization of the penstock as well as ODE solver options in MATLAB are examined by simulation, and are discussed. The simulation model thus obtained is validated using available charts for pressure rise in case of uniform gate closure. Then available models for the other parts of the waterway (inelastic models) are included to give an interface to the elastic penstock model. Finally, the model of the whole power generation unit with a classic transient droop controller and a synchronous generator connected to an infinite bus is simulated in MATLAB.

Appendix C: ODE solver

Due to large amount of computing and Matlab coding are involved in this study, a simplified ODE solver has been introduced and used throughout the entire research activity. The solver was developed from the candidate's summer job within a team of ' Automatic startup of ESP-lifted wells' in Statoil ASA. The detailed coding as following:

```
function Y = ode4(odefun,tspan,y0,varargin)
%ODE4  Solve differential equations with a non-adaptive method of order 4.
%   Y = ODE4(ODEFUN,TSPAN,Y0) with TSPAN = [T1, T2, T3, ... TN] integrates
%    the system of differential equations y' = f(t,y) by stepping from T0 to
%   T1 to TN. Function ODEFUN(T,Y) must return f(t,y) in a column vector.
%    The vector Y0 is the initial conditions at T0. Each row in the solution
%   array Y corresponds to a time specified in TSPAN.
%
%   Y = ODE4(ODEFUN,TSPAN,Y0,P1,P2...) passes the additional parameters
%   P1,P2... to the derivative function as ODEFUN(T,Y,P1,P2...).
%
%    This is a non-adaptive solver. The step sequence is determined by TSPAN
%   but the derivative function ODEFUN is evaluated multiple times per step.
%   The solver implements the classical Runge-Kutta method of order 4.
%
%   Example
%         tspan = 0:0.1:20;
```

```
%         y = ode4(@vdp1,tspan,[2 0]);
%         plot(tspan,y(:,1));
%     solves the system y' = vdp1(t,y) with a constant step size of 0.1,
%     and plots the first component of the solution.
%

if ~isnumeric(tspan)
  error('TSPAN should be a vector of integration steps.');
end

if ~isnumeric(y0)
  error('Y0 should be a vector of initial conditions.');
end

h = diff(tspan);
if any(sign(h(1))*h <= 0)
  error('Entries of TSPAN are not in order.')
end

try
  f0 = feval(odefun,tspan(1),y0,varargin{:});
catch
  msg = ['Unable to evaluate the ODEFUN at t0,y0. ',lasterr];
  error(msg);
end

y0 = y0(:);   % Make a column vector.
if ~isequal(size(y0),size(f0))
```

```
  error('Inconsistent sizes of Y0 and f(t0,y0).');
end

neq = length(y0);
N = length(tspan);
Y = zeros(neq,N);
F = zeros(neq,4);

Y(:,1) = y0;
for i = 2:N
  ti = tspan(i-1);
  hi = h(i-1);
  yi = Y(:,i-1);
  F(:,1) = feval(odefun,ti,yi,varargin{:});
  F(:,2) = feval(odefun,ti+0.5*hi,yi+0.5*hi*F(:,1),varargin{:});
  F(:,3) = feval(odefun,ti+0.5*hi,yi+0.5*hi*F(:,2),varargin{:});
  F(:,4) = feval(odefun,tspan(i),yi+hi*F(:,3),varargin{:});
  Y(:,i) = yi + (hi/6)*(F(:,1) + 2*F(:,2) + 2*F(:,3) + F(:,4));
end
Y = Y.';
```

Doctoral dissertation no. 33
2017

—

Modeling, Control and Optimization of a Hydropower Plant

Dissertation for the degree of Ph.D

—

Wenjing Zhou

—

ISBN 978-82-7206-457-9 (print)
ISBN 978-82-7206-458-6 (electronic)

usn.no